GAS HYDRATES, FLARES SEEPS OFFSHORE ROMANIA, A REVIEW

Corneliu DINU[1], Ioan MUNTEANU[2], Dorina TAMBREA[3], Nicolae PANIN[4]

[1]University of Bucharest, Faculty of Geology and Geophysics, 6 Traian Vuia, 020956, Bucharest, Romania,
e-mail: corneliu.dinu@g.unibuc.ro
[2]Repsol S.A., 44 Mendez Alvaro, 28045, Madrid, Spain
[3]Danubian Energy Consulting SRL, 35-37 Academiei St., Entrance A, 6th Floor, 11th Suite, 010013, Bucharest, Romania
[4]National Institute of Marine Geology and Geo-Ecology (GeoEcoMar), 23-25 Dimitrie Onciul St., 024053 Bucharest, Romania

Abstract. The civilisation is in the continuous search for energy resources, either already in use or new ones, for future needs. The gas hydrates are one of the unconventional resources that have been identified, evaluated and in the future will be probably exploited. The semi-enclosed Black Sea Basin has an excellent potential for free gas and gas hydrate accumulation, on account of its anoxic water regime which favours the preservation of organic matter in the sediments (the chemocline lies at 110–140 m depth). Regions outside the stability field of gas hydrates, namely, the shelf and upper slope, show a high gas content in the sediments.
The Black Sea Basin has been the focus for numerous research projects, which led to the identification of the BSR that might be associated with the gas hydrate zones. Beside the gas hydrates, numerous gas occurrences have been recognized on the seafloor of the Black Sea in different sectors and at different depths, including shelf and slope of Romanian Black Sea area, and a significant amount of data have been published.
The current synthesis aims to make a review of the results published in the last 15 years describing geological structure and evolution of the Black Sea Basin, as well as bottom sediments, gas hydrates, flare and escape structures Offshore Romania.

Key words: Black Sea, unconventional resources, Danube Canyon, landslides, heat flow, deep water

1. INTRODUCTION

The gas hydrates are one of the unconventional resources that might be in the future available for the humanity. Although the exploration and production is still in the early and experimental stages respectively, numerous research programs have been carried out for the identification and mapping of the gas hydrates around the world. The Black Sea has been part of some of those projects and PhD thesis, which led to the identification of the BSR, which might be associated with the gas hydrates zones.

The semi-enclosed Black Sea is a potential candidate for free gas and gas hydrate accumulation on account of its anoxic water regime which favours the preservation of organic matter in the sediments (the chemocline lies at 110-140 m depth). Regions outside the stability field of gas hydrates, namely the shelf and upper slope, show a high gas content in the sediments.

In the Black Sea and elsewhere, significant volumes of both deep thermogenic and shallow biogenic gases are escaping continuously to the seafloor and into the water column over long periods. These processes have occurred over geologic time (Kruglyakova *et al.*, 2004). Migration of hydrocarbon gases to the seafloor and into the water column occurs as direct seepages, mud volcanoes, and during the development of fluidized deformations such as diapirs (Kruglyakova *et al.*, 2004). Gas discharges on the floor of the Black Sea shelves are widespread.

Numerous gas occurrences have been recognized on the seafloor of the Black Sea in different sectors and different depths, including shelf and slope of Romanian Black Sea area, and a significant amount of data have been published.

The current synthesis aims to make a review of the results published over the last 15 years describing gas hydrates, flare and escape structures offshore Romania.

2. WESTERN BLACK SEA BASIN GEOLOGY

2.1. Tectonic model for the Black Sea basin-tectonic evolution with impact over the heat flow.

The Black Sea Basin formed in a back-arc domain due to the roll-back associated with the N-ward subduction of Neotethys under the Rhodope-Pontides Arc, which opened the Western Black Sea back-arc basin during Early Cretaceous times (Letouzey *et al.*, 1977; Zonenshain & Le Pichon, 1986; Görür, 1988; Dinu *et al.*, 2005). The extension affected a larger area during the Uppermost Cretaceous times, and by the Paleocene the Eastern Black Sea has been included into the Black Sea system (Robinson *et al.*, 1995; Spadini *et al.*, 1997; Kazmin *et al.*, 2007; Munteanu, 2012). The extensional settings continued in the Black Sea up to Lower Eocene times (Munteanu *et al.*, 2011), and resulted in the formation of two oceanic crust areas overlain by an up to 15 km thick sedimentary sequence in their centre, separated by the Andrusov Ridge into Western and Eastern Black Sea Basin (Fig. 1, Neprochnov *et al.*, 1970; Shillington *et al.*, 2008; Graham *et al.*, 2013; Nikishin *et al.*, 2015a). The age of the oceanic crust ranges from Lower Cretaceous to Eocene (see Kazmin *et al.*, 2007, Munteanu *et al.*, 2014); with a limited distribution in the Western Black Sea, but with a wide transition zone (Nikishin *et al.*, 2015b).

The far-field transmission of contractional deformation from the Balkan-Pontides Indentor to the Romanian-Ukrainian Offshore resulted in the inversion of pre-existing extensional structures and the formation of a North-vergent thick-skinned thrust system in the Western Black Sea, with the formation of Lebada-Heraclea main oil structures offshore Romania, during the Late Eocene-Middle Miocene inversion (Figs. 1 and 4, Munteanu *et al.*, 2011).

The complex tectonic evolution from extension to compression disturbs lithospheric thermal structure producing positive or negative thermal anomalies expressed through heat flow measurement, in particular the anomalous low heat flow in the WBS deep basin, ~20 – 30 mW/m^2 (Golmshtok *et al.*, 1992, Kutas *et al.*, 1988; Kutas & Poort, 2008). A higher heat flow values were recorded on the Romanian Shelf, where thick continental lithosphere is present (Fig. 28, Veliciu, 2002).

The structural features have been inherited from the prolongation of the onshore well known tectonic units, Pre-Dobrogea Depression (Scythian Platform), North Dobrogea Orogen, Central and South Dobrogea sectors of the Moesian Platform, well defined by their specific lithology as shown by the wells (Fig. 1, Dinu *et al.*, 2005). A synthetic lithological column for the Romanian Black Sea shelf is presented in Fig. 4, as well as the main tectonic events. Starting with Paleogene the sedimentary cover gets thicker and uniform for the entire West Black Sea Basin (Fig. 4).

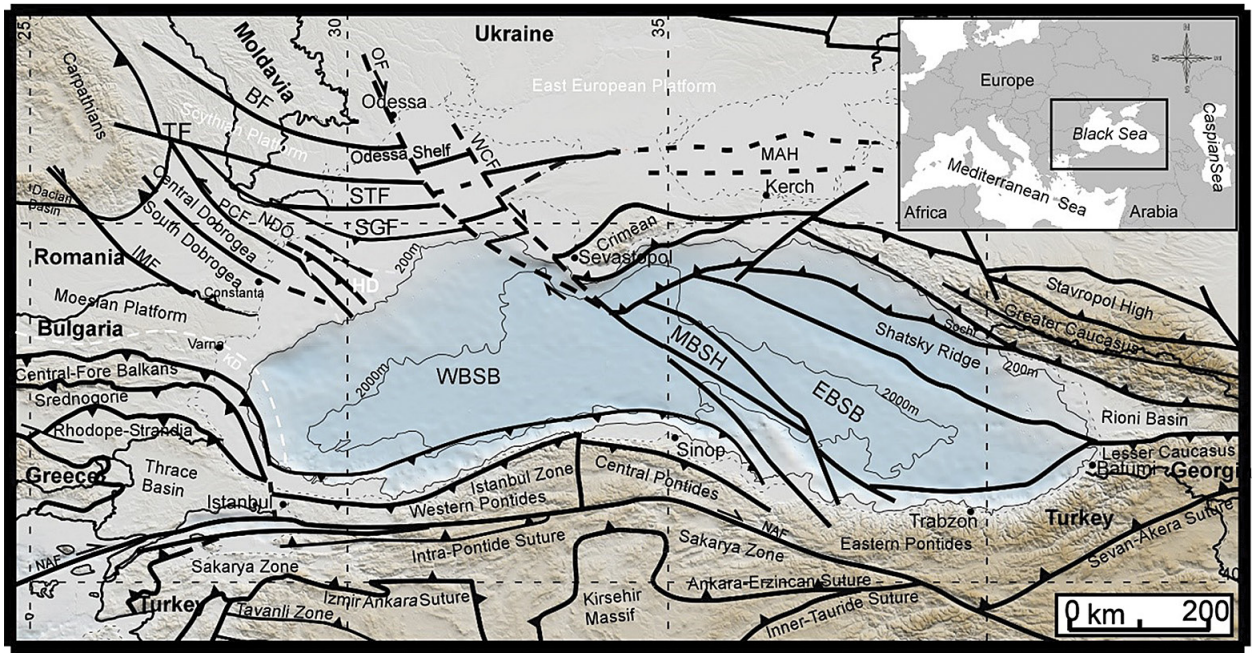

Fig. 1. Tectonic map of the Black Sea and adjacent areas (compiled from, Finetti *et al.*, 1988; Doglioni *et al.*, 1996; Okay and Sahinturk, 1997; Dinu *et al.*, 2005; Afanasenkov *et al.*, 2007; Khriachtchevskaia *et al.*, 2009, 2010; Nikishin *et al.*, 2010; Munteanu *et al.*, 2011). **BF** – Bistriţa Fault, **PCF** – Peceneaga Camena Fault, **IMF** – Intra-Moesian Fault, **NAF** – North Anatolian Fault; **OF** – Odessa Fault, **SGF** – Sfântul Gheorghe Fault, **STF** – Sulina-Tarhankut Fault, **TF** – Trotuş Fault, **WCF** – West Crimea Fault, **EBSB** – Eastern Black Sea Basin, **WBSB** – Western Black Sea Basin, **HD** – Histria Depression, **KD** – Kamchya Depression, **MAH** – -Mid Azov High, **MBSH** – Mid Black Sea High, **NDO** – North Dobrogea Orogen, **NKD** – North.

2.2. Black Sea in the Parathetys Basin framework

The Black Sea back-arc Basin is one of the last active sink from the Neogene Paratethys Basin (Senes, 1973; Rögl, 1999), currently draining most of the Europe largest river systems like Danube, Dnieper and Dniester (Popov *et al.*, 2006). The Black Sea Basin had semi-permanent connections with its epicontinental appendixes, such as the Dacian Basin (*e.g.* Popov *et al.*, 2006; Fig. 2). The exchange of waters between the Black Sea and the marginal Dacian Basin took place through a shallow-water corridor, Scythian Gateway, located north of Nord Dobrogea Orogen and extended, which was active during Late Miocene – Pliocene time (Figs. 2 and 3, Matoshko *et al.*, 2009).

2.3. Miocene-Quaternary sedimentation pattern on the Romanian Shelf

Although the overall Miocene-Quaternary sedimentation was reduced in the entire Western Black Sea Basin, higher subsidence rates have been recorded for uppermost Miocene-Quaternary times for the Romanian-Ukrainian NW Black Sea shelf (Cloetingh *et al.*, 2003; Nikishin *et al.*, 2003, Tambrea, 2007). At the Miocene-Pliocene transition a sea level fall of debated amplitude (100–2300 m), led to large-scale shelf erosion and significant progradation during the subsequent high-stand (Hsü & Giovanoli, 1979; Gillet *et al.*, 2007, Munteanu *et al.*, 2012). Subsequent rapid sea-level changes have also been interpreted during the Late Pliocene-Quaternary endemic evolution of the Black Sea (Fig. 3, Winguth *et al.*, 2000; Lericolais *et al.*, 2010), when sea-level fall enhanced the transport of large volumes of sediments towards the deep-sea part of the basin.

The present-day position of these rivers discharge in the NW part of the Black Sea basin (Fig. 2, Danube, Prut, Dnieper, Dniester) is interpreted to be a Quaternary feature or locally as young as the Holocene (*e.g.* Popescu *et al.*, 2001; Panin, 2003). A detailed geometry of the paleo-drainage network during the Late Miocene – Pliocene remains poorly constrained, but the large-scale deltaic sedimentation recorded in the Dacian Basin during the Upper Pliocene suggests that the main fluvial discharge had not reached this western segment of the Black Sea basin at this time (Jipa & Olariu, 2009).

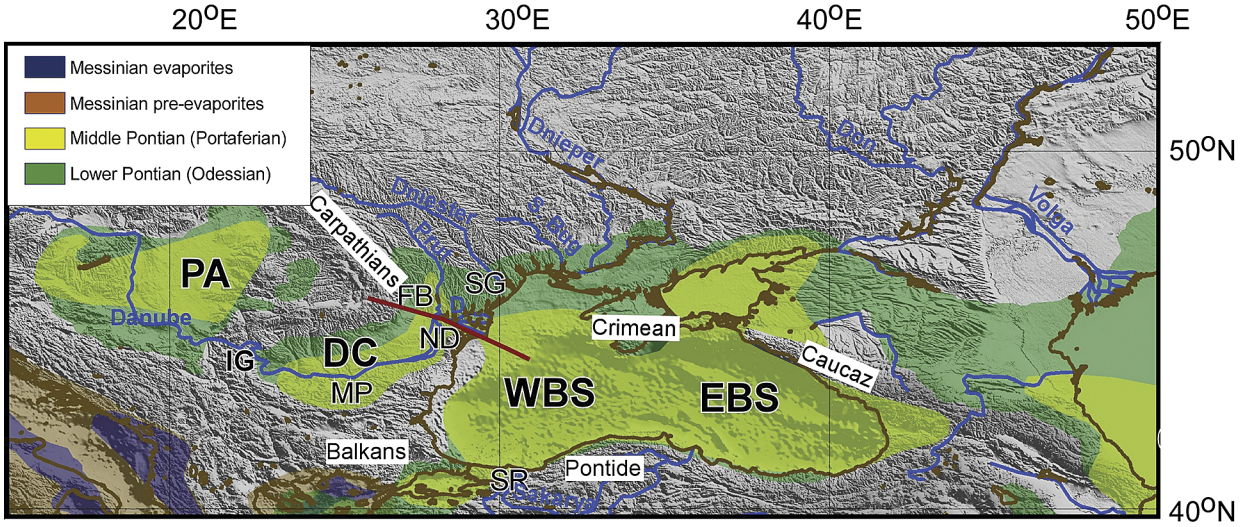

Fig. 2. Extent of Paratethys basins during the Lower Pontian high-stand and subsequent Middle Pontian (MSC) low-stand system tract (simplified after Popov *et al.*, 2006). **DC** – Dacian Basin, **EBS** – East Black Sea, **FB** – Focsani Basin, **ND** – North Dobrogea Orogen, **PA** – Pannonian Basin, **WBS** – West Black Sea. **SG** – Scythian Gateway.

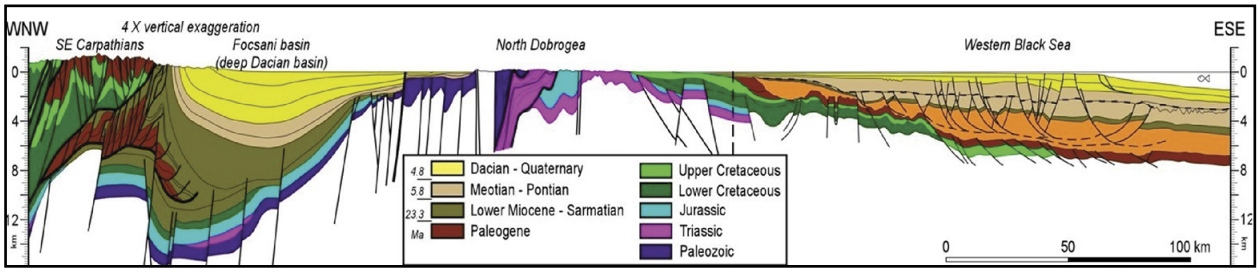

Fig. 3. Regional cross-section (4x vertical exaggeration) spanning from SE Carpathians, Dacian Basin and Dobrogea highland to the deep-sea part of Black Sea (compiled from Steininger *et al.*, 1988; Tarapoanca *et al.*, 2003; Dinu *et al.*, 2005; Matenco *et al.*, 2007; Munteanu *et al.*, 2012).

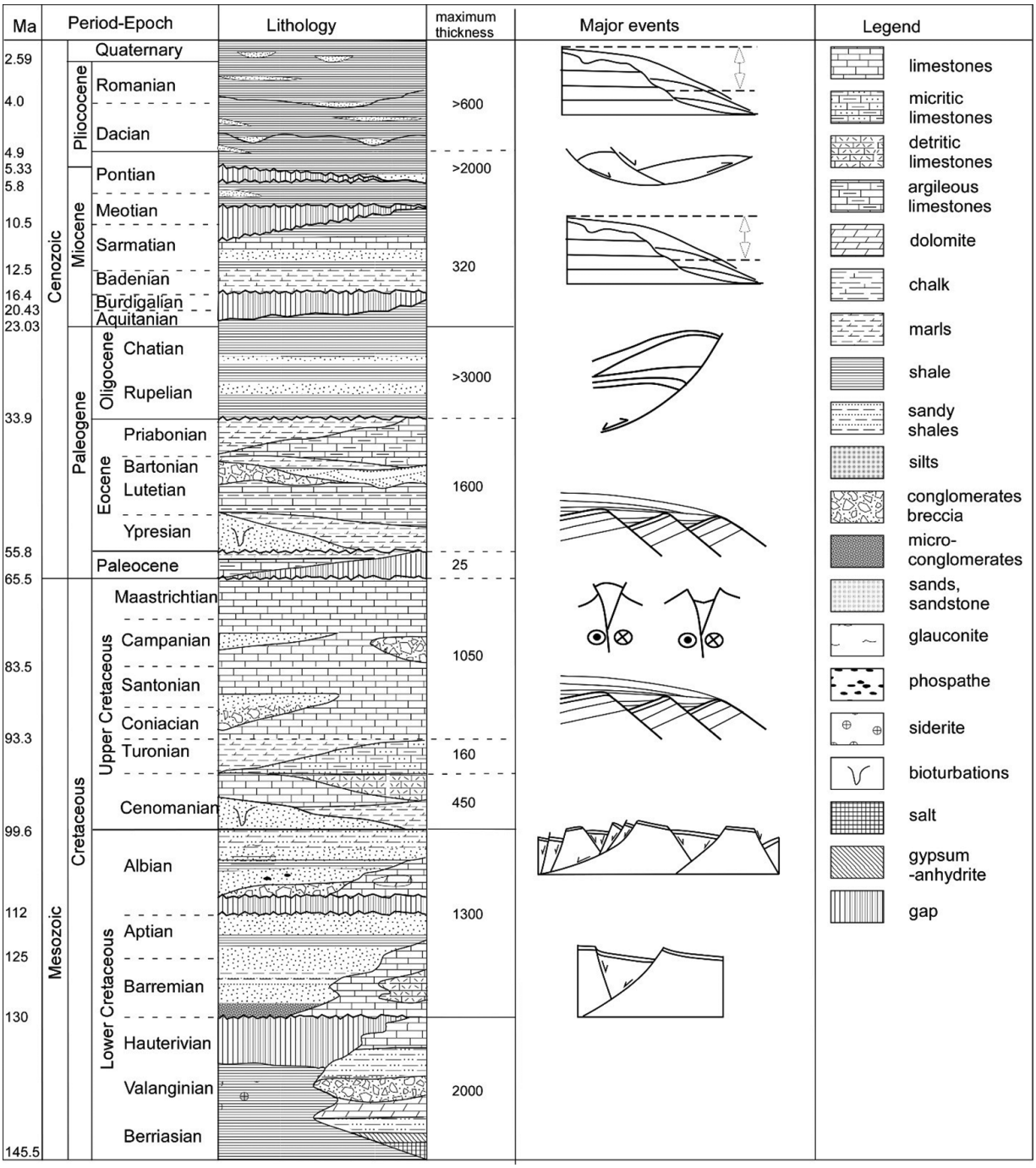

Fig. 4. Tectono-stratigraphic chart of the Western Black Sea part situated in the offshore Romania (compiled from Dinu *et al.*, 2005a; Munteanu *et al.*, 2011; Tambrea *et al.*, 2002). The tectonic events derived from the study of Munteanu *et al.*, 2011.

The sediments filling the Dacian and Black Sea basins have been sourced by the uplift and/or exhumation of Balkanides starting with Late Eocene and then from the Carpathian Orogen since Miocene times (Ivanov, 1988; Ricou *et al.*, 1998; Matenco *et al.*, 2010; Merten *et al.*, 2010). With the fill of the Dacian Basin the sediments fluxes have been shifted towards the Black Sea main sink, from the uppermost Pliocene (Upper Dacian in local scale) onwards resulting in a large scale progradation of the NW Black Sea shelf (Munteanu *et al.*, 2012).

Direct lithological constrains for the Upper Pliocene-Quaternary deposits are limited, the recent exploration wells data have not been disclosed, while the research drop coring are limited to the uppermost part of the system, a few meters, depending on the gravity core penetration (Konerding, 2005; Lericolais *et al.*, 2013; Constantinescu *et al.*, 2015). The available data shows a shelly-marly dominated system, with sands associated with topsets deltaic facies and shelf canyons or with deep-water turbiditic lobes facies (Fig. 5, Tambrea *et al.*, 2000; Bega & Ionescu, 2009; Duley & Fogg, 2009).

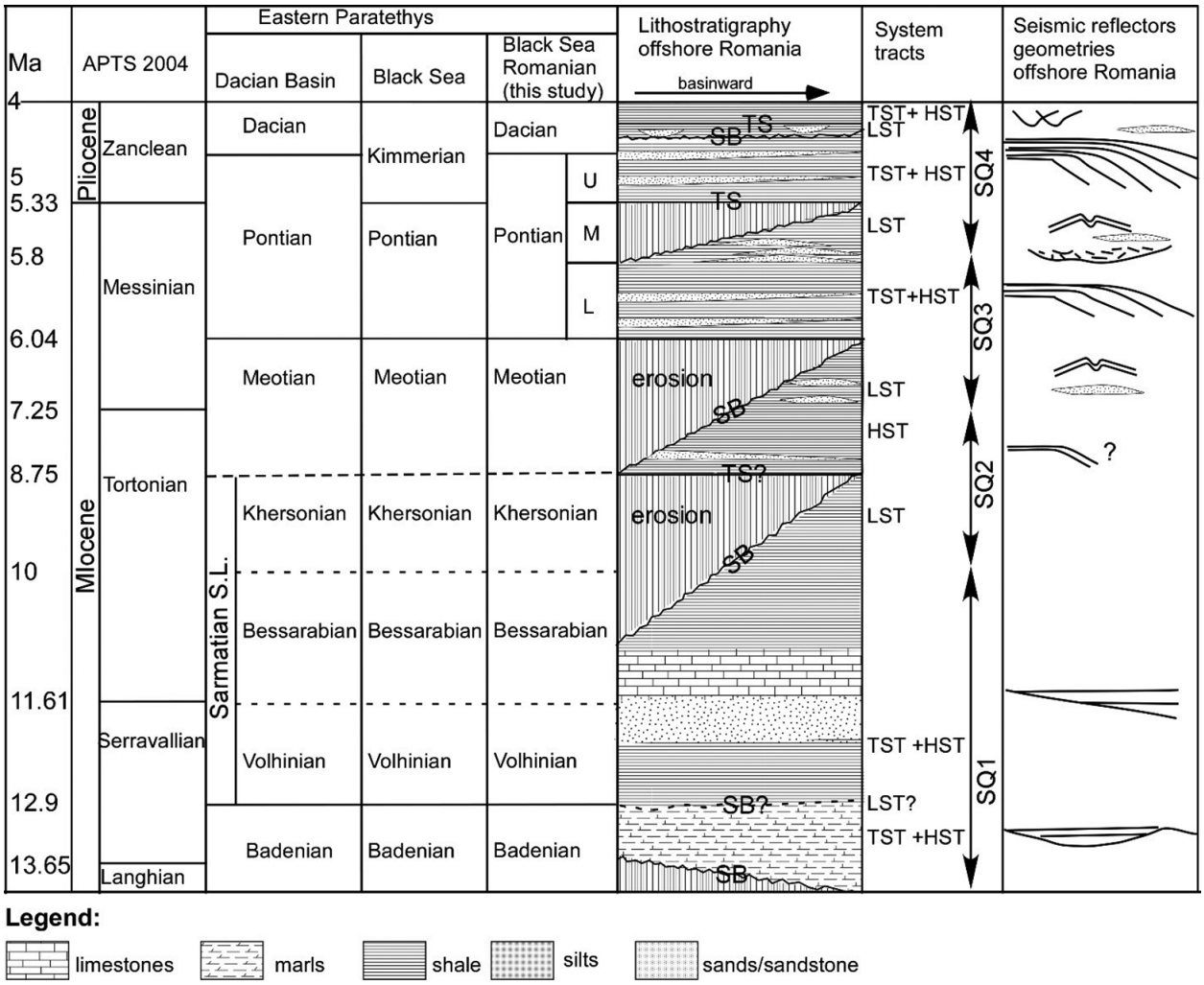

Fig. 5. Detailed chrono-stratigraphic chart for the Middle Miocene-Pliocene section of the Black Sea shelf, offshore Romania. The Miocene-Pliocene biostratigraphic ages are a combination between the endemic Central and Eastern Paratethys stages used by the local petroleum exploration (see Rögl, 1996 for further biostratigraphic correlations). The absolute ages and correlation between Paratethys and international scales are according with Vasiliev *et al.* (2005); Vasiliev *et al.* (2011). The system tracts and seismic geometries are the result of Munteanu *et al.*, 2012.

3. GAS HYDRATES RESEARCH IN THE ROMANIAN BLACK SEA SECTOR

Gas hydrate occurrence in the Danube fan is known since the first hydrate discovery in shallow subbottom sediments (Yefremova & Zhizhchenko, 1974, cited in Ginsburg and Soloviev, 1998). The presence of gas hydrates in deep sediments was inferred from Bottom Simulated Reflector (BSR) observations in the southern part of the fan (du Fornel, 1999).

In 2002, Ion *et al.*, based on a multifold high resolution seismic data acquired by IFREMER during BLASON (Black Sea Over the Neoeuxinian), French-Romanian scientific campaign in the Black Sea in 1998, had investigated the canyon of the Danube and had searched for the gas presence in the continental shelf, continental slope and deep-sea zones. They have concluded that the gas is present in the sedimentary features of the palaeo-Danube realm, on the continental shelf and slope and in the deep sea zone. In the shelf area the biogenic gas is prevailing, but the thermogenic gas is also present. On the continental slope the gas signature on seismoacoustic facies is less present. In the deep-sea area the gases in association with other fluids are present and produce mud volcanoes and BSR structures which have been reported for the first time in the Danube deep sea fan area.

Later on, in 2003, Egorov *et al.*, based on detailed research about methane gas emissions in the Black Sea, created a map of the location of gas seeps, as well as the distribution of methane along the vertical extend into the water column. They conclude that the distribution of the gas seeps, gas flares and gas hydrates in the Back Sea area is closely related to the presence of the channels and mud volcanoes and the gas has both biogenic and thermogenic origin. The biogenic origin of methane gas emissions from depths up to 370 m is related to the diagenesis of bottom sediments occurring at active participation of methane-forming bacteria. On the other hand, they showed that in the places of gas discharge

the density and salinity of the water do not change and the carbonate formations are present.

Zillmer *et al.*, in 2005, detected for the first time in seismic data of the Black Sea, a bottom simulating reflector (BSR), which marks the base of the gas hydrate stability zone, using the seismic wide-angle ocean bottom hydrophone (OBH) and ocean bottom seismometer (OBS) data, with the goal to quantify the gas hydrate and free gas saturation in the sediment and highlighted the BSR at 205–270 m depth below the seafloor and six to eight discrete layer boundaries between the seafloor and the BSR. Unfortunately, the top of the hydrate layer and the bottom of the gas layer cannot be identified by seismic reflection signals. A gas hydrate saturation–depth profile is obtained, which shows that there is 38 ± 10 per cent hydrate in the pore space at the BSR depth, where the porosity is 57 per cent (OBS 24). This value is derived for the case that the gas hydrate does not cement the sediment grains, a model that is supported by the low S-wave velocities. There is 0.1 - 0.9% free gas in the sediment below the BSR, depending on the model for the gas distribution in the sediment. The free gas layer may be more than 100 m thick because of a zone of enhanced reflectivity, which can be identified in the subsurface image.

In the paper 'Multiple bottom-simulating reflections in the Black Sea: Potential proxies of past climate conditions' in 2006, Popescu *et al.*, put in evidence the gas hydrate based on the high-resolution reflection seismic data acquired during the BlaSON surveys of IFREMER and GeoEcoMar (1998 and 2002). They mapped three areas of BSR occurrence in the Danube fan, located between 750 and 1830 m water depth (A, B, C). In the zones A and B, situated in the southern part of the fan, they detected an unusual succession of two, three or four BSR-type distinct reflections with similar amplitude, all of them subparallel to the seafloor, showing reversed polarity and crosscutting the sedimentary structure. A fifth very weak and discontinuous BSR possibly lies below the four-BSR occurrence. A low-frequency conventional industry-seismic profile across the zone C shows that the two BSRs have a reversed polarity.

Taking into consideration the hypothesis that the enhanced reflections and acoustic turbidity indicates the presence of gas hydrates and free gas in the sediment pore space they interpreted the BSR1 and its prolongation along the bottom-simulating boundary at the top of the enhanced reflections as the limit between gas hydrates and free gas, and thus the current BGHSZ. High amplitude anomalies located beneath this interface suggest that free gas occurs under the gas hydrate-bearing sediments. The amounts of free gas below lower BSRs are locally attested by segments of enhanced reflections that change amplitude where they cross multiple BSRs. This gas appears to focus along specific sedimentary horizons, probably in relation with their higher permeability. High amounts of free gas are not required to create these reflections, as gas concentration may be as low as a few percent of the sediment pore space.

At the same time, they linked multiple BSRs to geological background and they found a relationship between the gas hydrate presences with the architecture of the Danube deep-sea fan: occurrences of gas and hydrates correspond to specific channel–levee systems (A, B, C). In all cases:

(1) The Base of Gas Hydrates Stability Zone (BGHSZ) is visible only on a limited segment inside the channel-levee system,
(2) Multiple BSRs crosscut the parallel horizons of the levee that is situated downslope of the channel axis (considering the present seafloor gradient) and terminate against the base of the channel-levee system, and
(3) Free gas accumulation corresponds to the channel axis area.

They define a specific pattern of relatively closed gas and hydrate accumulations under a combined lithological, structural and stratigraphic control. This pattern represents the background for the formation of multiple BSRs, and most probably influences the multiple BSR-forming processes. They tried to explain the presence of these multiple BSRs and concluded that until new direct information becomes available, any discussion on this topic is inevitably limited to theoretical assumptions. Under these circumstances, they used modelling to test the compatibility of these alternative hypotheses against the generally known background of multiple BSR occurrences.

In 2007, Popescu *et al.*, analysed the seismic expression of gas and gas hydrates across the western Black Sea. The study was a synthesis of gas-related features in recent sediments across the Western Black Sea basin. The investigation was based on an extensive seismic dataset, and integrates published information from previous local studies.

The data reveal widespread occurrences of seismic facies indicating free gas in sediments and gas escape in the water column. The presence of gas hydrates was inferred from bottom-simulating reflections (BSRs). The distribution of the gas facies shows: (1) major gas accumulations close to the seafloor in the coastal area and along the shelfbreak, (2) ubiquitous gas migration from the deeper subsurface on the shelf and (3) gas hydrate occurrences on the lower slope (below 750 m water depth). The coastal and shelfbreak shallow gas areas correspond to the highstand and lowstand depocentres, respectively. Gas in these areas most likely results from in situ degradation of organic material, probably with a contribution of deep gas in the shelfbreak accumulation. On the western shelf, vertical gas migration appears to originate from a source of Eocene age or older and, in some cases, it is clearly related to known deep oil and gas fields. Gas release at the seafloor is abundant at water depths shallower than 725 m, which corresponds to the minimum theoretical depth for methane hydrate stability, but occurs only exceptionally at water depths where hydrates can form. As such, gas enter-

ing the hydrate stability field appears to form hydrates, acting as a buffer for gas migration towards the seafloor and subsequent escape.

In 2007, Lüdmann *et al.*, characterised the gas hydrates and free gas occurrence in the north-western Black Sea. They found out that a BSR occurs only locally in the western Black Sea, namely at the continental margin of Romania and near the Dnieper Canyon southwest of the Crimea Peninsula. The associated gas hydrate accumulations are probably characterized by a higher free gas content below the BGHSZ compared to the surrounding areas. In the Ukrainian sector, the seeps of gas appear in connection with mud diapirs, which penetrated the sedimentary column below the BGHSZ (Lüdmann *et al.* 2004). The top of the diapirs are characterized by extensive fracturing, allowing fluids to ascent and accumulate beneath the GHSZ. In the Romanian sector, the free gas flux is controlled by the specific lithostratigrahy of the channel-levee system of the Danube River. The coarse channel deposits provide excellent migration paths and the low-permeability condensed sections overlying the channel-levees and the GSHZ function as a perfect seal. In addition, numerous faults in this area allow the ascent of thermogenic gas from deeply-buried oil-bearing subbottom layers into the channels of the deep-sea fan system.

Multiple BSRs which occur only in the Romanian sector probably represent boundaries of GHSZs containing different mixtures of methane and higher homologues. The latter originated from leaky Oligocene oil reservoirs, and migrated along deep-seated faults into the channels of the Danube deep-sea fan system. The alternative explanation, namely that the multiple BSRs are relicts of the former GHSZ under different P-T conditions, seems less likely. For example, the time required to produce a 5 °C decrease in temperature at the present BSR position would be about 50 kyr. It is suggested that the influence of temperature fluctuations might be only relevant near the upper slope where the GHSZ pinches out and the heat could propagate much more rapidly into the subbottom.

They summarized that the gas hydrates and free gas accumulations off Romania are characterized by a complex interplay of the lithology of the host sediments, stratigraphic background and local tectonic pattern.

In 2007, Tambrea analysing the P-T conditions and several seismic data established the areal distribution of the gas hydrate in Istria Depression.

Merey and Sinayuc, 2016, in their study, by using the literature, seismic and other data from the Black Sea such as salinity, porosity of the sediments, common gas type, temperature distribution and pressure gradient, have selected the gas production method of depressurization as the most favourable for the Black Sea gas hydrates. Numerical simulations were run to analyse gas production from gas hydrate deposited in turbidites in the Black Sea by depressurization.

The most common gas hydrate reservoirs considered as possible energy sources are Class 1, Class 2 and Class 3 hydrate reservoirs. Class 1 hydrates are characterized with a hydrate layer above a zone with free gas and water. Class 2 deposits exist where the hydrate bearing layer, overlies a mobile water zone. Class 3 accumulations are characterized by a single zone of hydrate and the absence of an underlying zone of mobile fluids. When all other conditions and properties being equal among these hydrate reservoirs, Class 1 hydrates appear to be the most promising targets for gas production, because its pressure is close to hydrate equilibrium conditions and it would be easy to produce (only small changes in pressure and temperature are needed for hydrate dissociation) and the existence of a free gas zone guarantees gas production even when the hydrate contribution is small. It seems that the high reservoir-quality in gas hydrate accumulations are expected in permeable sandy-silty deposits, such as turbidites and channel-levee-systems of the large paleo-river systems around the Black Sea.

The main objectives of the study carried out by Zander *et al.*, 2017, were to analyse the compaction caused by gas production from an assumed gas hydrate reservoir in the study area, to establish if the production-induced compaction affects seafloor subsidence and to define the optimal strategy to avoid a production-related geo-hazards.

Based on geophysical data from the Danube deep-sea fan, they created a two-dimensional geomechanical model to analyse the hazards of hydrate-production-induced slope failures in a channel-levee system. Initial results estimated the failure surface at the levee slope that has a low Factor of Safety of about 1.25, which is considered to be critically affected by seabed subsidence. The estimated subsidence at the seafloor after pore pressure depletion of the reservoir is only in the order of centimetres. The preliminary estimation concludes that the effect of production-induced subsidence on the stability of critical slopes will be minor. However, the inherent stability of the slope is still under marginal ranges (less than 1.5); and the material properties and production scenario still have big uncertainties due to lack of information.

The Romanian sector of the Black Sea deserves attention because the Danube deep-sea fan is one of the largest sediment depositional systems worldwide and is considered the world's most isolated sea, the largest anoxic water body on the planet and a unique energy-rich sea. Due to the high sediment accumulation rate, presence of organic matter and anoxic conditions, the Black sea sediments offshore the Danube delta is rich in gas and explain the presence of BSR. The cartography of the BSR over the last 20 years, exhibits its widespread occurrence, indicative of extensive development of hydrate accumulations and a huge gas hydrate potential. By combining old and new datasets acquired in 2015 during the GHASS expedition, Riboulot *et al.*, 2017, performed a geomorphological analysis of the continental slope north-east

of the Danube canyon (also called Viteaz Canyon) compared with the spatial distribution of gas seeps in the water column and the predicted extent of the gas hydrate stability zone. This analysis provides new evidence of the role of geomorphological setting and gas hydrate extent in controlling the location of the observed gas emissions and gas flares in the water column. Gas flares are today considered an important source of the carbon budget of the oceans and, potentially, of the atmosphere.

The authors have detected 1409 active seeps within the 1200 km^2 of the shelf and slope north-east of the Danube canyon. Most of the gas seeps (96%) are not randomly distributed in this area. They occur along canyon flanks, scarps, crest lines, faults and in association with pockmarks and mounts. Moreover, the depth limit for 98% of the gas seeps coincides with the predicted landward termination of GHSZ. This suggests GHs formed at the base of the GHSZ act as an effective seal preventing gas to reach the seafloor and the water column. The extent and the dynamics of GHs have a probable impact on the sedimentary destabilization observed at the seafloor and the stability of the GHs is dependent on the salinity gradient through the sedimentary column and thus on the Black Sea recent geological history.

Zander *et al.*, 2017, after detailed analyses of the multiple BRSs conclude that they do not represent gas composition changes or over-pressured compartments, but reflect past pressure and temperature conditions. The modelling results suggest that temperature effects of rapid sediment deposition rather than bottom-water temperature change or sea level variations dominate the pressure and temperature conditions leading to the multiple BSRs. These changes are more distinctive in the Black Sea and especially in the Danube area because of the isolation of the Black Sea from the Mediterranean during sea level lowstands. Because hydrate dissociation may not occur for several thousands of years, such paleo BSRs remain well defined in seismic data. The authors propose that small amounts of free gas are present beneath each of the paleo BSRs. The gas saturation is high enough to cause an impedance contrast in seismic data, but low enough to inhibit buoyancy-driven upward migration. The paleo BSRs possibly reflect the real geotherm in the order of 35 ± 5° C/km, which is higher than the local geotherm of 24.5 ± 0.5° C/km derived from the shallowest (current) BSR. This also suggests that the Danube area is not in thermal steady state and still adapting to increasing bottom water temperatures since the last glacial maximum.

4. GAS FLARES, GAS SEEPS, GAS CHIMNEYS IN THE BLACK SEA

Gas flares in the water column have been recorded in over 5000 locations in the Black Sea and range from seeps related to deep seated mud volcanoes (Greinert *et al.*, 2006) to widespread seepage in water depths shallower than the upper limit of the gas hydrate stability zone (Egorov *et al.*, 2003, 2011; Naudts *et al.*, 2006; Römer *et al.*, 2012). The number of the seeps is of course more higher taking in account that only in a limited area of 1540 km^2 located in the transition zone between the continental shelf and slope of Dnieper Canyon, in water depths of 66 to 825m were detected on echosounding records.

More than 200 gas plumes have been documented along the shelf break of the north-western part of the Black Sea by a Simrad EA-500 acoustic survey (Fig. 6, Shnyukov, 1999; Kutas *et al.* 2004).

With the recent increasing interest in gas seeps, detection tools and methods have been developed and adapted to discover and investigate seep sites. In addition to echo sounder and high-resolution seismic recordings, multibeam and side-scan sonar have been used to detect gas seepage and shallow gas and also ROVs, submarines and CTDs have been used for ground truth, mapping and sampling sea-floor seeps. Recent work also paid attention to the sub-surface with a focus on seismic sub-bottom signatures and indications of shallow gas (acoustic turbidity, enhanced reflections, acoustic blanking, etc.) and possible conduits (faults, mud diapirs, etc.), which can be indirect indications for seepage at the sea floor (Naudts *et al.*, 2006).

4.1. Gas flares in the Romanian Western Black Sea

The north-western Black Sea is dominated by a rather wide shelf (60–200 km) with a shelf break at 120 to 170 m water depth and canyon systems with large deep-sea fan complexes, mainly developed during sea level lowstands (Winguth *et al.*, 2000; Popescu *et al.*, 2001).

The main canyon systems in the western Black Sea are the Danube and Dnieper Canyons, each with their own typical morphology. The Danube Canyon system and Danube deep see fan are well-studied (Popescu *et al.*, 2001, 2004, 2006, 2007, Winguth *et al.*, 2000, Ion *et al.*, 2002, Wong *et al.*, 1997, Lüdmann *et al.*, 2007, Zillmer et al, 2005, Zander, 2017, Riboulot *et al.*, 2017, Hillman et al, 2018).

On the shelf, the highest concentration of seeps is found in elongated depressions (pockmarks) above the margins of filled channels. On the continental slope where no pockmarks have been observed, seepage occurs along crests of sedimentary ridges. There, seepage is focussed by a parallel-stratified sediment cover that thins out towards the ridge crests. On the slope, seepage also appears in the vicinity of canyons (bottom, flanks and margins) or near the scarps of submarine landslides where mass-wasting breaches the fine-grained sediment cover that acts as a stratigraphic seal.

Upward migration of gas through the sedimentary column is typically associated with faults or lithological contacts, which facilitate the movement of gas and can be observed in seismic records as so called **gas chimneys,** characterized by chaotic seismic facies.

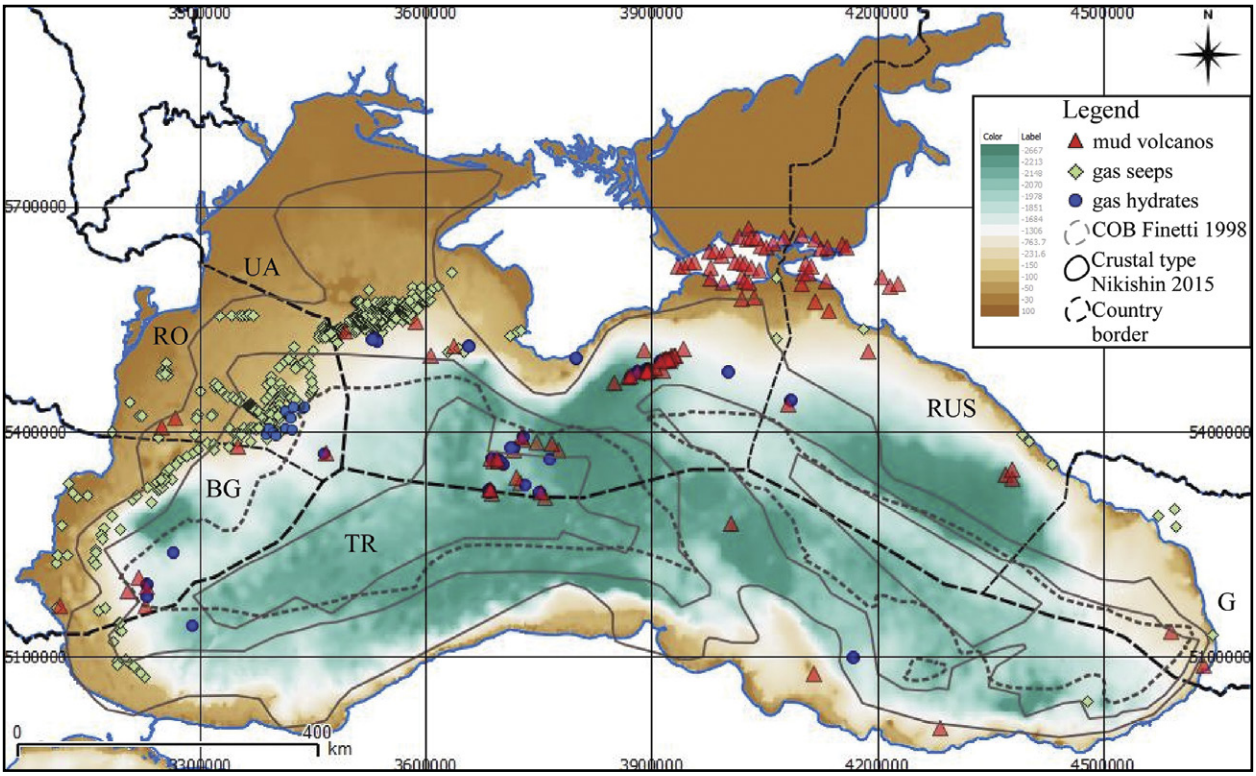

Fig. 6. Map of oil and gas seeps, gas hydrates and mud volcanos occurrences in the Black Sea. Compiled from: Tambrea, 2007, Egorov *et al.*, 2011, Kruglyakova *et al.*, 2004, Popescu *et al.*, 2006. DEM extracted from GEBCO (Crustal types after Nikishin *et al.*, 2015a and Finetti *et al.*, 1988. Note that Romanian offshore is located according with Nikishin *et al.*,2015 on the continental and stretch continental crust, and at the transition to oceanic crust according with Finetti *et al.*, 1988. **BG** – Bulgaria, **G** – Georgia, **RO** – Romania, **RUS** – Russia, **TR** – Turkey, **UA** – Ukraine.

Gas chimneys are defined as an area of gas migrating upwards from a gas accumulation at depth. Gas chimneys act as conduits for vertical migration of fluid and/or gas and can be imaged in seismic data as anomalies characterized by distorted reflections and low velocities caused by incoherent scattering, absorption and poor stacking due to nonhyperbolic normal moveout (NMO) (Karstens & Berndt, 2015 and references therein).

Gas chimneys are common in the Black Sea. On the inner shelf these features tend to terminate against a major unconformity which is interpreted as Oligocene to Upper Miocene in age (Gillet *et al.*, 2003; Popescu *et al.*, 2007). On the outer shelf these chimneys may reach the seafloor, resulting in active venting and gas flare formation at the seafloor (Ion *et al.*, 2002, Popescu *et al.*, 2007). This is thought to be a function of the permeability of the base of the Miocene sediments, and may also be related to increased gas supply by some chimneys associated with known hydrocarbon fields (Popescu *et al.*, 2007).

It has been suggested that flares in the Black Sea may be aligned along faults as such structural features commonly act as conduits for fluid and/or gas flow (Popescu *et al.*, 2007, Lüdmann *et al.*, 2007, Fig. 13). In many cases, there appears to be a direct correlation, based on seismic observations, between the distribution of faults and the occurrence of flares. However, they are also observed in the absence of fault systems, frequently in the vicinity of submarine slope failures and canyons (Kutas *et al.*, 2004; Starostenko *et al.*, 2004), or they can be aligned along the crest of submarine ridges (Naudts *et al.*, 2006).

Methane escapes into the water column are observed at numerous sites in the coastal areas and along the shelf-break, but also in areas within the GHSZ, i.e. deeper than 720 m water depth, and at mud volcanoes in the deep basins (Fig. 6).

Many studies were elaborated about the gas flares in the Romanian area of continental margin of Western Black Sea, following the international and Romanian cruises in the period 2001 – 2017.

Popescu *et al.*, 2007 present the results obtained using high-resolution reflection seismic data from two seismic sources: GI gun (central frequency 70 Hz) and mini-GI gun (central frequency 150 Hz). The data have been acquired during the BlaSON surveys of IFREMER and GeoEcoMar (1998 and 2002). Additionally for investigating the shallow sediments, the 3.5-kHz sub-bottom profiler was used by GeoEcoMar in 1979–1983 across the Romanian Shelf (Fig. 7).

The presence of free gas in sediments significantly affects the acoustic properties of the sub-bottom records and creates a variety of seismic gas signatures. The study reveals

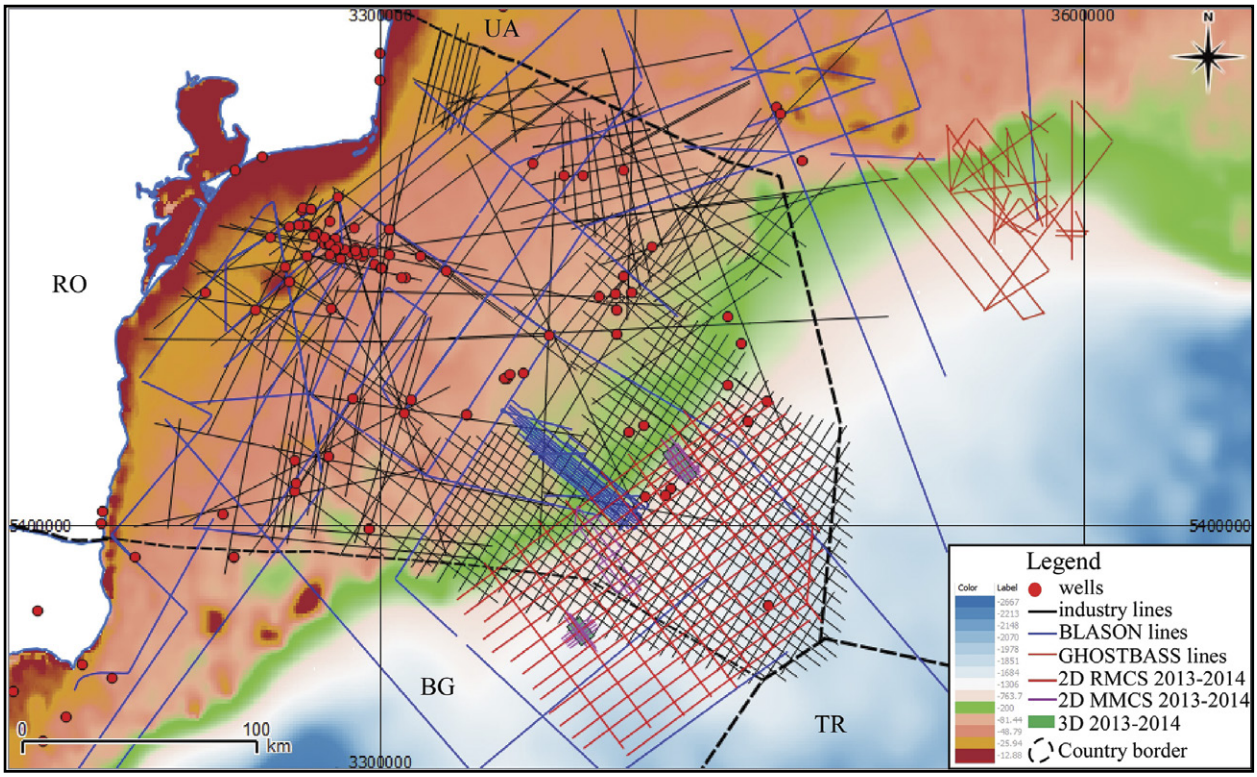

Fig. 7. Location of seismic profiles across the Western Black Sea. **BG** – Bulgaria, **RO** – Romania, **TR** – Turkey, **UA** – Ukraine.

widespread occurrences of these types of seismic facies in the recent sediments of the Black Sea. Most commonly, free gas dispersed in sediment scatters acoustic energy, resulting in a variable degree of disturbance of the seismic reflections. This effect is usually described as "acoustic turbidity".

Turbidity often fades out to areas of complete "wipeout" where sediments appear to be acoustically impenetrable (Figs. 8 and 11), in relation to high gas content. Extensive areas are marked by a succession of strong "multiples" both on high-resolution data (Fig. 8) and on higher-frequency sub-bottom profiles. Repetition of the seafloor reflection is caused by very gassy sediment layers located close to the seafloor. Columnar disturbances by upward fluid migration disrupt the normal sequence of seismic reflections (Figs. 9 and 10). The disturbances originate from a source deeper than the penetration limit of our profiles (ca. 2 s), and either reach the seafloor or terminate within the sediment layers (Popescu *et al.*, 2007). These disturbances appear most often as narrow pipes, described elsewhere as "acoustic columns" or "acoustic chimneys" (*e.g.* Garcia-Gil *et al.* 2002).

Locally, columns occur in association with wider, turbid "acoustic curtains" with irregular tops (Fig. 10) usually up to 100 m high on the continental shelf. Acoustic plumes commonly correspond to areas where acoustic columns or turbidity reaches the seafloor (Fig. 9). At some places, alignments of seeps follow the direction of recent faults, with gas escape clearly originating from the fault displacement (Fig. 11a).

Discussing about the distribution of the gas facies, Popescu *et al.*, 2007 separated a **shallow gas facies** and **a deep gas facies.**

Shallow gas facies

Two major gas accumulation areas occur in the shallow sediments of the western Black Sea. The first shallow gas zone is located along the coast, whereas the second one lines up along the shelf break (Fig. 13). The seismic data from these areas are characterized by repeated multiples, associated with acoustic turbidity, wipeouts and enhanced reflections, masking almost completely the structure of the sedimentary systems (Fig. 9).

First shallow gas zone is widespread up to 1.3–4 ms (1–3 m) beneath the seafloor and it is located close to the Danube delta, corresponding to the Danube delta front and the inner prodelta (Fig. 13). This gas zone extends southwards following the direction of the present-day coastal drift current. The coastal drift current is associated with the Danube and Dnieper rivers, and is restricted to a quite narrow coastal zone (Panin&Jipa, 2002).

The second shallow gas zone accumulation is developed along the shelf break, including the outer shelf and the upper slope down to ca. 750 m water-depth. Gas occurrences follow the shelf break all along the western Black Sea basin in a band with variable width, from 3 km in front of the Bulgarian coast to ca. 50 km on the northern Romanian shelf (Fig. 13). The gas front is relatively flat and close to the seafloor (ca.

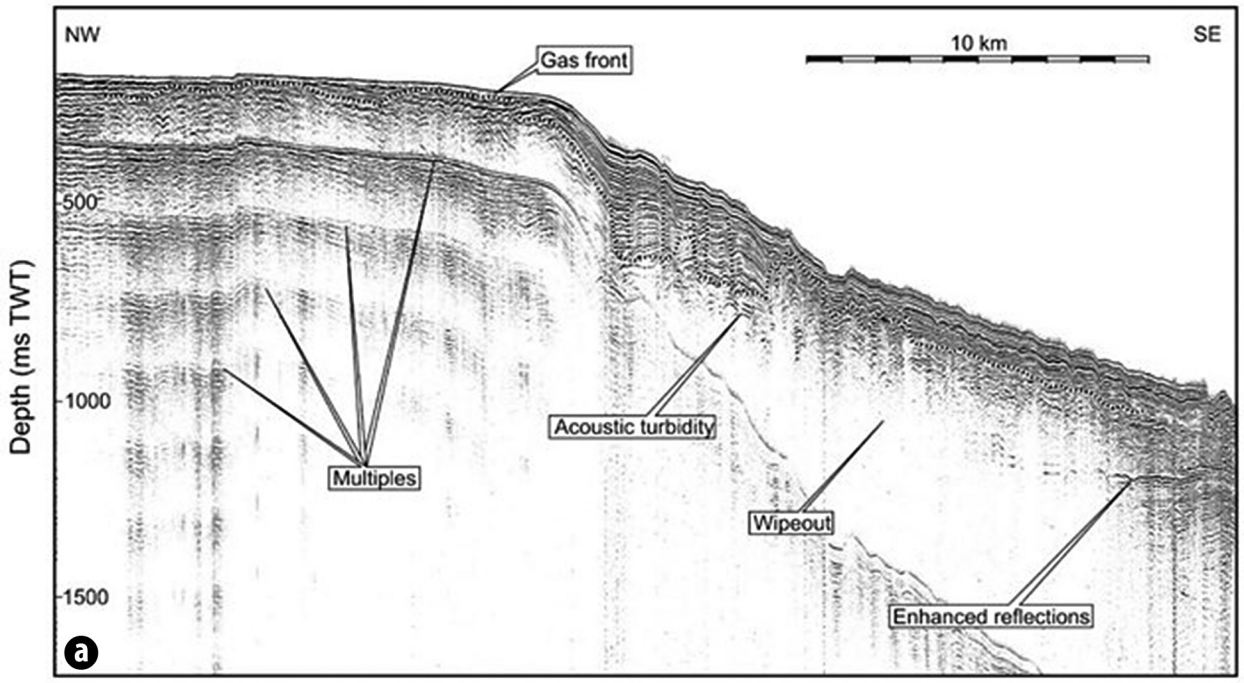

Fig. 8. Gas-related seismic facies in the western Black Sea: multiples, acoustic turbidity, wipeout, enhanced reflections. Part of high-resolution reflection seismic profile b008. (location of the profiles is shown in Fig. 12) (Popescu *et al.*, 2007).

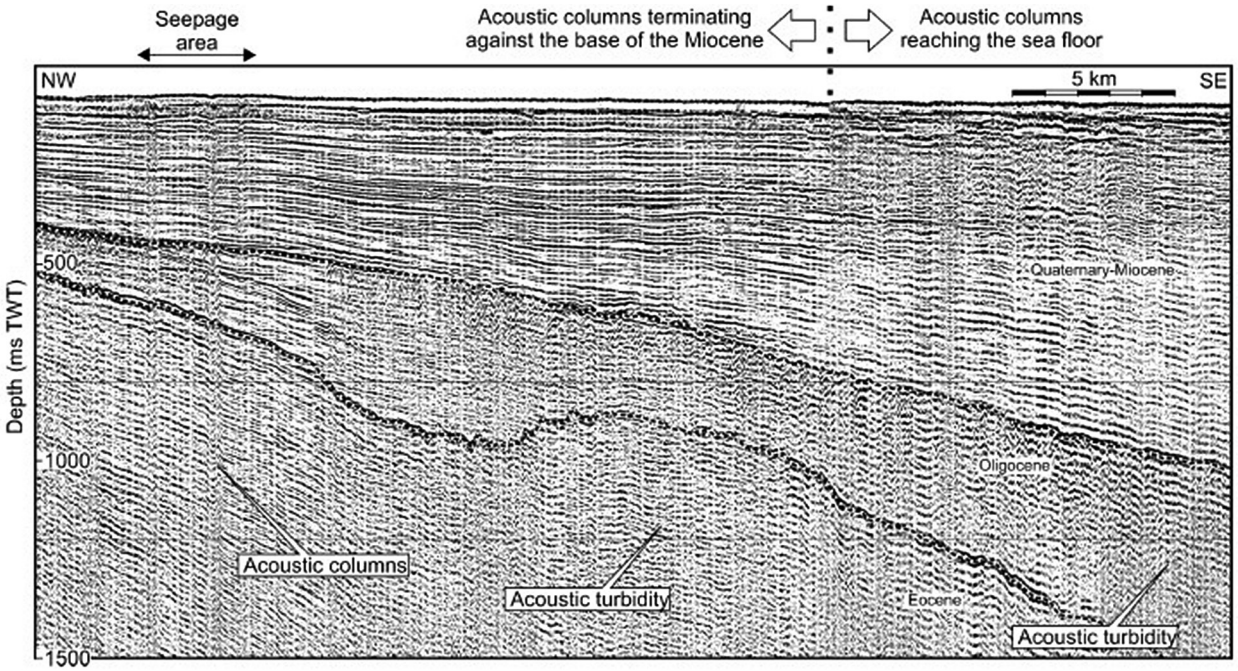

Fig. 9. Gas-related seismic facies in the western Black Sea: acoustic columns, acoustic turbidity. The figure shows part of high-resolution reflection seismic profile b038-GI, location in Fig. 12. Acoustic columns reach the seafloor on the outer shelf (right part of figure), whereas on the inner shelf they usually terminate against the regional Oligocene/Miocene unconformity. Locally, acoustic columns on the inner shelf may, however, penetrate this surface and rise up to the seafloor, in areas, which correspond with gas seepage. Stratigraphic limits are from Gillet (2004) (Popescu *et al.*, 2007).

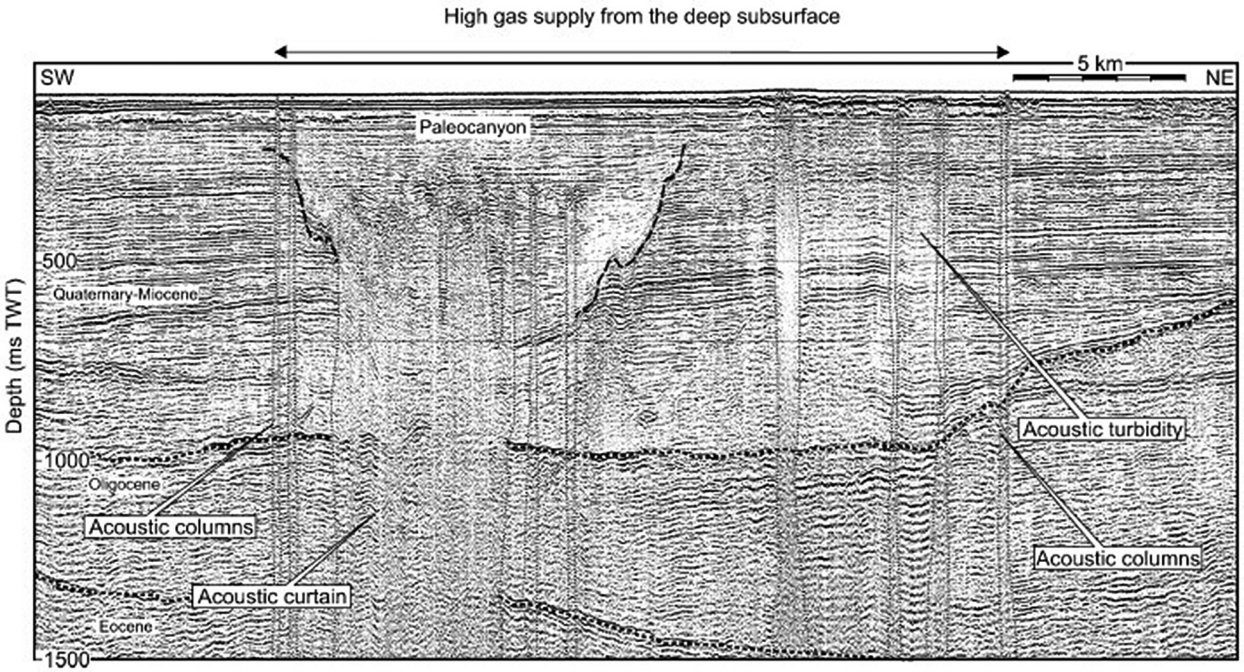

Fig. 10. Gas-related seismic facies in the western Black Sea: acoustic columns, acoustic curtains, acoustic turbidity. The figure shows part of high-resolution reflection seismic profile b005 (location in Fig. 12). Areas with particularly high gas supply from the deep subsurface often coincide with the location of major palaeo-canyons (Popescu *et al.*2007).

20–40 ms/15–30 m depth) on the outer shelf, and becomes more irregular and deeper (up to 300 ms/ca. 220 m) on the upper slope. Gas accumulations in this setting represent the most prolific gas seeping areas across the western Black Sea (Fig. 13).

Deep gas

Acoustic columns occur ubiquitously on the western Black Sea shelf on high-resolution reflection seismic data (Fig. 9). Two distinct settings can be distinguished:

(1) The inner shelf, where most of the columns terminate upwards against a major unconformity interpreted previously as the limit between the Oligocene and the Middle-Upper Miocene (Badenian- Sarmatian; see Gillet *et al.,* 2003; Gillet, 2004) and

(2) The outer shelf, where columns penetrate this stratigraphic surface and reach the seafloor (Fig. 9).

The gas migration is a function of the permeability of the base of the Miocene sediments. Several patches of columns reaching the seafloor occur inside the zone with buried columns, possibly in relation with higher gas supply, and often correspond to gas seeps at the seafloor (Figs. 8 and 13). Some of these areas are situated above known deep oil and gas fields such as Lebada, Ana, Doina, Cobalcescu, etc. (Fig. 13). Wider areas of deep gas coincide usually with the location of major palaeo-canyons buried in the Plio-Quaternary deposits of the north-western Black Sea shelf (Fig. 10). However, gas supply does not originate in the canyon fill, but the canyons seem to be located in the fracture zones with a stronger gas supply. The modern Danube Canyon also developed along a narrow zone with subsurface gas and a seepage alignment (Fig. 13; Popescu *et al.,* 2004). The results are in agreement with previous studies that have suggested vertical gas migration along faults or more permeable paths from the deeper sediments of the Black Sea (Ion *et al.,* 2002; Kutas *et al.,* 2004). Another indication of deep gas is the alignment of gas seeps along major faults, such as Peceneaga-Camena (Popescu *et al.,* 2004; Fig. 13) and the Kalamit Ridge bounding fault zone (Peckmann *et al.,* 2001).

A deep gas supply was demonstrated in the central Black Sea at 2000 m water depth, where mud volcanoes occur in association with gas venting and pockmarks (Ivanov *et al.*1996; Limonov *et al.* 1997, Fig. 6).

Discussing about **gas origin** we can conclude that the most of the geochemical studies of core and drilling samples from the Western Black Sea have indicated that gas in sediments is mainly methane of biogenic origin (Hunt, 1974; Ross *et al.,* 1978; Ivanov *et al.,* 1983, 2002; Dimitrov, 2002; Neretin *et al.,* 2004). However, the presence of higher hydrocarbons and methane isotope signatures indicating a contribution of thermogenic gas have been reported from the mud volcanoes in the central Black Sea (Limonov *et al.,* 1997). Coastal gas accumulations have a shallow sub-bottom depth and they are located in areas currently characterized by high depositional rates associated with the organic-rich sediment input from the Danube River. Isotopic compositions of methane sampled from near-surface sediments from this zone have indicated a microbial origin (Ivanov *et al.,* 1983, 2002). We thus conclude

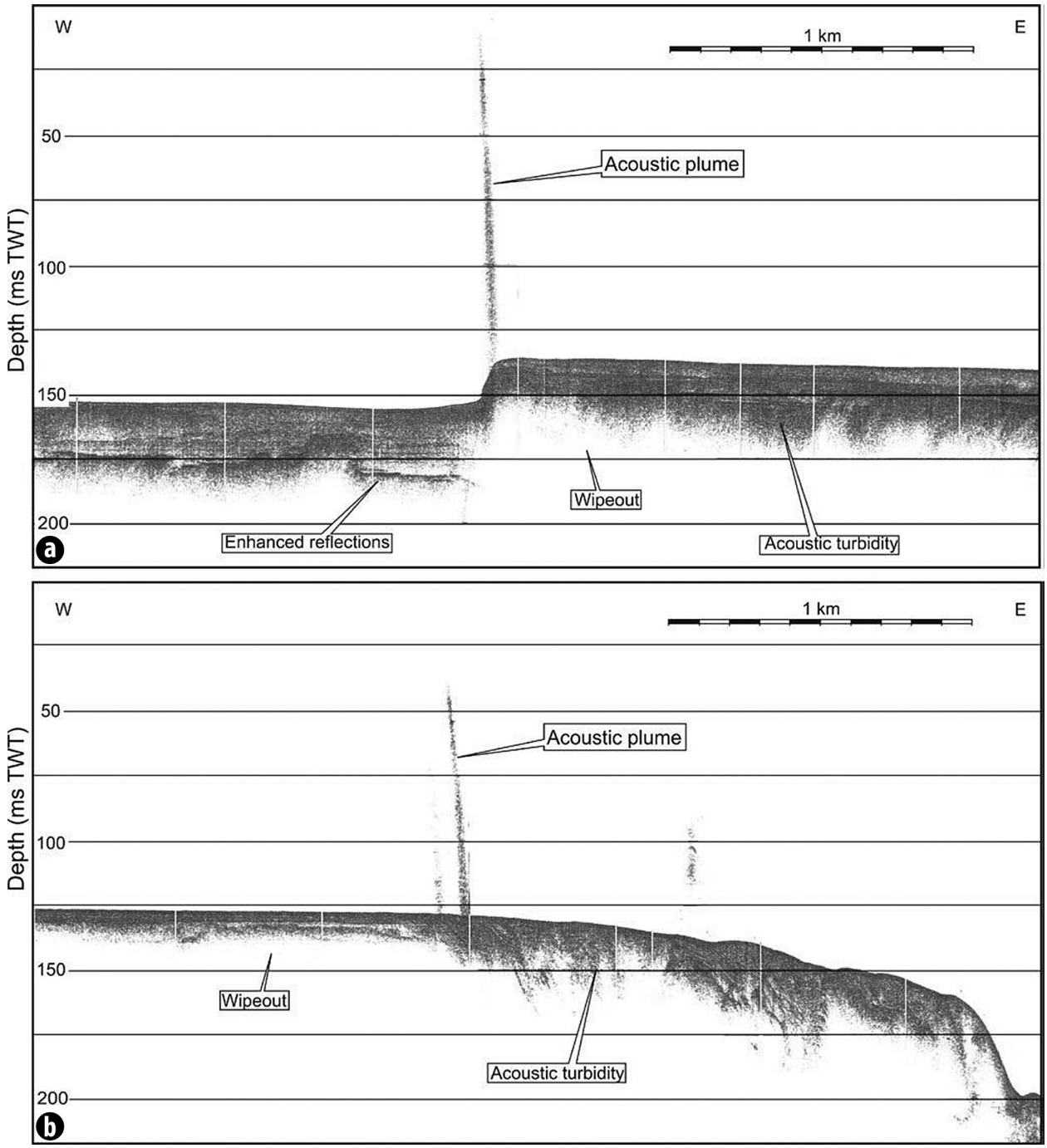

Fig. 11. Gas-related seismic facies in the western Black Sea: acoustic plumes, acoustic turbidity, wipeouts, enhanced reflections. The location of the profiles is shown in Fig. 12. (**a**) Part of 3.5-kHz subbottom profile 4/82. The acoustic plume originates from an active fault visible at the seafloor. (**b**) Part of 3.5-kHz sub-bottom profile 5/82. The acoustic plumes are located near the head of the modern Danube canyon, but outside the main erosional canyon trough (Popescu *et al.*, 2007).

that the source of this gas is most probably related to in situ degradation of high amounts of organic matter contained in river-supplied sediments (Popescu *et al.*, 2007).

Gas from the shelfbreak area is mainly methane (Michaelis *et al.,* 2002), and was proposed to derive from organic-rich sediments with a possible contribution of thermogenic gas (Peckmann *et al.* 2001). The shallow gas accumulations along the shelfbreak are likely to represent the lowstand equivalent of the coastal gas area. However, gas derived from in situ organic-rich palaeo-coastal sediments may coexist with gas migrating from the deeper subsurface, as suggested by the wide occurrence of upward gas migration on the rest of the shelf, and by the preferential location of gas seeps and subbottom gas along deep fault directions (Popescu *et al.*, 2007).

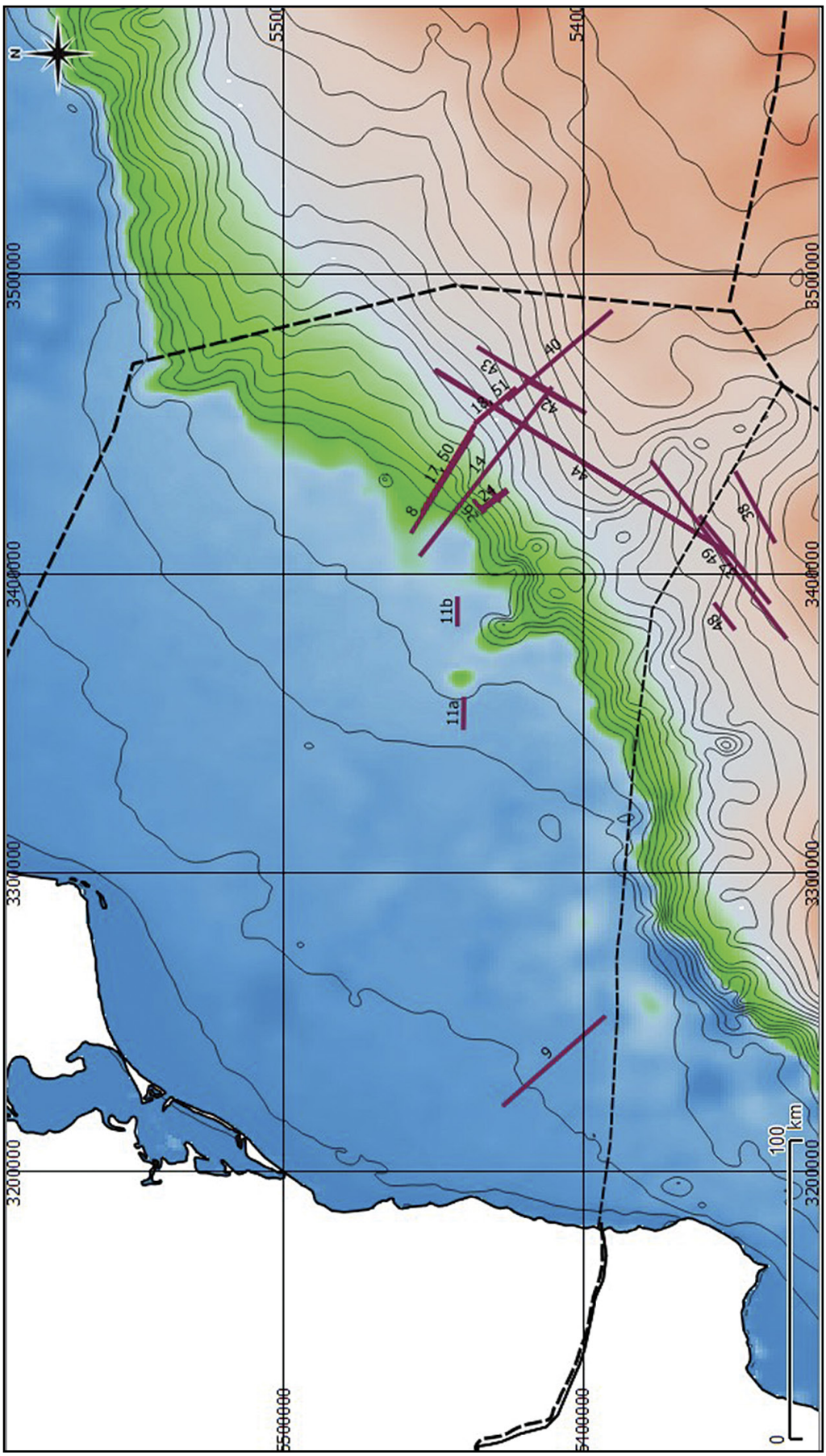

Fig. 12. Map showing the localization of the 2D profiles explained in text that have been used by different authors in their studies for the gas and gas related structures.

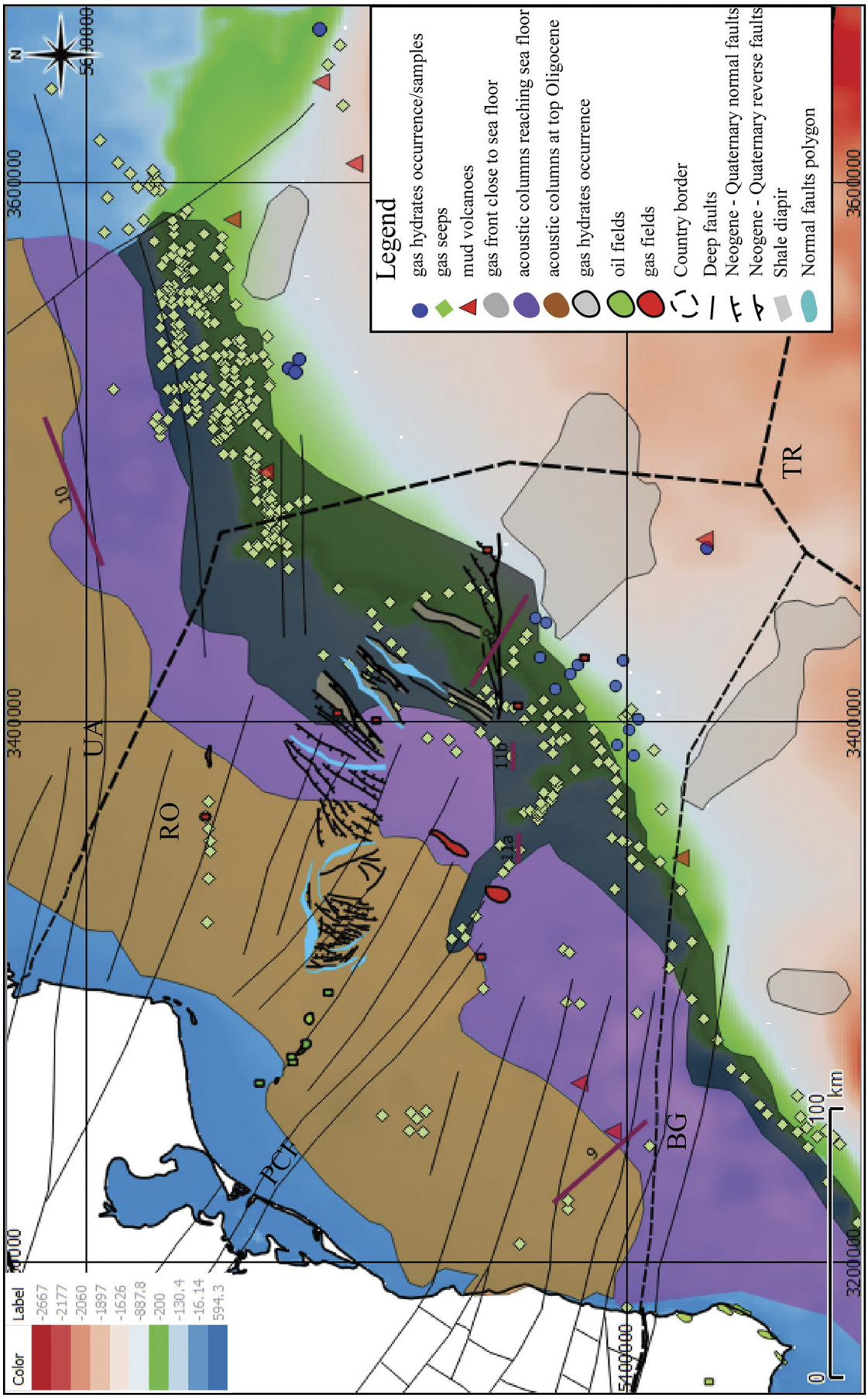

Fig. 13. Distribution of the gas-related seismic facies and BSRs in the Western Black Sea (redraw after Popescu *et al.*, 2007 and reference therein) and updated with information from Tambrea, 2007, Egorov *et al.*, 2011, Kruglyakova *et al.*, 2004. Deep seated faults after Dinu *et al.*, 2005; Neogene-Quaternary faults after Tambrea, 2007; **PCF** – Peceneaga Camena Fault; **BG** – Bulgaria; **RO** – Romania; **TR** – Turkey; **UA** – Ukraine.

Upward gas migration from a deep source is common on the western Black Sea shelf. This area is known to contain hydrocarbon fields (Fig. 13), some of which produce oil (Lebada, Sinoe) and gas condensate (Gallitzin). The main regional hydrocarbon source is the Maikopian facies.

The gas seeps concentrated on the shelf edge off Romania could be related to gas content in the subsurface layers. Profile 33 shows extensive acoustic masking due to free gas (Fig. 14). These gas accumulations may originate from gas, which migrated unhampered through channel-levees of the older sequences 3-4 because they are situated below the BGHSZ. The gas could therefore follow the up-ward dip of the channel-levee to the break point of the shelf edge, where the layers become horizontal (Fig. 14, grey arrows). This process may have also played an important role when, after flooding of the Black Sea, the GHSZ started to shrink and gas hydrate dissociation produced a large amount of free gas. Part of this gas may have formed new gas hydrates, but may have also migrated farther upslope to the shelf break where the channel-levees terminate. This process might still be continuing because the present BGSZ has not yet reached thermal equilibrium. At the shelf edge, a vertical gas flux as indicated in Fig. 8 (grey arrows) could not be excluded; here, faults may provide additional pathways.

In the Romanian sector, the free gas flux is controlled by the specific lithostratigrahy of the channel-levee system of the Danube River. The coarse channel deposits provide excellent migration paths and the low-permeability condensed sections overlying the channel-levees and the GSHZ function as a perfect seal. In addition, numerous faults in this area allow the ascent of thermogenic gas from deeply-buried oil-bearing sub bottom layers into the channels of the deep-sea fan system.

Riboulot *et al.,* 2017, consider that gas flares are today an important source of the carbon budget of the oceans and, potentially, of the atmosphere.

The study is based on the analysis of bathymetry and water column acoustic data acquired during the 2015 GHASS cruise on board the R/V Pourquoi Pass, High-resolution reflection seismic data were acquired during the 1998 BLASON and 2002 BLASON2 surveys of IFREMER and GeoEcoMar (Figs. 15 and 16).

The continental slope morphology of the Romanian sector of the Black Sea is affected by several landslides inside and outside canyons. It is a complex study area presenting sedimentary processes such as seafloor erosion and instability, mass wasting, formation of GHs, fluid migration, gas escape, where the imprint of geomorphology and local lithology seem to dictate the location where gas seep occurs (Fig. 15). The authors have detected 1409 active seeps within the 1200 km^2 of the shelf and slope north-east of the Danube canyon. Most gas seeps (96%) are not randomly distributed in this area. They occur along canyon flanks, scarps, crest lines, faults and in association with pockmarks and mounts. Moreover, the depth limit for 98% of the gas seeps coincides with the predicted landward termination of GHSZ. This suggests GHs formed at the base of the GHSZ act as an effective seal preventing gas to reach the seafloor and the water column.

The seepage activity does not appear homogenous, as the density of gas flares varies with bathymetry and laterally. Many of the numerous and widespread gas flares that were recorded at the scale of the Romanian sector of the Black Sea reach several hundreds of meters above the seafloor, attesting to a vigorous seepage activity with high fluid fluxes. Gas emissions may be particularly numerous within some sectors between 200 m and 800m. No gas flares were detected in deeper areas. Gas emissions can be classified into 6 groups based on their distribution and origin:

(1) Non-random gas seeps along the canyons/gullies;
(2) Non-random gas seeps along headwall scarps and lateral margin of the mass transport complexes (MTC);
(3) Non-random gas seeps along fault/ crest line;
(4) Non-random gas seeps at the landward termination of the GHSZ above small mounts;
(5) Non- random gas seeps right above pockmarks;
(6) Other random gas seeps (Figs.10, 13).

Evidence of free gas in seismic data. The 2D seismic profiles show a relatively well-preserved sedimentary stratification (Figs. 17 and 18). Seismic facies is dominated by high amplitude parallel seismic reflectors. From the shelf down to the slope, a MTC is identified buried under 40 m of sediment. The source area of the MTC is delimited to the north in about 200 m water depth by the shelf edge. The MTC is characterized by a transparent chaotic seismic facies. The thickness of the mass deposit, about 20 m at 300 m water depth, progressively increases seawards to attain 75 m at 700 m water depth. The thickness is not homogeneous and varies in function of the inherited relief. The compressional domain of the MTC show many bulges draped by overlying sediment resulting from the presence of small mounts at the seafloor.

Under the MTC, the seismic signature of sediment shows anomalies interpreted as the localized accumulation of free gas. In marine sediments, free gas often yields anomalous seismic signatures, making seismic methods a useful tool for the identification and characterization of the sub-seafloor gas charged body and the gas migrating system.

Overall, the distribution of gas flares observed in the water column of the study area are in agreement with the free gas areas defined in Popescu *et al.,* (2007). However, in some cases, several gas flares are detected downward the areas defined in the literature: many gas flares are inside the BSR zone defined in (Popescu *et al.*, 2006) close to the landward termination of the BSR (Figs. 19).

The distribution of the gas seeps in the Romanian sector of the Black Sea coincides in most cases with the presence at the seafloor of sediment deformation features. 96% of the gas flares are located above canyons, landslides, pockmarks, and fault/crest line. Studies about the geomorphological

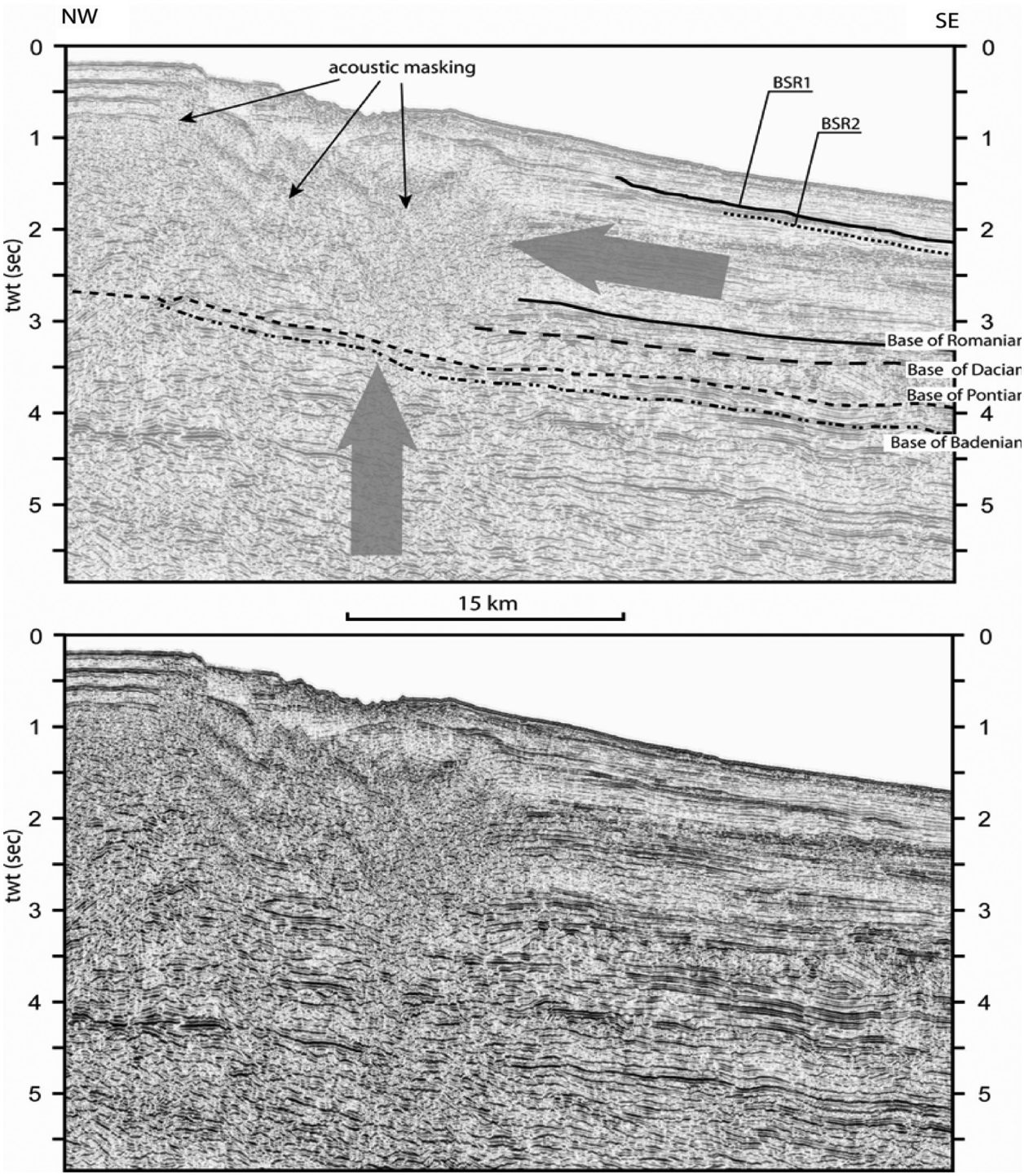

Fig. 14. Part of profile 33, which shows areas of gas accumulation near the shelf edge indicated by extensive acoustic masking. Grey arrows show possible migration paths of free gas (location in Fig. 12) (Lüdmann *et al.*, 2007).

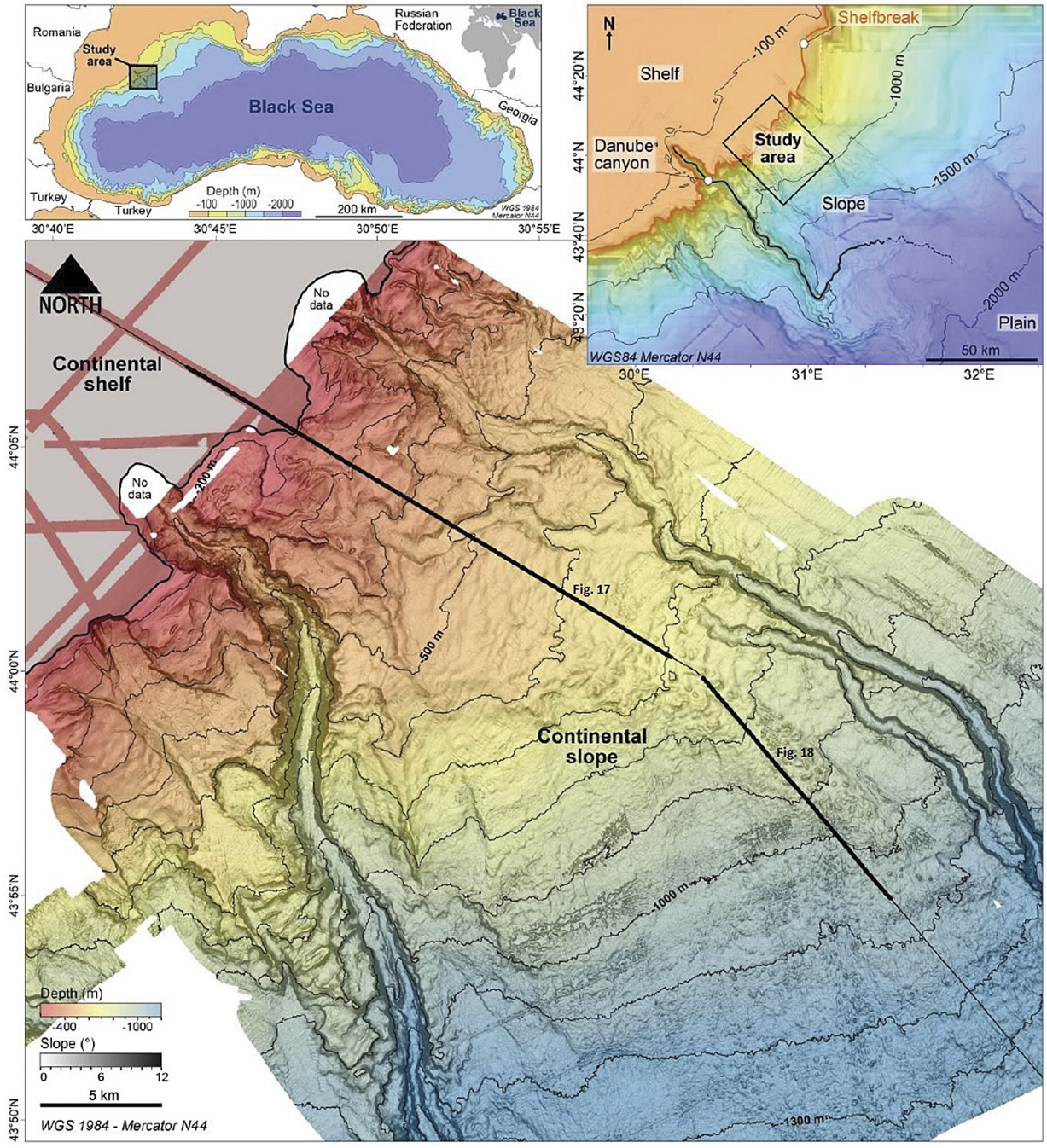

Fig. 15. Bathymetric map, acquired during the 2015 GHASS cruise, showing the study area with the location of seismic profiles. The continental slope is dissected by several canyons, including Danube canyon with several submarine landslide scars along canyon flanks (Riboulot *et al.*, 2017).

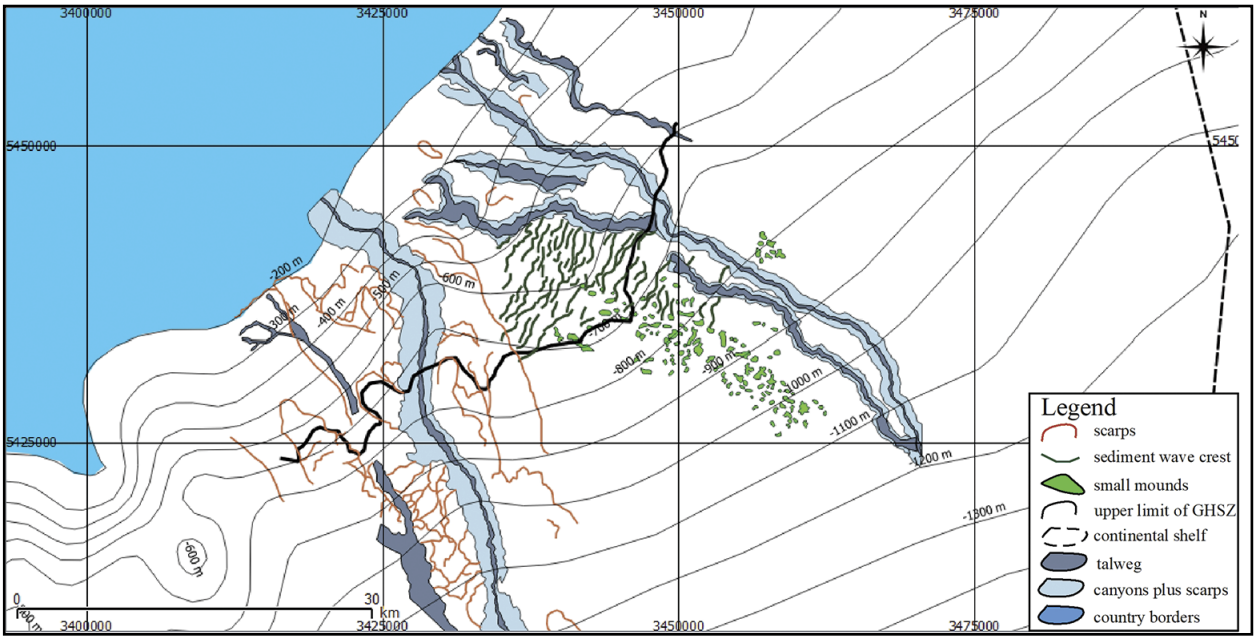

Fig. 16. Geomorphologic map of the study area of the Romanian Black Sea slope (Riboulot *et al.*, 2017).

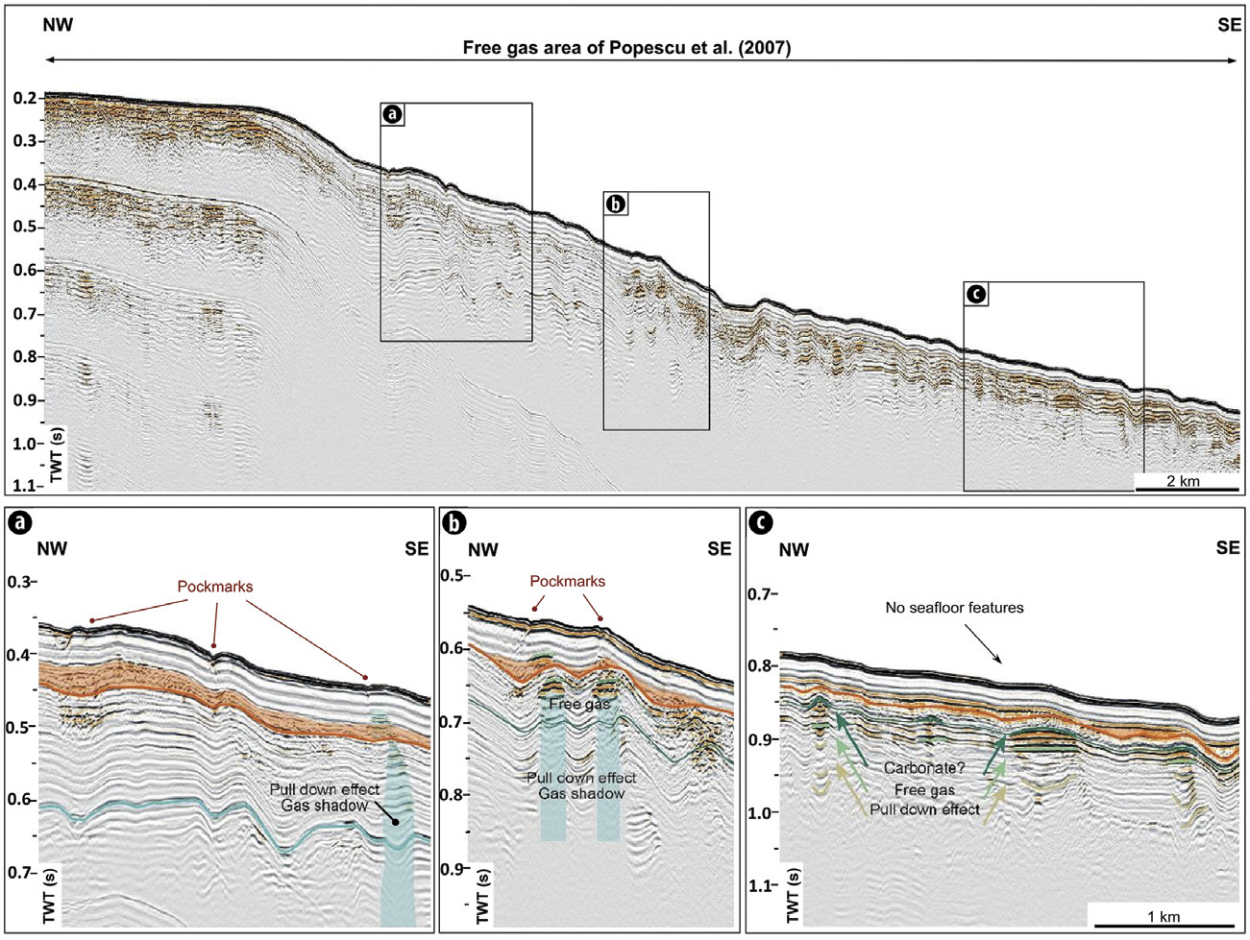

Fig. 17. Seismic reflection profile BlaSON 1-8 (BLASON cruise). Across the shelf break and the upper slope within the free gas area defined in Popescu *et al.* (2007; location in Fig. 12). The close up views (**A**, **B** and **C**) show how the occurrence of free gas affects seismic data. The most apparent free gas zones are identified under a mass transport complex (in orange). Several free gas zones coincide with the presence of gas chimneys and pockmarks (**A** and **B**) while when the seafloor depth is deeper we have a lack of seafloor fluid features. The gas seems to be trapped under the MTC (Riboulot *et al.*, 2017).

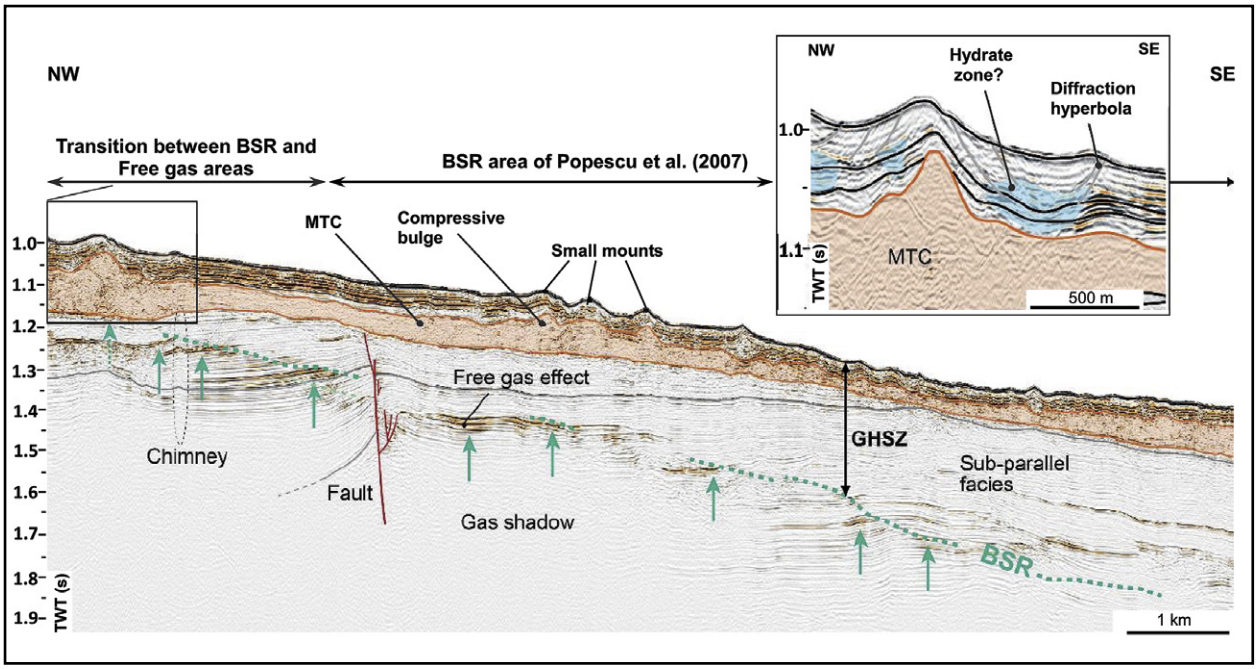

Fig. 18. Seismic reflection profile BlaSON 1-7 (BLASON cruise): across the slope partly within the BSR area defined in Popescu *et al.* (2006; location in Fig. 9). The presence of a BSR is suggested by a strong and negative polarity reflector associated to an increase in the attenuation and amplitude anomalies (seismic signature of the free gas – green arrows). Within the predicted GHSZ, right above the BSR, we do not observed seismic signature of the presence of free gas. The free gas seems to be trapped under the MTC. The black rectangle indicates the area of inset. The inset highlights the location of the supposed GH occurrence within deformed sedimentary layers at the landward termination of the BSR (Riboulot *et al.*, 2017).

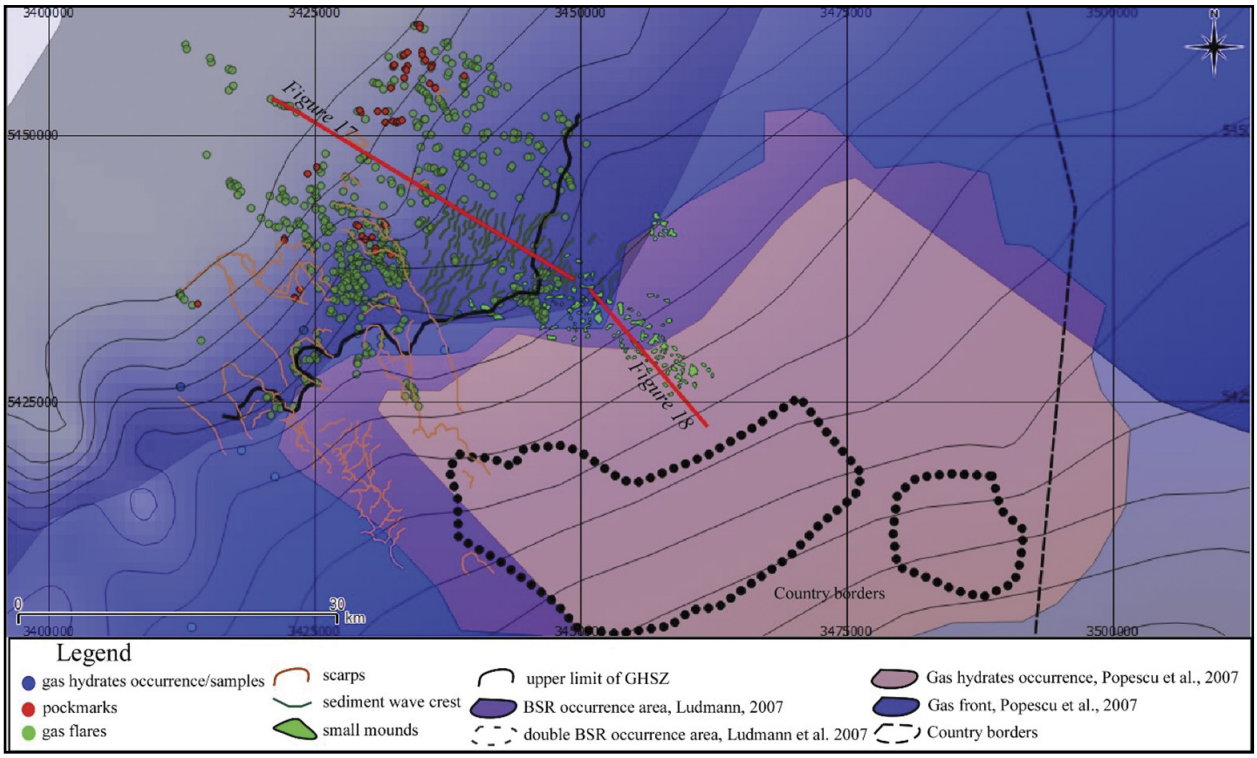

Fig. 19. Bathymetric map of the study area with superimposed, geomorphological features/zones, (**2**) limits of the GHSZ and (**3**) presence of measured gas bubbles in the water column and GH and BSR occurrence (Popescu *et al.*, 2007; Lüdaman *et al.*, 2007; Riboulot *et al.*, 2017).

control of the distribution of gas seepages finally show they follow the same pattern as the control of the distribution of pockmarks. Studies published during the last 20 years have demonstrated that the spatial organization of pockmarks (seafloor deformation due to fluid expulsion) may be the result of fluid seepage from underlying sedimentary structures such as fault systems, channels, mud volcanoes, mud diapirs, glaciogenic deposit, and mass transport deposits.

The extent and the dynamics of GHs have a probable impact on the sedimentary destabilization observed at the seafloor and the stability of the GHs is dependent on the salinity gradient through the sedimentary column and thus on the Black Sea recent geological history.

Hillman *et al.*, 2018, based on seismic data acquired during the R/V Maria S. Merian (MSM34) cruise of 2013–2014, produced a study concerning the gas migration pathways in the Danube Fan, in an area comprising Danube Canyon and two others smaller canyons, defined like S2 and S3 (Fig. 20). The purpose of the study is to demonstrate that there are several settings that are conducive to gas migration in the region, including lithological contacts acting as flow pathways and vertical gas migration structures, or gas chimneys. The precise mechanisms by which gas migrates from depth to reach the seafloor in the Danube Fan are still poorly understood. Understanding shallow gas migration and the potential relationship with the hydrate system in this region is of interest for offshore hydrocarbon exploration due to the potential hazard of shallow gas accumulations when drilling, and also the possible connection to submarine slope failures which pose a risk to seafloor infrastructure.

Upward migration of gas through the sedimentary column is typically associated with structural or lithological contacts, which facilitate the movement of gas and can be imaged in seismic data as so called gas chimneys.

There are several factors that may play a role in controlling the migration of gas through the sediments. The formation of gas chimneys and other vertical fluid flow anomalies is generally controlled by (Hillman *et al.*, 2018):

(1) Overpressure - induced hydro-fracturing of overlying deposits;
(2) High-permeability sediments;
(3) Faulting and deformation;
(4) Lithological heterogeneity and upper layers overpressure which play an important role in lateral gas migration.

Several of the flares were observed during multiple crossings. Gas flares are abundant near the S2 Canyon and S2 slump, with several gas flares imaged along the headwall and sidewalls of the S2 slump (Figs. 20 and 21).

Migration of gas

Evidence of gas migration through the sedimentary column can be observed in seismic data as enhanced amplitude seismic reflections associated with the presence of free gas in sediments which scatters acoustic energy, resulting in the disturbance of seismic reflections, an effect known as acoustic turbidity (Judd & Hovland, 2007; Popescu *et al.*, 2007). Where gas content is high, turbidity may fade out to complete 'blanking' where sediments appear to be acoustically impenetrable (Popescu *et al.*, 2007). Such features are commonly associated with anomalously high-amplitude enhanced reflections or bright spots, which result from high concentrations of free gas trapped in the sediments.

Previous studies show that the Danube Canyon is located above the presumed offshore position of the Peceneaga-Camena fault, a feature which could act as a migration pathway for gas (Popescu *et al.*, 2004; Winguth *et al.*, 2000). The seismic data acquired during the cruise MSM34 show several amplitude anomalies that are interpreted as potential gas migration pathways. They are subdivided into migration pathways related to lithology, and gas chimney-like structures.

Migration pathways related to lithology. In the vicinity of the S2 slump the BSR is closer to the seafloor than in adjacent areas, although the BSR does not actually intersect the seafloor in the seismic data (Figs. 23 and 24). In this area, the BSR appears to approach the base of the chaotic, deformed strata (MTD 4) beneath the S2 slump (Fig. 24). Beneath the S2 Canyon, the BSR is clearly defined by the termination of several high amplitude reflections, with patches of enhanced amplitudes along the BSR and in the sediments underlying the S2 slump. Several of these high amplitude reflection packages near the seafloor underlie the southwestern sidewall of the S2 slump (Fig. 25), and correlate with the position of observed flares at the seafloor. In the levee sediments to the northeast of the S2 Canyon, there are two high amplitude horizons; at the base of the package of well-laminated near seafloor sediments, and within a unit characterized by relatively seismically transparent facies (Fig. 23). These two horizons are truncated along the canyon wall and correlate with the position of flares observed during the MSM34 cruise. A similar relationship is observed further to the northeast along the canyon (Hillman *et al.*, 2018).

Gas migration structures

Gas migration structures are abundant in the vicinity of the S2 Canyon and the surrounding sediments of the Danube Fan, occurring at water depths of<700 m. Where these structures reach the seafloor, they correspond to observed gas flares in the water column. Hillman *et al.*, 2018 classified the structures into three groups based on their seismic characteristics, size, and geometry. Groups A and B are more reminiscent of true gas chimneys at varying scales and complexities, whereas Group C contains anomalous gas accumulations and features related to MTDs.

The location of these structures appears to be controlled by:

(a) Overlying units acting as seals,
(b) Variations in lithology across heterogeneous sediments (particularly MTDs),
(c) Intermittent/gradual gas supply leading to the development of stacked accumulations of gas.

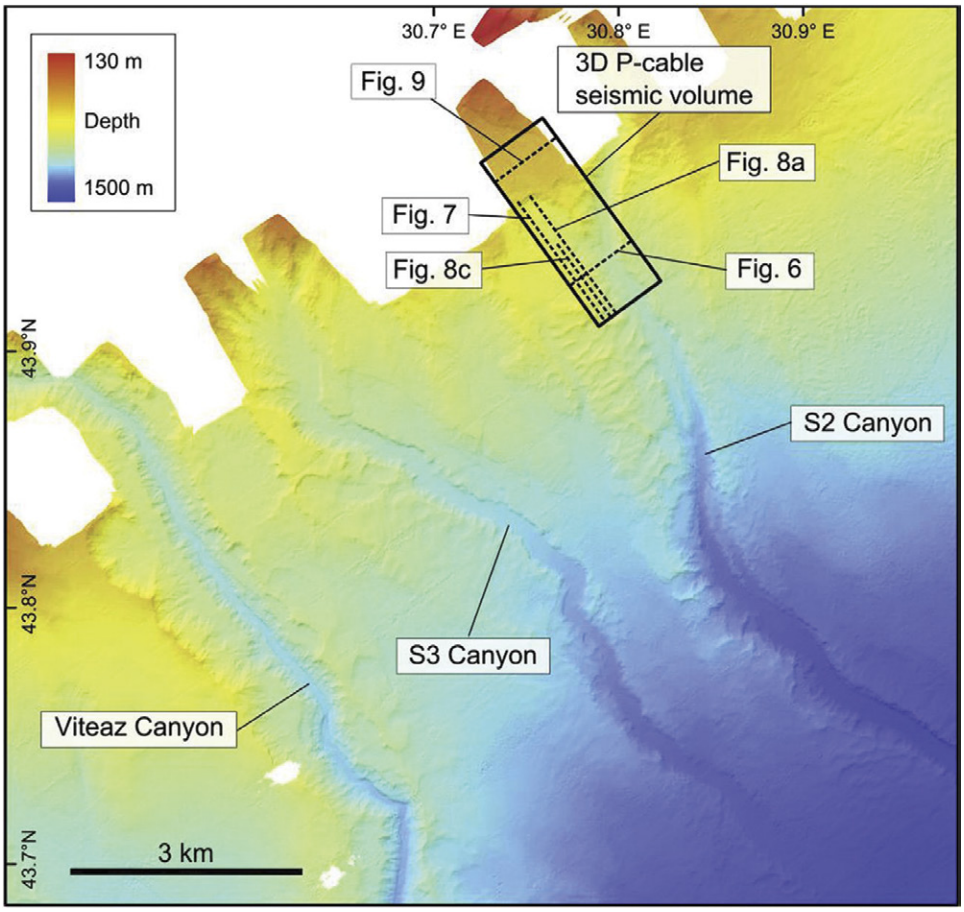

Fig. 20. Map of the Danube Fan study area (MSM34 cruise). The location of seismic lines included in this paper is indicated by the black dashed lines (Hillman *et al.*, 2018).

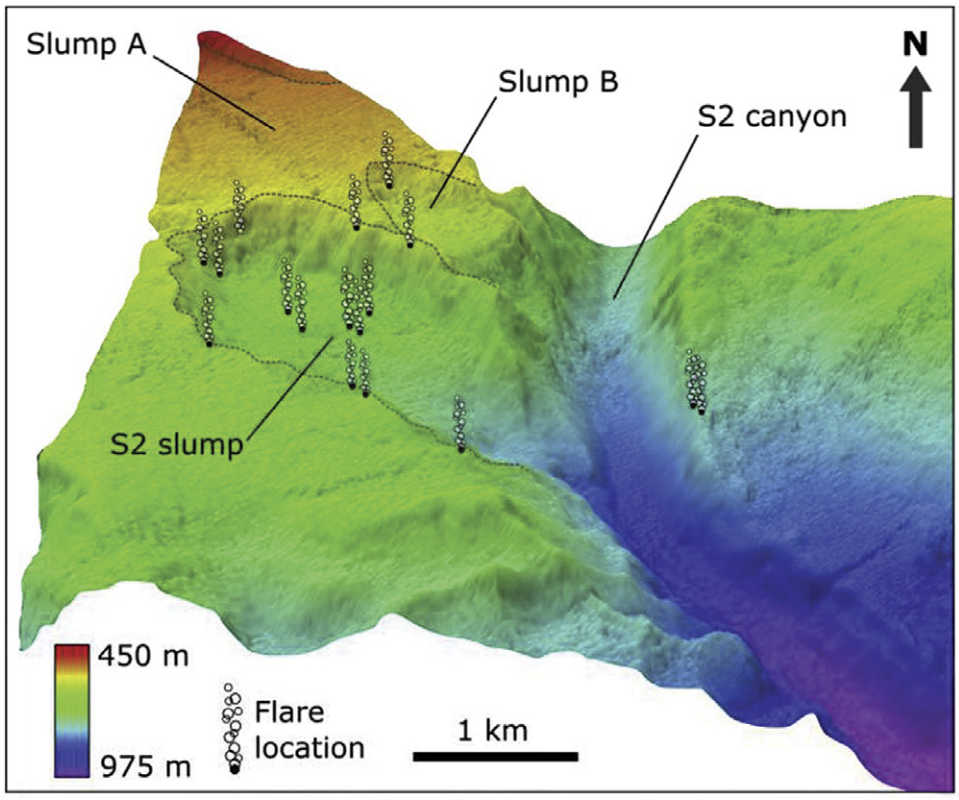

Fig. 21. 3D perspective view of the S2 canyon and slump to show the location of flares identified during the MSM34 cruise in the area. The dashed lines delineate the edges of the 3 slope failure features – the S2 slump, slump A, and slump B. The majority of slump A is not imaged in the MSM34 bathymetry (Hillman *et al.*, 2018).

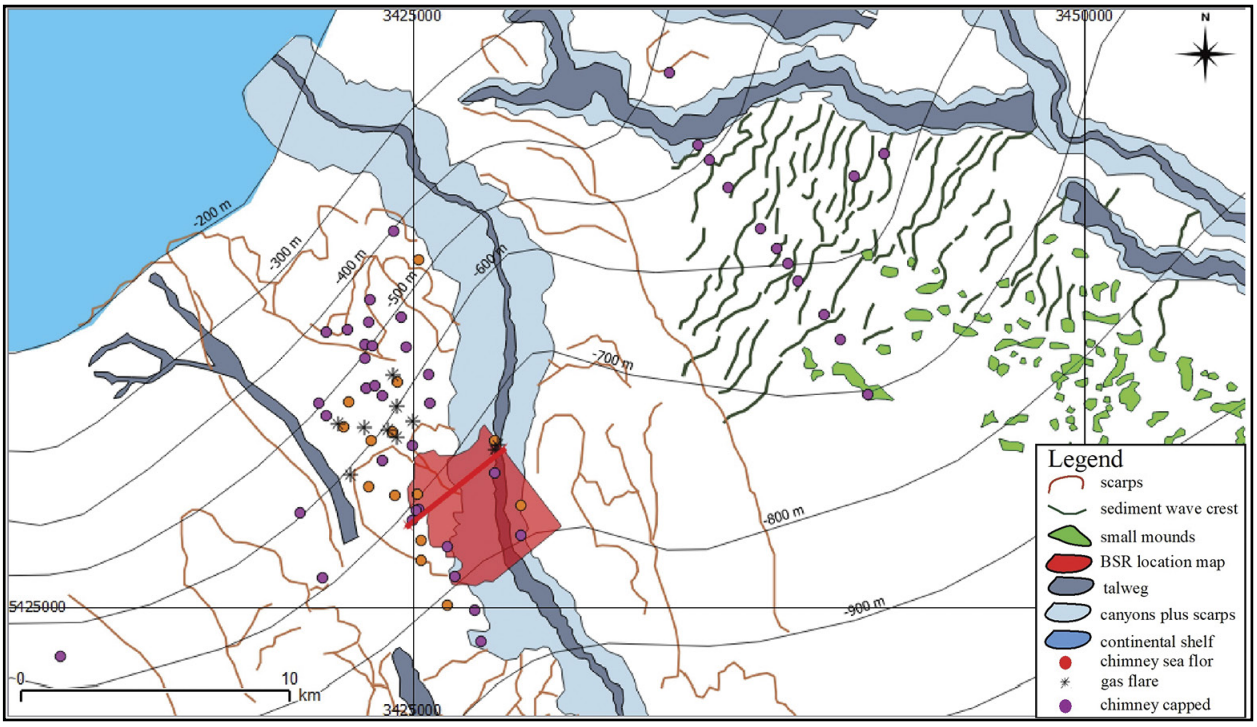

Fig. 22. Map of gas migration structures identified on seismic data, and flares observed in high frequency sub-bottom profiler data in the vicinity of the S2 canyon (Hillman *et al.*, 2018). Morphology from Riboulot *et al.*, 2017. Red line represents the location of seismic line 1730.

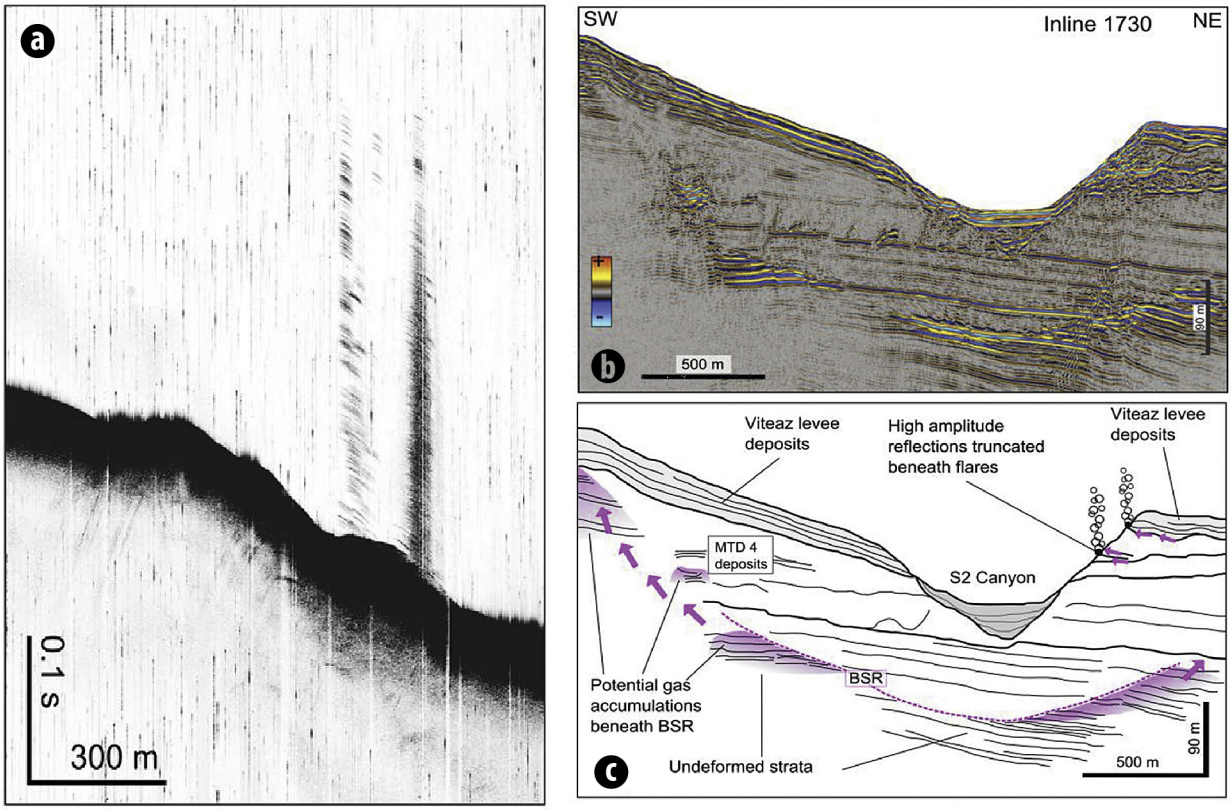

Fig. 23. (**a**) Example of a flare observed in the water column, location of the line is shown in (a). (**b**) Inline 1730: seismic profile. (**c**) Inline 1730: Line drawing. The BSR bends upward beneath the S2 slump. Increased amplitudes terminating and stacking along the potential pathway of the BSR image vertical gas migration leading to potential gas accumulations near the seafloor along the southwestern sidewall of the S2 slump. Along its eastern flank the S2 Canyon truncates two high-amplitude horizons in the levee deposits that correlate to the position of flares along the canyon (Hillman *et al.*, 2018).

In the seismic data, numerous structures that are tens-of-meters in diameter, conical in geometry, and are capped by high amplitudes underlain by zones of acoustic blanking (Figs. 24-27). Based on observations in the seismic data these structures can be categorized into Groups A, B and C, based on their dimensions, amplitude characteristics and geometry.

The structures in Group A and B are both characterized by distinct high amplitude anomalies, and/or acoustic blanking, and are differentiated primarily by their geometry and size, with Group B being more complex in structure and larger in size (100s of m in diameter). Group B is also frequently associated with high amplitude strata at depth, which fades into zones of acoustic blanking at the base of these structures (*e.g.* Fig. 25). Several of the larger features in Group B show stacked concentric circles of high seismic amplitudes, centred on a zone of acoustic blanking (Fig. 26). Both Group A and B are characterized by distinct chimney-like shapes, with circular to elliptical horizontal geometry when observed in the 3D seismic data. The Group C structures are less well defined in the seismic data, and do not exhibit the same 'chimney-like' shape, with some characterized by discrete, broad high-amplitude anomalies, and others as clusters of chaotic seismic facies with patchy high amplitudes (*e.g.* Fig. 25).

The main characteristics of these groups can be summarized as (Hillman *et al.*, 2018):

- **Group A structures** are characterized as narrow, steep sided gas migration features, with an overall simple geometry. Several such structures are observed beneath the

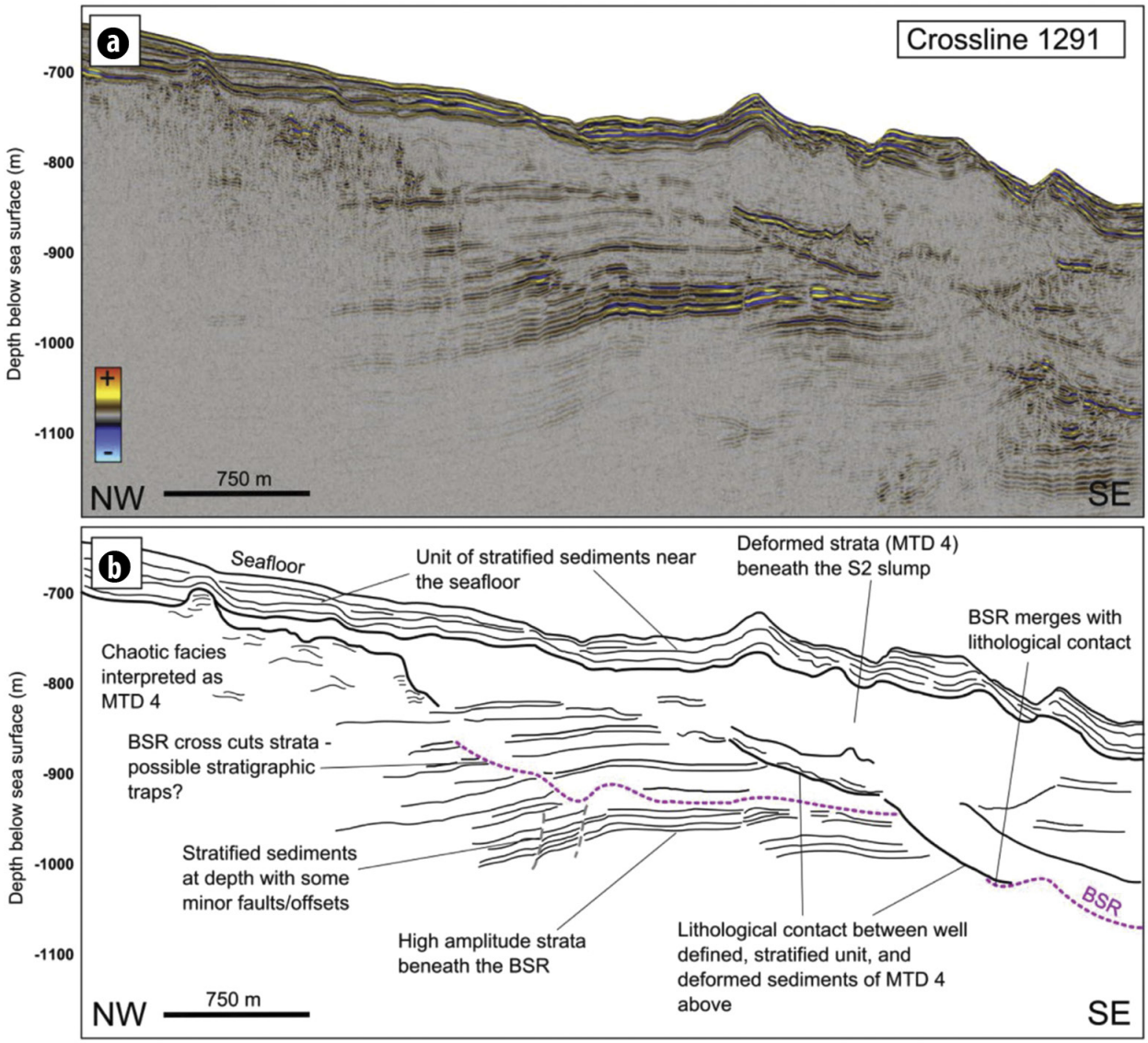

Fig. 24. (**a**) Cross line 1291: seismic line showing the position of the BSR relative the lithological contact beneath the MTD. The position of the BSR is reinforced through observations of Inline 1730 (Fig. 12). See Fig. 2 for line location. (**b**) Cross line 1291: interpreted line drawing. The position of the BSR merges with the lithological contact to the SE. To the NW the BSR is clearly distinguished by the termination of high amplitudes. The stratified sediments beneath the BSR are offset by minor faults, with possible small stratigraphic traps along the BSR (Hillman *et al.*, 2018).

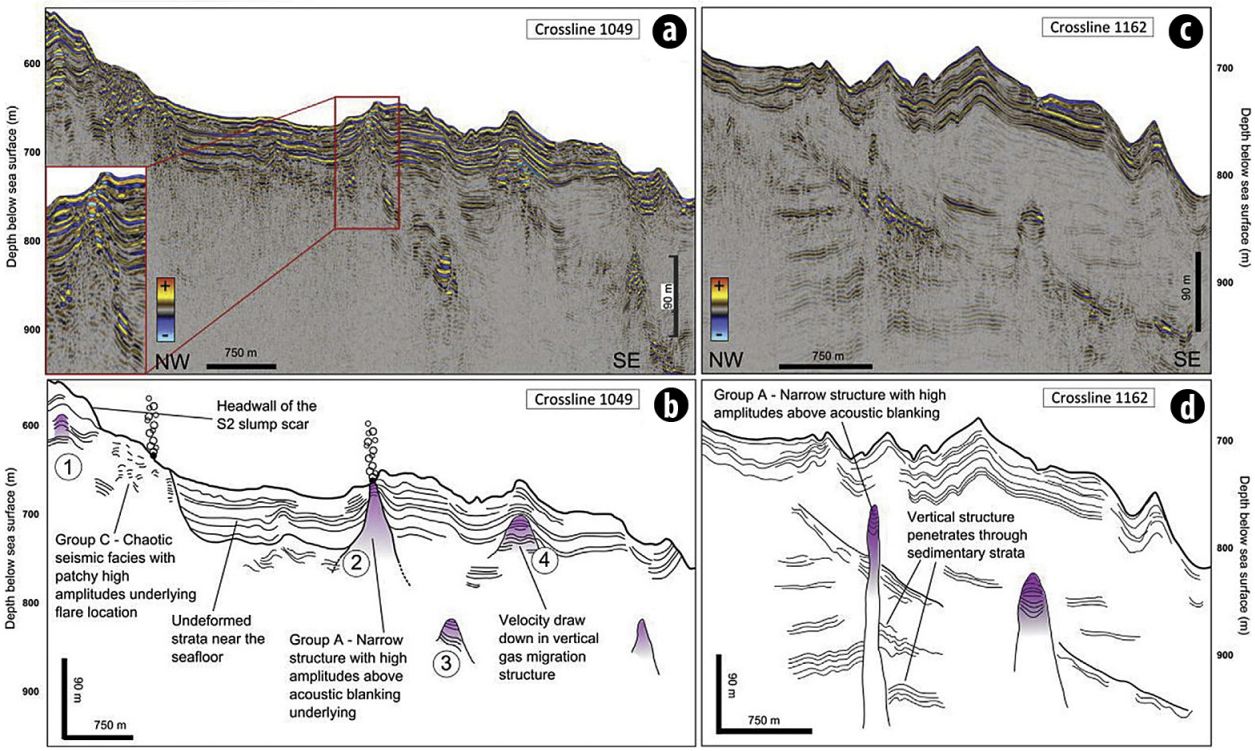

Fig. 25. (**a**) Cross line 1049: seismic line showing examples of Group A and C gas migration features. Inset – enlarged view of narrow, conical structure showing high amplitude reflections capping a column of acoustic blanking. See Fig. 2 for line location. (**b**) Cross line 1049: interpreted line drawing. Structures 1, 3 and 4 are capped by overlying sediments and do not reach the seafloor. Structure 2 reaches the seafloor and underlies the location of an identified flare. There is also a flare above the chaotic seismic facies interpreted as MTD deposits associated with the S2 slump. (**c**) Cross line 1162: seismic line showing an example of Group A gas migration features. See Fig. 14 for line location. d) Cross line 1162: interpreted line drawing. These narrow, vertical structures clearly cross-cut the sedimentary strata at depth (Hillman *et al.*, 2018).

S2 slump, where they appear to correlate with locations where the overlying unit of stratified sediments thins out (Fig. 25), suggesting that upward gas migration exploits the thinned, weakened overburden at such points. However, as some of these chimney-like structures are capped and do not extend to the seafloor, the gas accumulation most likely did not result into an overpressure strong enough to initiate fracturing. Where these chimney-like structures do reach the seafloor, they correlate to the observed flares.

- **Group B structures** are generally larger in size, typically with a more complex internal geometry than those of Group A. In particular, the near-circular, capped gas migration structures upslope of the S2 slump (Fig. 26) have a geometry that is reminiscent of a larger (km-scale) feature. There, high amplitudes that correlate with high seismic velocities are observed on the edges of a chimney-like feature, with blanking and low velocities at the centre and below. This is interpreted as gas hydrates forming at the boundary of the chimney structure (corresponding to high seismic amplitudes and velocities), with free gas at the centre (corresponding to seismic blanking and low velocities). The presence of free gas in sediments can be characterized in seismic data by both high and low amplitudes, and it may be that the variation across these chimney structures is due to a change in the concentration of free gas in the sediments, or the degree of disruption in the sediments caused by the upward flow of free gas. The possible deformation or minor folding of sediments in the vicinity of these larger chimney structures (*e.g.* Fig. 26), suggests that may have resulted in gas being channelled towards a particular location, allowing the build-up of an accumulation sufficient to generate hydro-fracturing and to form a large chimney.
- **Group C structures** are more anomalous and do not follow the same characteristics like groups A and B. Some of the structures in Group C are likely the result of small, shallow gas accumulations, the locations of which are controlled by minor structural traps in the channel-levee complexes of the Danube Fan. The structures in Group C that are associated with flares at the seafloor are characterized by patchy distributions of high amplitudes in the seismic data (*e.g.* Figs. 23 and 25). These are likely due to the dispersed accumulation of gas within the sediments, which may be controlled by localized, small-scale heterogeneity in the lithology. This is particularly evident at the foot of the S2 slump headwall, where an MTD is exposed at the seafloor, and corresponds with the location of several flares (Figs. 21 and 27).

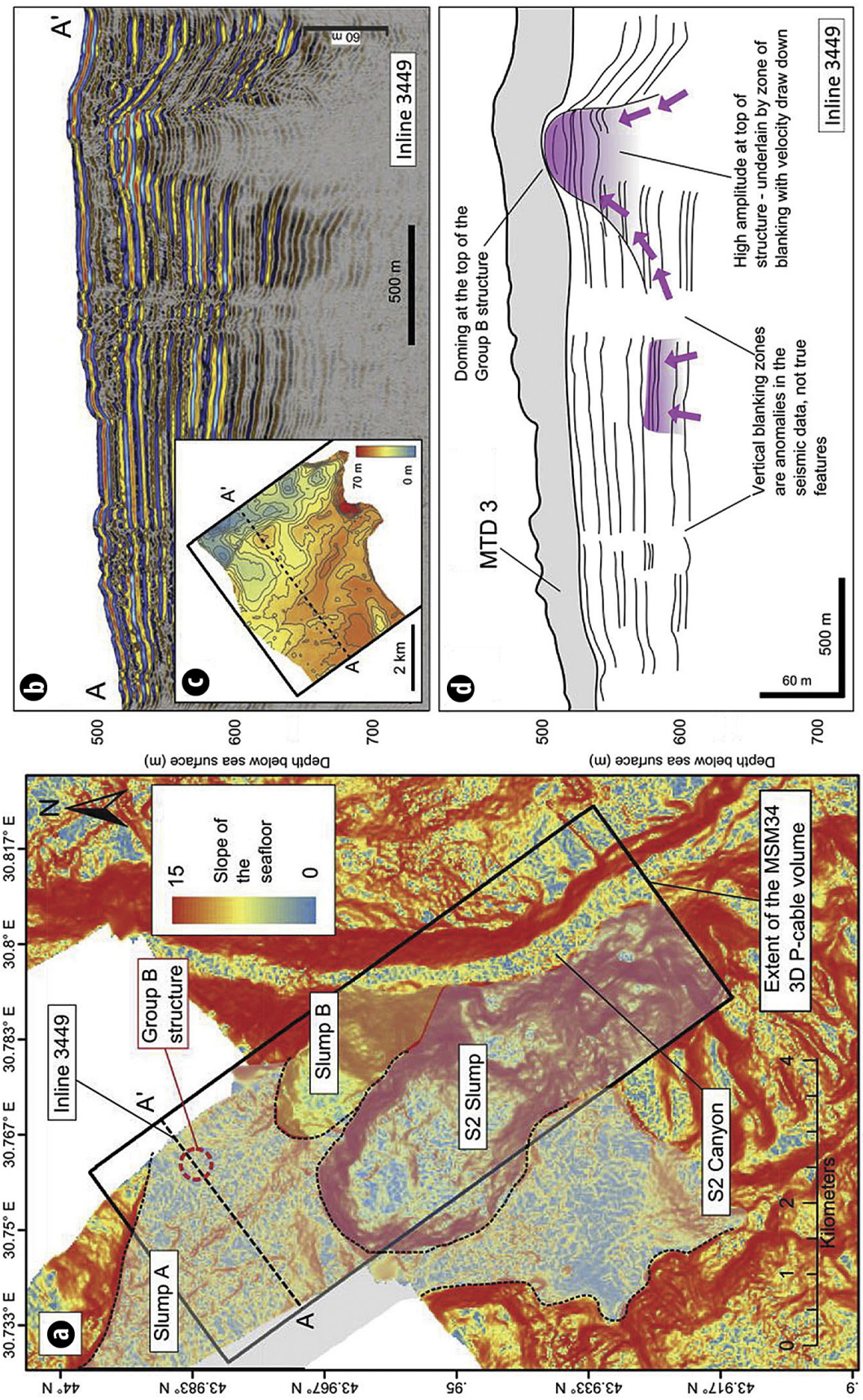

Fig. 26. (**a**) Slope map of the seafloor – the three slump features near the S2 canyon are outlined. Slump A is associated with MTD 3, shown in (b) and (d) that caps the chimney. (**b**) Line 3449: seismic line showing an example of a Group B gas migration structure. (**c**) Isopach map of the MTD 3 unit. The thickness of the unit decreases above the large gas-migration feature and dome structure (c) in the NE of the study area. The heavy black line indicates the extent of the 3D seismic volume. (**d**) Line 3449: interpreted line drawing. The Group B structure here does not reach the seafloor; it is capped by MTD 3 associated with the slope failure (Slump A) upslope of the S2 slump. There appears to be doming at the top of the structure, resulting in thinning of the overlying sediments (Hillman *et al.*, 2018).

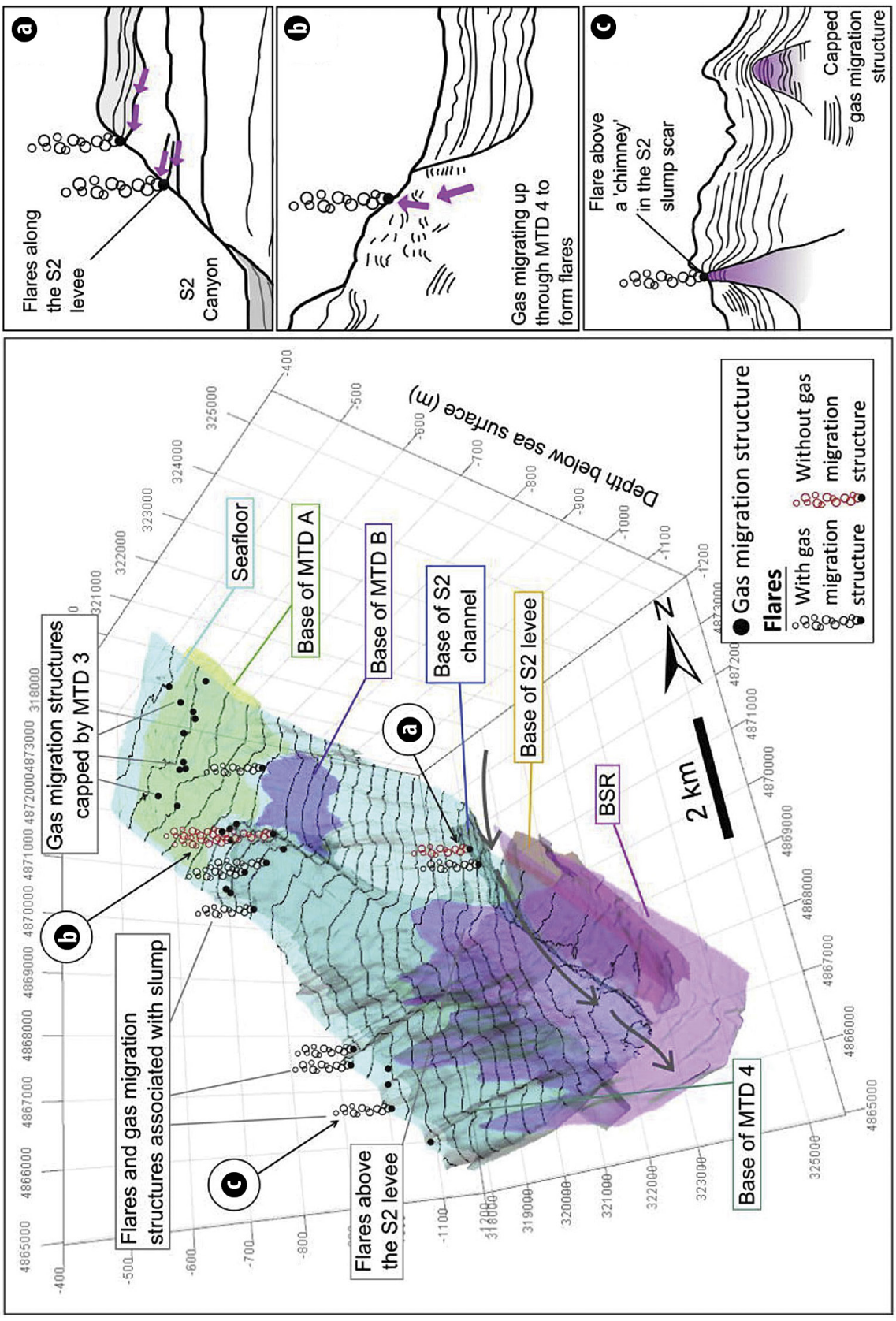

Fig. 27. 3D view of the BSR, flares and gas migration structures in relation to key stratigraphic units across the extent of the 3D seismic volume. (**a**) Gas charged horizons truncated by the S2 canyon forming flares. (**b**) Chaotic MTD unit allowing upward migration of gas to form flares in the S2 slump. (**c**) Gas migration structure extending upwards to the seafloor along the western edge of the S2 slump, and a capped gas migration structure. In this area gas clearly migrates up from beneath the up-bending BSR (see Fig. 21) (Hillman *et al.*, 2018).

- **Mass transport deposits (MTD) and gas migration.** Based on the observation of the position of the BSR corresponding with the base of MTD 4 deposits beneath the S2 slump scar in the seismic data, it would appear that the sediments of MTD 4 also facilitate the migration of gas, with discontinuities in the chaotic seismic facies likely providing flow conduits that result in the formation of gas migration features and flares. Upward migration of gas through the sediments is also prevented by MTD deposits in some cases. This would explain the capped structures that are observed upslope of the S2 slump (Figs. 21 and 26). Here, the chimneys terminate at the contact with MTD 3 associated with Slump A, which indicates that the sediments of the MTD form a seal, preventing upward gas migration. Minor variations in porosity and/or permeability of sediments may already be sufficient to allow or control the movement of gas. MTD deposits on continental slopes generally involve a mixture of lithologies from the original failed area that are transported by various gravitational processes. Short transport distances would prevent effective sorting and consequently result in low permeability of the MTD, forming a seal unit, unless the failed deposits were already well sorted. As the primary source of failed material in the Danube Fan is likely to be levee sediments, representing a mixture of fine-grained and slightly coarser spill-over deposits. The thickness of deposits from failure of such material most likely corresponds to sealing effectiveness as shown by the correlation between the thickness of the MTD 4 and the location of flares, which generally occurs where the MTD thins to <25 m. On the other hand, active gas migration structures capped by an MTD unit should lead to gas accumulation at the base of the MTD, or to gas migration along its base.

5. RECOGNITION OF THE GAS-HYDRATES OCCURRENCE BASED ON THE THERMOBARIC CHARACTERISTICS

The Istria Depression as part of the Black Sea is offering favourable conditions for the gas-hydrate occurrence due to its particular features related with the water depth (see Chapter 1), the Miocene-Quaternary sedimentary characteristics (see Chapter 2.3) and the geothermal and pressure conditions.

According with the previous studies of the gas-hydrate occurrence in the Black Sea (Lüdmann et al, 2004, Kutas *et al.*, 2004, Ivanov et al, 1998), the gas-hydrates are present both in the continental coastal areas and in the deep basin under the interface water-sediment, in Quaternary sediments that are generally 1-3 km thick.

The data used for establishing the presence of gas hydrate occurrence in the Istria Depression based on the thermobaric conditions are the heat flux data (Veliciu, 2002), information related to the depth, salinity and pressure of the Black Sea water.

Veliciu, 2002, considers that the heat production within the thick sedimentary layer present beneath most of the central Black Sea can be estimated by using the mean concentrations of uranium, thorium and potassium in the Black Sea sediments and calculated decay energies; an average density of 2.4 g/cm^3, which is comparable with data used in gravimetry, is assumed. A heat production of 1.7 mW/m^2 /km of sediment was calculated on the basis of these assumptions. If an average sedimentary thickness of 10 km is present on the floor of the Black Sea, it contributes with about 17 mW/m^2 to the observed flux, leaving 75 mW/m^2 as the sum of the flux contributed by the 6.4-7.0 km/sec layer and the upper mantle. Estimation of the heat produced within the 6.4-7.0 km/sec layer requires knowledge of the composition of the rock. If the 6.4-7.0 km/sec layer is former oceanic crust, its contribution is less than 0.5 mW/m^2, even for a thickness approaching 20 kms. However, if the „basaltic" layer is actually a 10 km thick layer of highly metamorphosed, deeply eroded continental rocks, its thermal contribution should range from 8 to 12 mW/m^2, if uranium, thorium and potassium concentrations within the layer are similar to the radiogenic content of rocks of the amphibolite and granulite facies exposed on shore in the surrounding platforms. The identification of the 6.4-7.0 km/sec layer within metamorphosed continental rocks seems preferable. On this assumption, the heat flux into the base of the crust is about 63 mW/m^2. If we assumed values of 3.8 HGU and 4 HCU for the heat production and thermal conductivity of the sediment respectively, the steady-state temperature at the base of the sediment ranges from 420 to 670 °C for sedimentary thicknesses of 10 and 15 km respectively. The heat flow values estimated by Veliciu ranges from 20 to 92 mW/m^2 in the north-western Black Sea basin (Fig. 28); the maximum values are located in the northern part of Istria Depression and the minimum values are located in the southern part of the analysed area.

In order to evaluate the geothermic gradient, the equation $q=k*G_t$, which links the heat flow (q), geothermic gradient (G_t) and thermic conductivity has been used taking in consideration that the thermic conductivity varies with depth. The thermic conductivity values were measured in the well 379A by Erickson and Von Herzen in 1978, which was part of the DSDP Leg 42B campaign of the Back Sea study (Fig. 29).

To determine the temperatures distribution of the various depths under the sea bottom, it was considered that the sea bottom of the sea is an isothermal line of 9.1°C, this value has been taken from the measurements made in 2002 by the IFREMER French Institute (Popescu *et al.*, 2006).

In this way, temperature distribution maps were made for the following depths below the sea bottom: 150 m, 200 m, 250 m and 300 m (Fig. 31). It is noted that the temperature distribution maps preserved the same shape as the heat flux map, having the maximum values in the northern central area of the Istria depression and minimum values in the southern area.

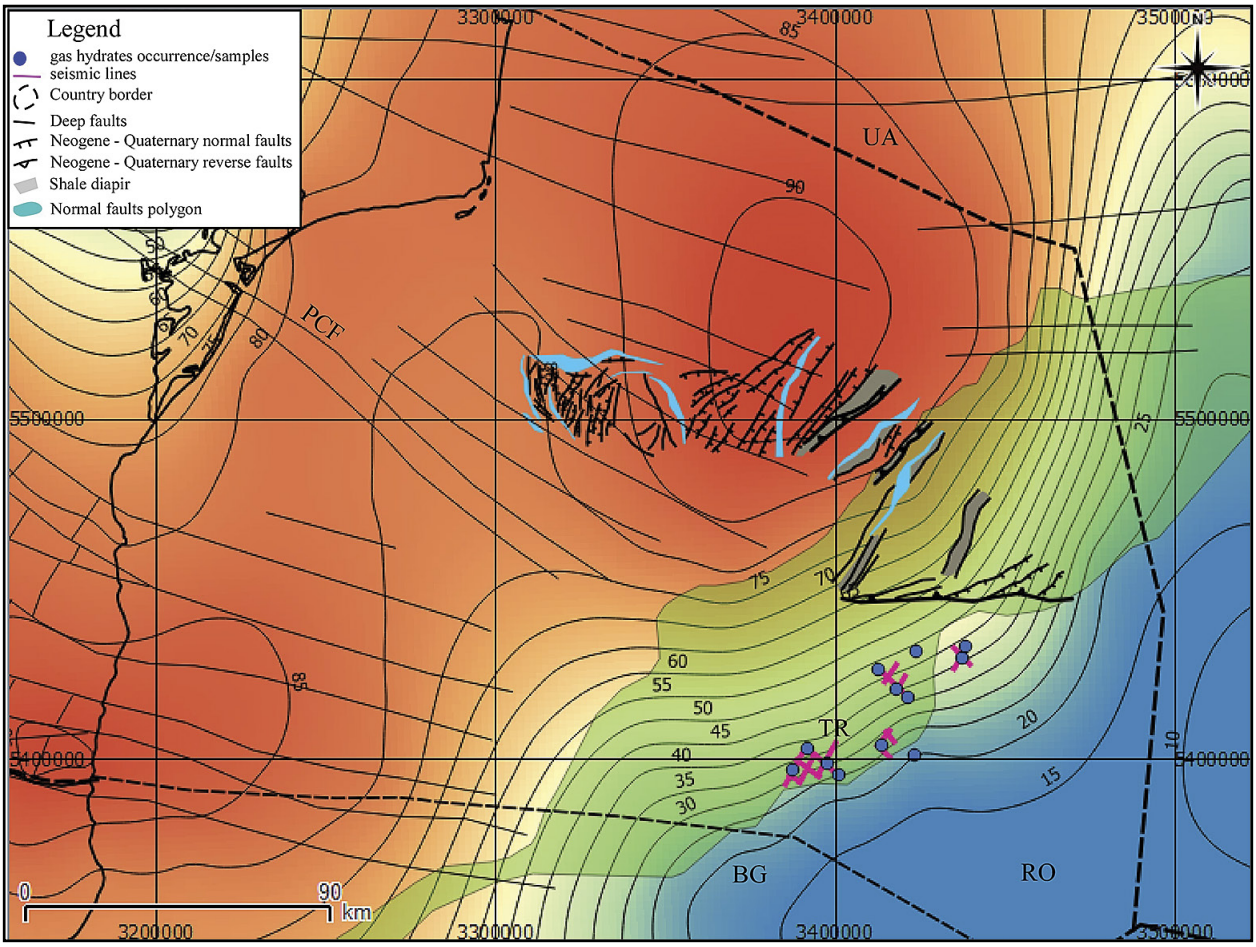

Fig. 28. Heat flow map offshore Romania (Veliciu, 2002). **BG** – Bulgaria, **RO** – Romania, **Tk** –Turkey, **UA** – Ukraine.

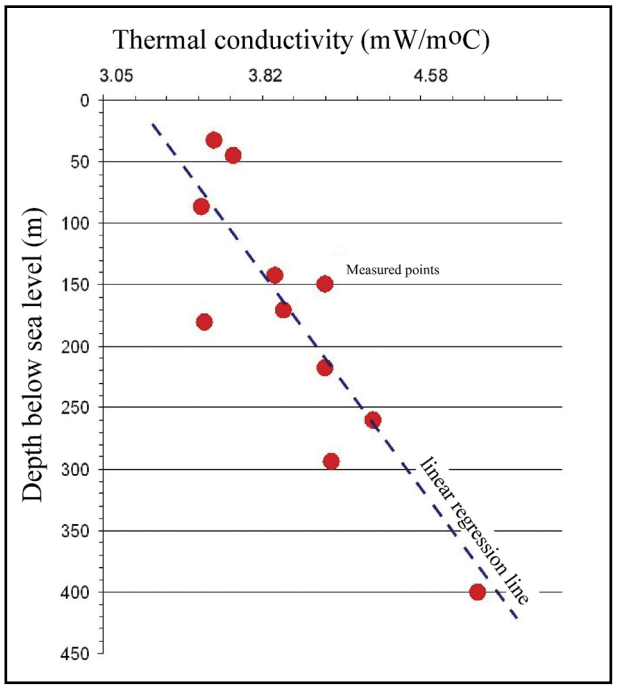

Fig. 29. Thermal conductivity of superficial sediments in the Black Sea according with data measured in DSDP Leg 42B (after Erikson and Von Hinze, 1978).

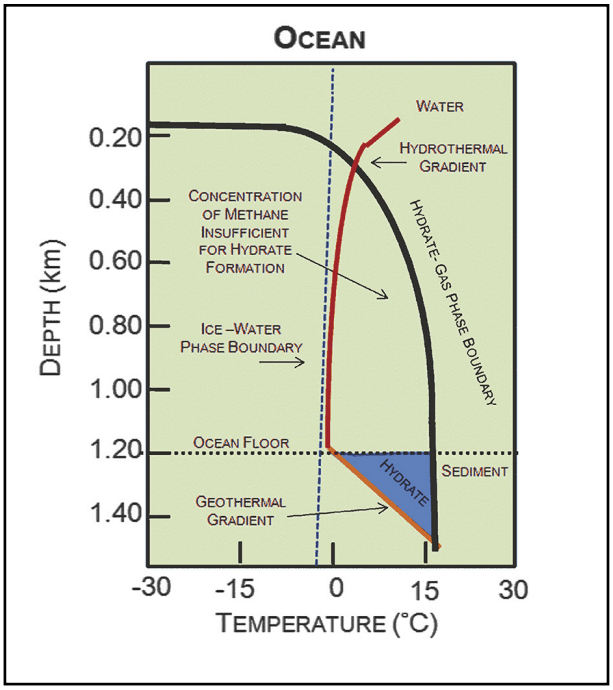

Fig. 30. Depth Temperature Zone in which Methane Hydrate is stable in oceans (after Collet, 2002).

Unfortunately, due to lack of information on thermal conductivity deeper than 400 m below the sea bottom, it was not possible to establish the maximum depth down to which there are thermal conditions for the gas-hydrate occurrence. It can be noticed that at the depth of 150 m under the sea bottom, the temperature varies from 12.4 to 9.6° C, at a depth of 200 m from 13.4 to 9.8° C, for the depth of 250 m ranges from 14 to 10° C and for the depth of 300 m, the temperature varies from 15 to 10.5° C.

Therefore, from the temperature point of view, on the Romanian Continental Shelf, the conditions for the gas-hydrates occurrence are fulfilled, the temperature are in the range of -10 to 32° C as it is required from theoretical point of view (Fig. 31) .

For the pressure determination, a hydrostatic pressure gradient of 0.010 MPa/m (Dickens & Quinby-Hunt, 1994) and a lithostatic pressure gradient of 0.026 MPa/m set for 2.6 g/cm^3 average density and 9.8 g/cm^2 gravity acceleration, were used.

Based on the above mentioned hydrostatic pressure gradient, the hydrostatic pressure map was created at the sea bottom (0 m below the sea bottom) (Fig. 31), which shows that the pressure varies directly proportional to the depth, for the sea depths of up to 200 m, the hydrostatic pressure is lower than 2 MPa, while at 1000 m sea depth the pressure reaches 10 MPa. Therefore, from pressure point of view, at the sea bottom level, the gas-hydrates could occur in the areas deeper than 200m. As it goes deeper into the sedimentary layer beneath the sea (150 m, 200 m, 250 m and 300 m), as it was expected, it is noticed a steady increase of the lithostatic pressure according to depth. Superposing the temperature distribution maps build for various depths with pressure distribution maps for the same depths it was settled the spatial distribution of the thermic and pressure favourable conditions to gas-hydrate occurrence in the Istria Depression area (Fig. 31). The favourable zones for the gas-hydrate occurrence from temperature and pressure point of view move from the deep basin to the shore as the analysis depth of the sedimentary column increases as it follows:

- at the level of the sea bed (0 m beneath the bottom sea bed), the gas-hydrates occurrence is located in the eastern part on the Istria Depression where the sea depth is higher than 100m;
- for 200 m depth below the bottom of the sea bed, the best conditions from temperature and pressure point of view for the gas-hydrate occurrence are encountered in the western part of the Istria Depression from 300 m sea depth to the shore line;
- at the level of 250 m depth under the bottom of the sea bed, the gas-hydrate occurrence is located in the western part of the Istria Depression from 200 m sea water depth to the shore line;
- at the level of 300 m depth below the bottom of the sea bed, the gas-hydrate occurrence is located in the western part of the Istria Depression from 150 m sea water depth to the shore line.

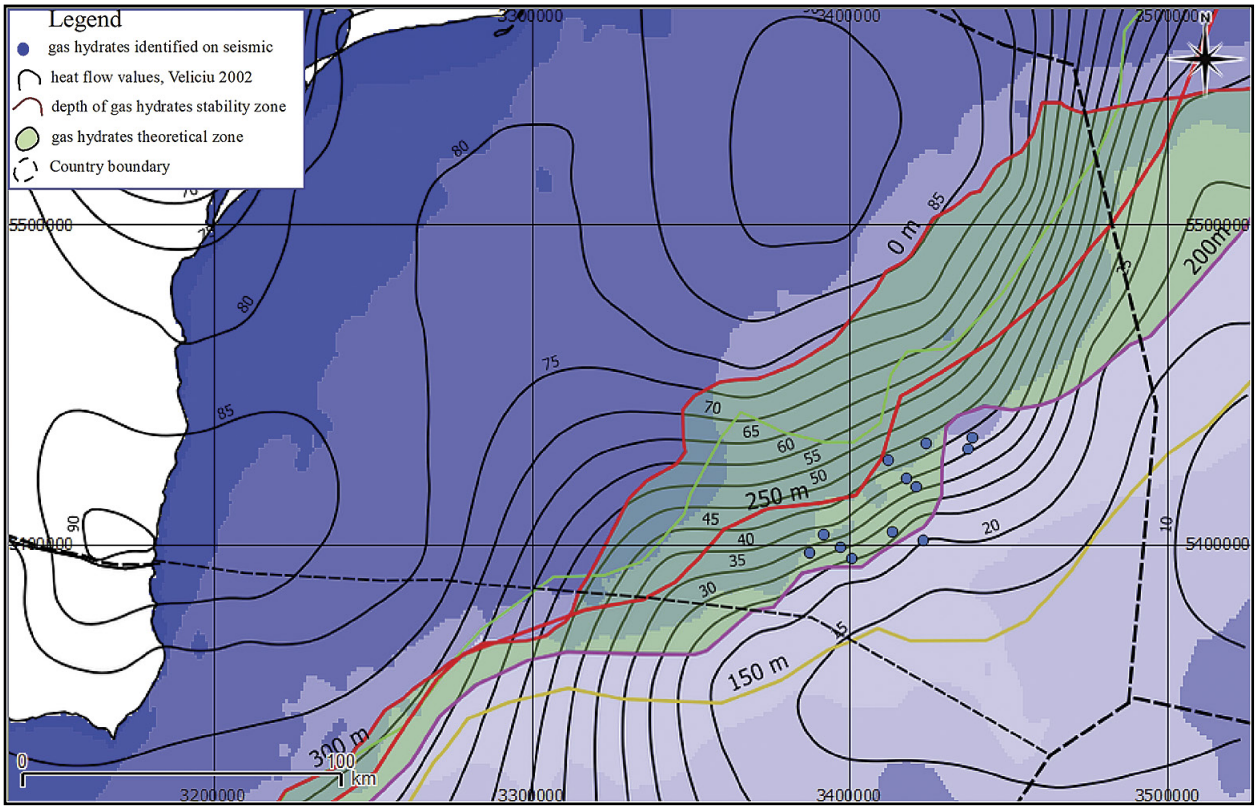

Fig. 31. Map showing the gas-hydrates thermobaric stability zones at different depths below sea level, **light red** – 0 m, **yellow** – 150 m, **magenta** – 200 m, **dark red** – 250 m and **green** – 300 m, bellow sea bed (Tambrea, 2007). Heat flow values after Veliciu, 2002.

6. RECOGNITION OF THE GAS-HYDRATES OCCURRENCE BASED ON THE SEISMIC DATA

For gas-hydrate identification in the Istria Depression, the BSR (bottom-simulating reflector) was identified on several 2D seismic profiles. Unfortunately, the identification of the BSR on the seismic data was difficult as the seismic data has been acquired and processed for deep hydrocarbon exploration purposes. On the seismic line in the Fig. 33, the marked BSRs with accompanying polarity reversal compared the seafloor reflector have been recognized. This BSR cross-cut the bedding planes of the sediment and is characterized by very high amplitude. Sediments shallower than the BSR may host gas hydrate and it is characterized by a blank seismic facies, while sediments deeper than the BSR may have gas bubbles in the pore space and is characterized by high amplitude.

The BSRs was observed only on several seismic profiles, in the depth range of sea water between 700 and 1300 m (Figs. 32 and 33). In order to evaluate the depth of the BSR, twelve values of the BSR TWT were read on the seismic lines and converted from time to depth. The interval velocity used to convert from time to depth were of about 1480 m/s for water interval according to the velocity analyses done for the seismic data processing and 1608 m/s for shallow sediments according to the analysis by Lüdmann *et al.* in 2004, in a similar sedimentary environment. The resulted depths for the BSR are in range of 160 to 350 m below the bottom of the sea which means 890 to 1600 m below sea bed (table 1).

Superimposing the gas distribution identified on the seismic profiles with the distribution areas resulting from the analysis of the temperature and pressure (Figs. 31 and 32), there is a relatively good correlation. Many of BSRs are located in the area where the temperature and pressure conditions for the gas-hydrate occurrence are satisfied.

7. EXAMPLES OF THE BSR OFFSHORE ROMANIA

Based on the multifold high resolution seismic data acquired by IFREMER during BLASON (Black Sea Over the Neoeuxinian) French-Romanian scientific campaign in the Black Sea in 1998, Ion *et al.*, 2002 have clearly put in evidence several BSRs in deeper part of Danube deep sea fan. On a seismic line, 4 levels of the BSR's can be distinguished placed in the deep sea fan complex of the Danube at water depths of 1500-1680 m and 400-600 ms twt bsf (Fig. 34). The authors think that the first two uppermost (A and B) BSR features are two layers with disseminated gas hydrates, without gas presence beneath them. The other two BSRs (C and D) appear to have basal fluids unless it is a single less permeable layer with clathrates which have basal gas and water below gas. This quite uncommon association of BSR features could be the result of the vertical migration of the gas hydrates stability

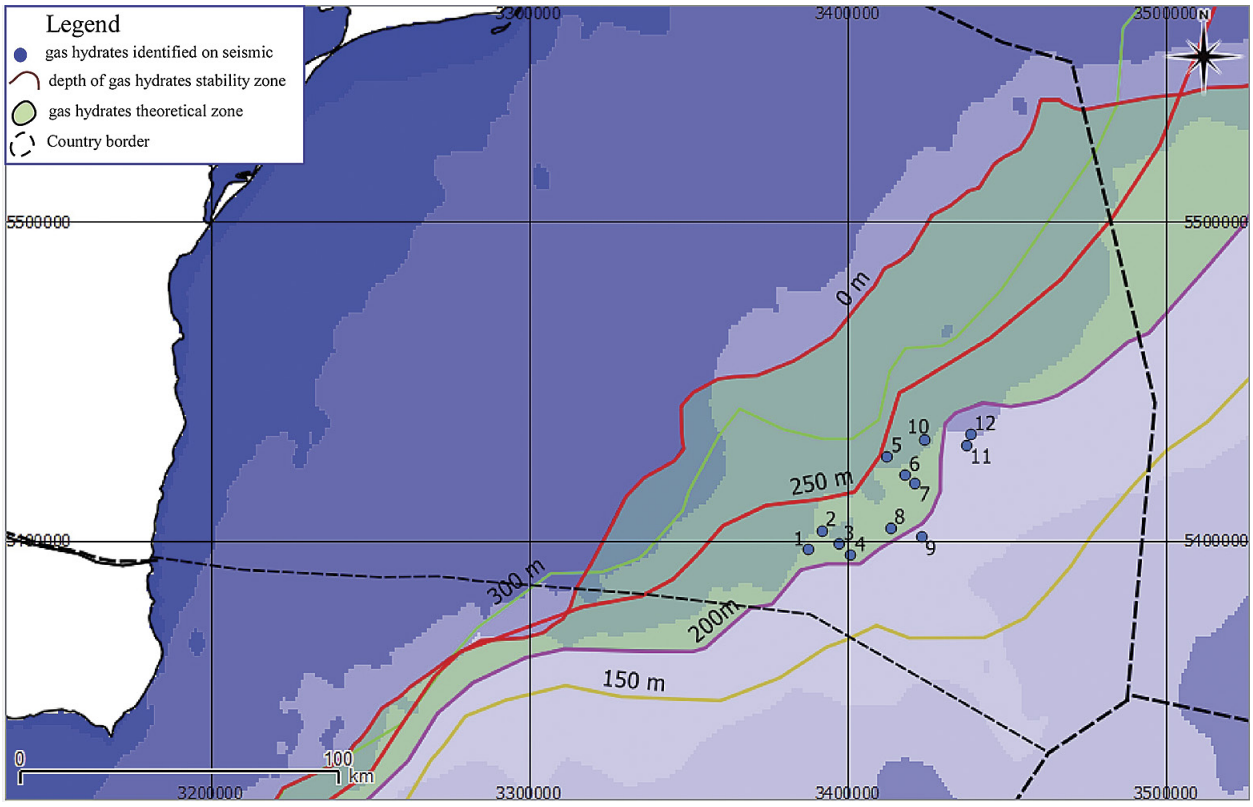

Fig. 32. Map showing the points where the gas-hydrates have been identified on seismic lines (in red colour) (Tambrea, 2007). The points description in table 1.

Table 1. Description of identified BSR (Tambrea, 2007). For localization, see Fig. 32

BSR points	Water depth TWT (ms)	Water depth (m)	TWT BSR (ms)	BRS thickness (ms)	BRS thickness (m)	BSR depth (ms)
BSR 1	976	722.24	1184	208	167	889
BSR 2	1172	867.28	1532	360	***289***	1157
BSR 3	1256	929.44	1688	432	***347***	1277
BSR 4	1352	1000.48	1652	300	241	1242
BSR 5	1388	1027.12	1684	296	238	1265
BSR 6	1156	855.44	1404	248	199	1055
BSR 7	1460	1080.40	1788	328	264	1344
BSR 8	1824	1349.76	2016	192	154	1504
BSR 9	2020	1494.80	2168	148	119	1614
BSR 10	1032	763.68	1336	304	244	1008
BSR 11	1300	962.00	1672	372	***299***	1261
BSR 12	1272	941.28	1676	404	***325***	1266

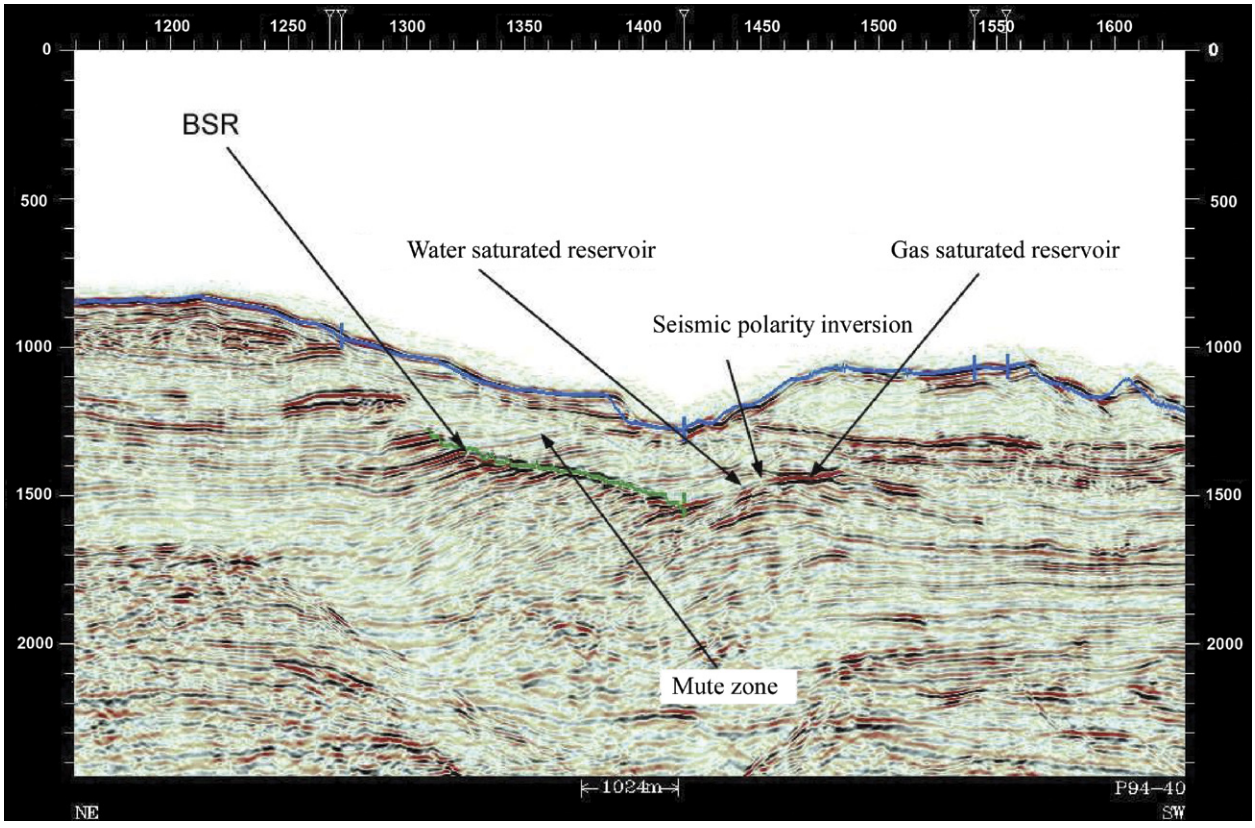

Fig. 33. Example of seismic line where gas hydrates have been identified (Tambrea, 2007).

zone (GHSZ), in response to the sea level variation during the Quaternary.

On another seismic line acquired during the Blason campaign, outside of the palaeo-Danube influence, a classical BSR feature was recorded (Fig. 35). This was the first time when BSR structures have been reported in the Danube deep sea fan area.

Popescu, et al 2006 based on an extensive seismic dataset, acquired during the BlaSON surveys of IFREMER and GeoEcoMar (1998 and 2002) (Fig. 7) and published information from previous local studies, analysed gas hydrates from Romanian Black Sea shelf.

The data reveal widespread occurrences of seismic facies indicating free gas in sediments and gas escape in the water column. The presence of gas hydrates is inferred from bottom-simulating reflections (BSRs). The distribution of the gas facies shows:

(1) Major gas accumulations close to the seafloor in the coastal area and along the shelfbreak,
(2) Ubiquitous gas migration from the deeper subsurface on the shelf and
(3) Gas hydrates occurrences on the lower slope (below 750 m water depth).

The coastal and shelfbreak shallow gas areas correspond to the highstand and lowstand depocentres, respectively. Gas in these areas most likely results from in situ degradation of biogenic matter, probably with a contribution of deep gas in the shelfbreak accumulation. On the western shelf, vertical gas migration appears to originate from a source of Eocene age or older and, in some cases, it is clearly related to known deep oil and gas fields. Gas release at the seafloor is abundant at water depths shallower than 725 m, which corresponds to the minimum theoretical depth for methane hydrate stability, but occurs only exceptionally at water depths where hydrates can form. As such, gas entering the hydrate stability field appears to form hydrates, acting as a seal for gas migration towards the seafloor and subsequent escape.

Three areas of BSR occurrence in the Danube fan, located between 750 and 1830 m water depth (A, B, C in Fig. 36) were mapped on the seismic data. Zone A is situated on the Bulgarian Black Sea area and the results will not be discussed in this paper. In the zone B, situated in the southern part of the fan, the authors detected an unusual succession of two, three or four BSR-type distinct reflections with similar amplitude, all of them subparallel to the seafloor, showing reversed polarity and crosscutting the sedimentary structure (Figs. 37-40). A fifth very weak and discontinuous BSR possibly lies below the four-BSR occurrence (Figs. 37 and 39). The depth of each BSR increases with water depth, and thus with pressure. The uppermost BSR (BSR1) continues laterally as the upper limit of an area containing seismic reflections of anomalously high amplitude, underlain by acoustic turbidity (Figs. 37 and 38). In the northern zone C, the BSR appears either as a defined reflection with reversed polarity or as an upper limit of enhanced reflections, mimicking the seafloor (Fig. 40). A faint double BSR occurs locally below the widespread BSR1 (Fig. 40).

Gas hydrate seismic features show an obvious relationship with the architecture of the Danube deep-sea fan. Occurrences of gas and hydrates correspond to specific channel–levee systems (A, B, C in Fig. 36). In all cases:

(1) The BGHSZ is visible only on a limited segment inside the channel–levee system,
(2) Multiple BSRs crosscut the parallel horizons of the levee that is situated downslope of the channel axis (considering the present seafloor gradient) and terminate against the base of the channel–levee system, and
(3) Free gas accumulation corresponds to the channel axis area (Fig. 36). Multiple BSRs in the Danube fan occur exclusively as part of a defined pattern: a gas-bearing channel–levee system whose top is situated above the BGHSZ (Fig. 37). This pattern is developed around a gas accumulation at the channel axis corresponding to coarser-grained deposits with higher porosity, and thus reflecting a lithological control. Trapping gas inside this

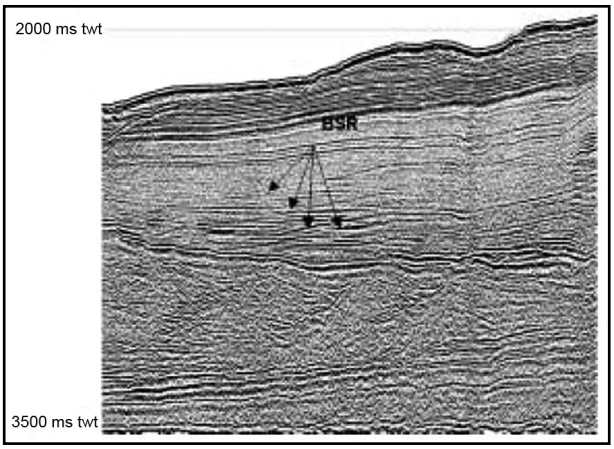

Fig. 34. Seismic line showing multiple BSR, offshore Romania (Ion *et al.*, 2002).

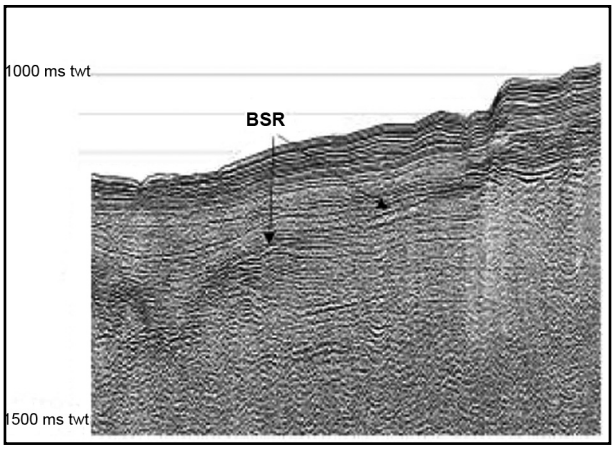

Fig. 35. Seismic line showing multiple BSR, offshore Romania (Ion *et al.*, 2002).

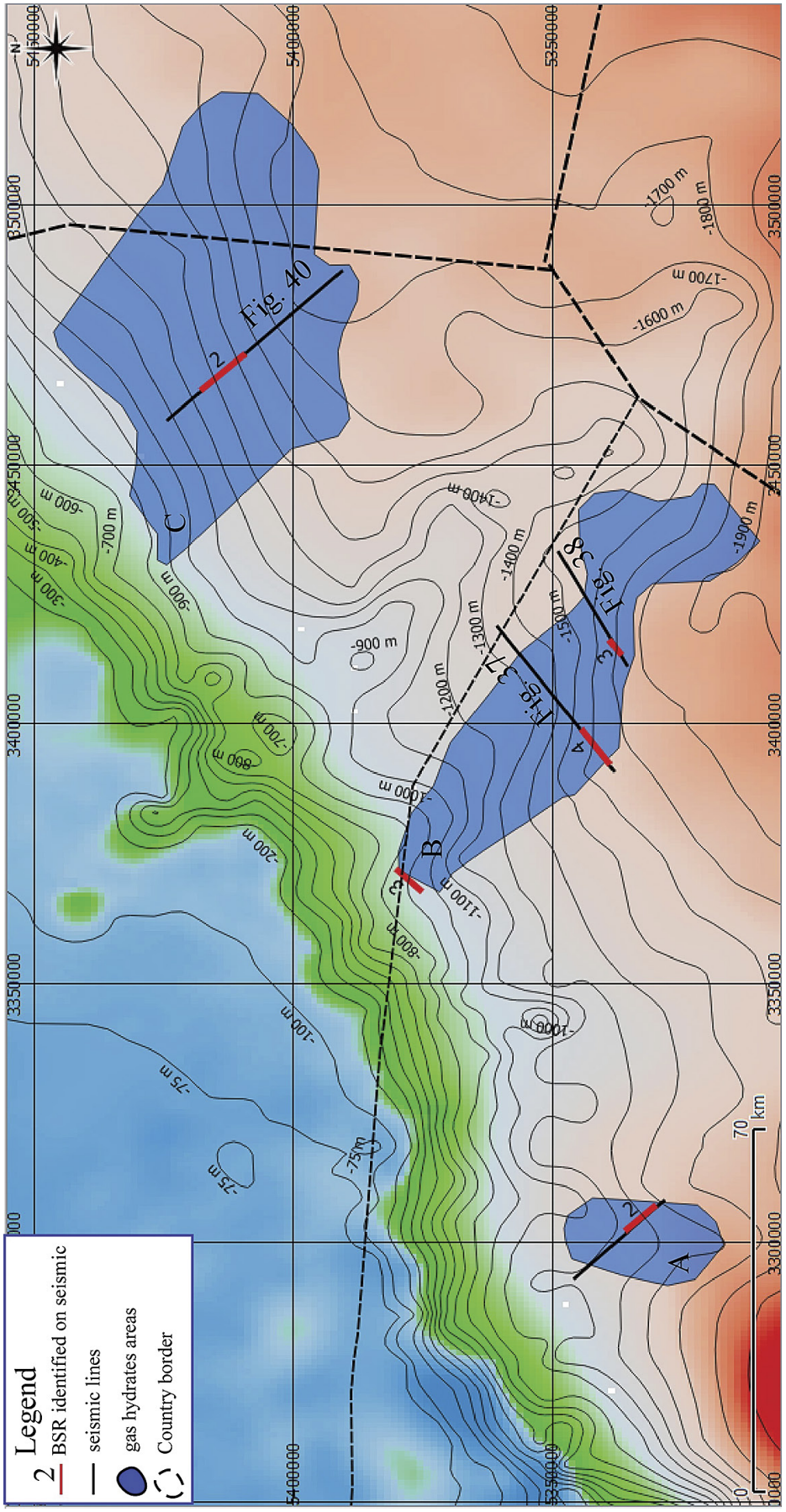

Fig. 36. Map showing the areas of BSR occurrence in the Danube deep-sea fan A, B, C (shown by light blue shading). Broad red tracklines show multiple BSRs, and associated numbers specify how many BSRs occur. Locations of profiles shown in Figures 37, 38 and 540 are indicated.

particular channel reservoir was favoured by burial under the fine grained stratified levees of the subsequent system, which resulted in the formation of relatively sealed isolated gas-bearing systems. Additionally, the typical lenticular shape of the channel–levee systems created topographic highs only partially buried, resulting in an anticlinal BGHSZ (Fig. 37) that is able to form a structural trap for free gas (Kvenvolden, 1998). In the lateral levees, free gas concentrates where the stratified deposits are sealed up-dip by the BGHSZ in a stratigraphic type gas trap (Fig. 37; Kvenvolden, 1998). We can thus define a specific pattern of relatively closed gas and hydrate accumulations under a combined lithological, structural and stratigraphic control. This pattern represents the background for the formation of multiple BSRs, and most probably influences the multiple BSR-forming processes.

Several characteristics of the BSR developed in the Romanian Black Sea shelf noticed by Popescu *et al., 2007* are similar with previous observations:

- (a) Multiple BSRs have a similar location and water-depth dependence as the upper hydrate-related BSR, which implies that the forming process is pressure and temperature controlled in a similar fashion.
- (b) All multiple BSRs show reversed polarity (Fig. 39) which reflects a negative acoustic impedance contrast and, which for the equilibrium BSR is associated with low velocity free gas below the BGHSZ. However, occurrence of free gas beneath the lower BSR is suggested by low velocities (Andreassen *et al.*, 2000). In this case, enhanced reflections are sometimes located below multiple BSRs, and indicate that amounts of free gas may lie beneath lower BSRs (Fig. 39).
- (c) The sediments hosting the double BSRs show a type of sedimentary facies characterized by mud-dominated stratified sediments with intercalations of sand. This convergence suggests that the mechanisms causing the multiple BSRs should be compatible with this specific facies.

Beyond these common points, the multiple BSRs in the Danube fan offer remarkable particular characteristics that may contribute to advance understanding of these features:

- (a) Multiple BSRs occur as groups of successive reflections, implying that the process that produced them has a repetitive character. In addition, this feature is in contradiction to the idea that double BSRs could represent the boundaries of a transitional zone between hydrates and free gas, as proposed by Baba and Yamada (2004).
- (b) Multiple BSRs form in relatively isolated gas-bearing systems, controlled by the architecture of the Danube deep-sea fan deposits. As the formation of gas hydrates in partially closed systems may lead to specific physical changes to the sediment (Clennell *et al.*, 1999), these conditions need to be considered in the investigation of the processes forming multiple BSRs.

Lüdmann *et al.*, 2007 studied the characteristics of gas hydrates in the northwestern Black Sea, using a dataset of 87 multi-channel reflection seismic lines acquired by industry offshore Romania in the years 1994 and 2001 (Fig. 41) and a second dataset consists of seismic profiles obtained by the University of Hamburg during the GHOSTDABS cruise of 2001 (Lüdmann *et al.* 2004). The study area lies approximately 130 km offshore Romania at water depths ranging from 100 to 1,800 m, where the sedimentary system is represented largely by the Danube deep-sea fan (*e.g.*, Wong *et al.,* 1994; Winguth *et al.,* 2000; Popescu *et al.,* 2001, 2004).

The authors recognized on the seismic data, the facies types associated with deep-sea fan complexes such as the levee, overbank, and HAR (high-amplitude reflector) facies in the channel-levee systems as well as HARPs (high-amplitude reflection packages) and mass wasting facies (namely slides, slumps and debris flows) elsewhere. The distribution of BSRs is patchy, suggesting that gas hydrates occur only locally offshore Romania (Ion *et al.* 2002; Popescu *et al.* 2006) and, usually the BSRs marking the BGHSZ are confined to the channel-levee and overbank facies of the major channel-levee systems of the Danube River.

In the Romanian sector, the hydrates are found in two areas covering a total of about 2,900 km^2 (Fig. 41) with water depths ranging from 650 to 1,450 m, but extends to >1,900 m in the adjacent environs. Seismic line 17 shows a typical example of a BSR (Figs. 42 and 43) with the following reflection characteristics:

- (1) It has a high reflection coefficient, reaching up to 50 % of that of the seafloor;
- (2) It is characterized by a polarity opposite to that of the seafloor reflector;
- (3) It mimics the topography of the seafloor and may in places cross-cut the original stratification (Hyndman & Spence 1992).

Lüdmann *et al.,* 2007 as Popescu *et al.,* 2006, found multiples BSRs in the northern part of the analysed area (Fig. 41).

As an alternative interpretation, Lüdmann *et al*, 2004 suggest that the multiple BSRs in the Black Sea are related to differences in gas composition (*e.g.* methane and 26.0-28.3 % ethane). Each major channel-levee acts as a closed system sealed at the base and top by impermeable layers, namely the condensed sections deposited during sea-level highstands. The channels are orientated perpendicular to the continental margin and in the direction of the bottom gradient. Free gas and fluids can migrate upslope within the coarser channel-fill sediments characterized by high-amplitude reflections (HAR). As they reach a certain concentration in the upper channels, migration into the overbank deposits takes place.

Where the channel-levee system penetrates the GHZ, fluids and free gas are captured below the BGHSZ and cannot migrate farther upwards. This may increase the pressure locally and the gas and fluids can spread laterally into the over-

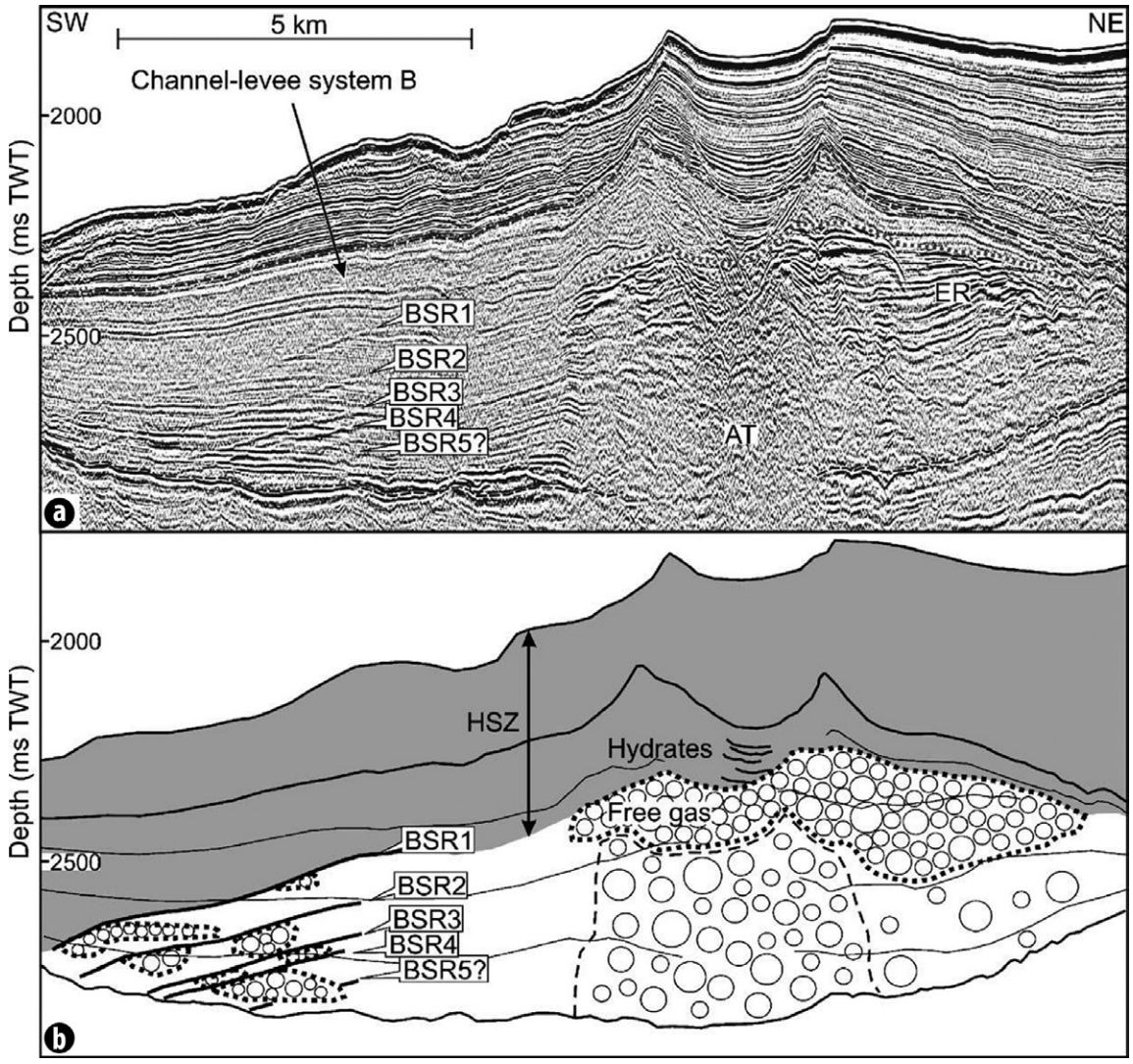

Fig. 37. Quadruple (quintuple ?) BSR accros zone B, location in Fig. 35. (**a**) Part of seismic reflection profile b039-GI. Seismic facies are indicated. ER=enhanced reflections, AT=acoustic turbidity. Dashed lines show top and bottom of the channel–levee system. Dotted line shows top of free gas. (**b**) Interpretation of the seismic image. Grey area is the hydrate stability zone (HSZ), circles indicate free gas. Note that free gas concentrates at the channel axis. Amounts of free gas also occur below BSRs 2, 3 and 4.

bank deposits, where the BSR is generally well-expressed (Fig. 43).

Lüdmann *et al.*, 2007 suggest that two processes contribute to gas hydrate accumulation on the slope off Romania: (1) microbial methane is generated by *in situ* methanogenesis; and (2) it is transported upwards with a significant amount of thermogenic hydrocarbons from deeper sources *via* permeable stratigraphic layers and/or along faults. A major hydrocarbon source rock in the study area is bituminous shales of the Oligocene Histria Formation (Dinu *et al.* 2005). Deep-seated Pontian to Dacian faults (Figs. 45 and 46) provided pathways for the ascent of wet hydrocarbons. These gases could have entered the channel-levee systems by diffusion or along minor faults or cracks. From there, they migrate upslope as a mixture with the lighter methane as free gas or in solution. During the ascent of the mixture, fractionation separates the hydrocarbons in accordance with their stability conditions. Hereby the lighter and smaller methane molecules migrate faster and may reach areas where the stability conditions for methane and water are satisfied.

Multiple BSRs with often a different number of BSRs occur in three separate channel-levee systems. This difference in BSR multiplicity may be a result of different gas mixtures in the systems.

Multiple BSRs which occur only in the Romanian sector probably represent boundaries of GHSZs containing different mixtures of methane and higher homologues. The latter originated from leaky Oligocene oil reservoirs, and migrated along deep-seated faults into the channels of the Danube deep-sea fan system. The alternative explanation, namely that the multiple BSRs are relicts of the former GHSZ under

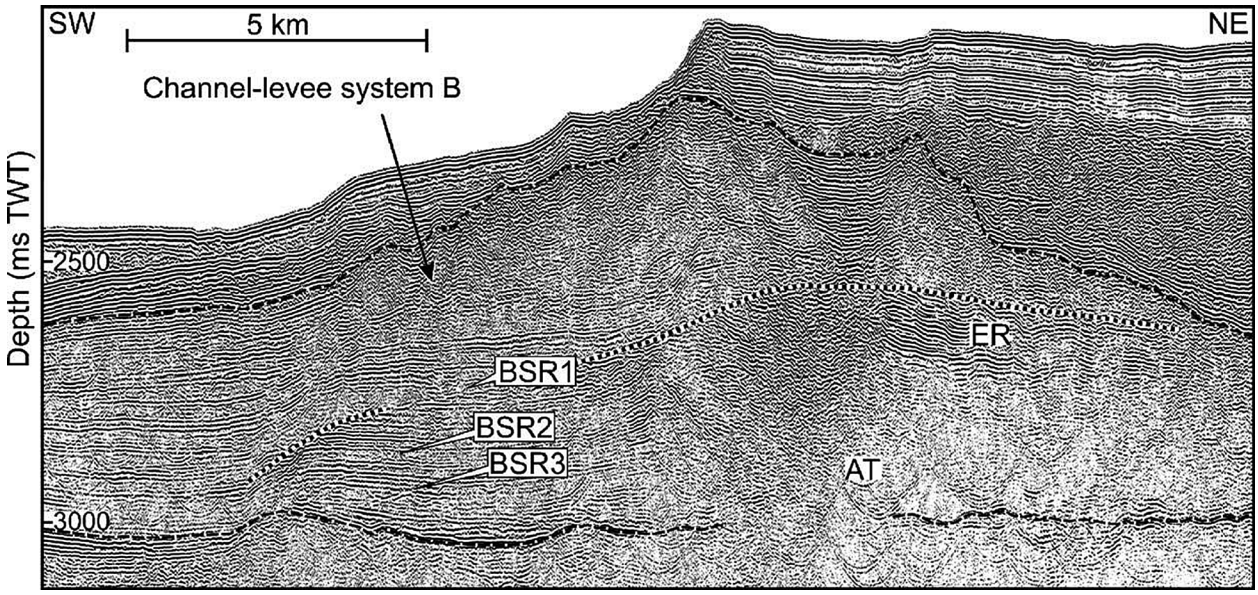

Fig. 38. Triple BSR across zone B: part of seismic reflection profile b102b-mini GI, location in Fig. 1. Seismic facies and limits are indicated as in Fig. 37.

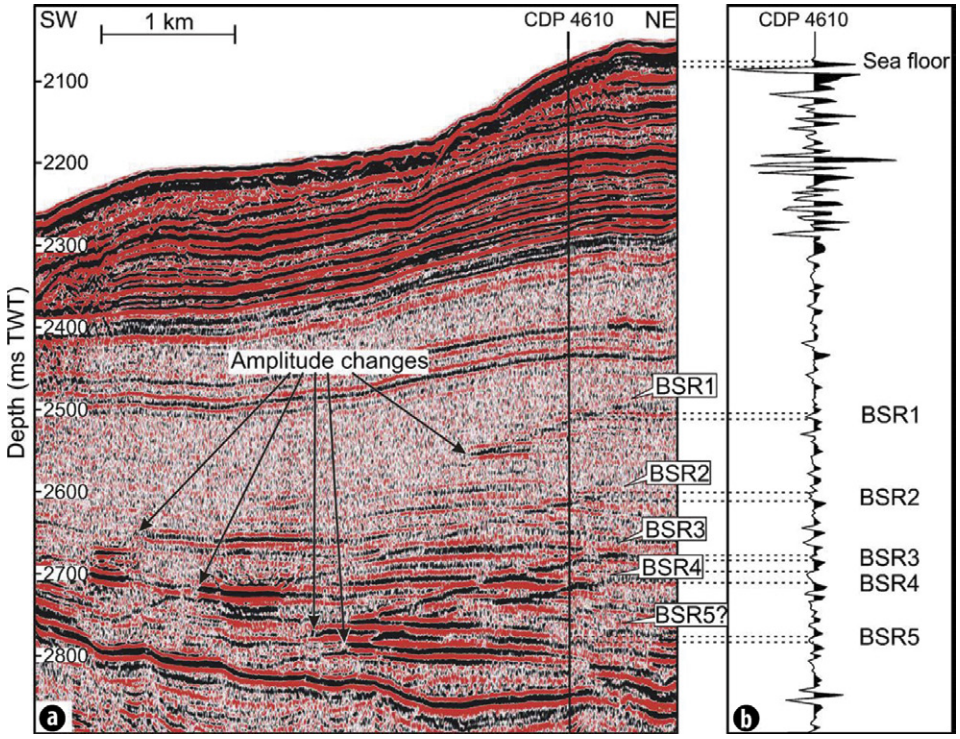

Fig. 39. Detail of the multiple BSRs shown in Fig. 40 (display in black–white–red scale). Some of the enhanced reflections change amplitude where they cross BSR1 but also lower BSRs 2, 3 and 4, indicating that free gas occurs locally beneath multiple BSRs.

different *P-T* conditions, seems less likely. For example, the time required to produce a 5 °C downward increase in temperature at the present BSR position would be about 50 kyr. The influence of temperature fluctuations might be only relevant near the upper slope where the GHSZ pinches out and heat could propagate much more rapidly into the sub-bottom.

Zander *et al.*, 2017 used 2D multichannel seismic data for identification and mapping of anomalous multiple bottom simulating reflectors (BSR), which were observed in the levee deposits of a buried channel-levee system in the Danube deep-sea fan.

The most recent active channel of the Danube fan is the Danube channel (Fig. 47), which was connected to the mouth of the Danube river by the Danube canyon at the shelf break (Popescu *et al.*, 2001). The erosive Danube canyon terminates in a channel-levee system at about 800 m water depth (Lericolais *et al.*, 2013) and developed during the last glacial period about 25 ka BP when the sea-level was up to 150 m lower than today (Winguth *et al.*, 2000). As observed in other river

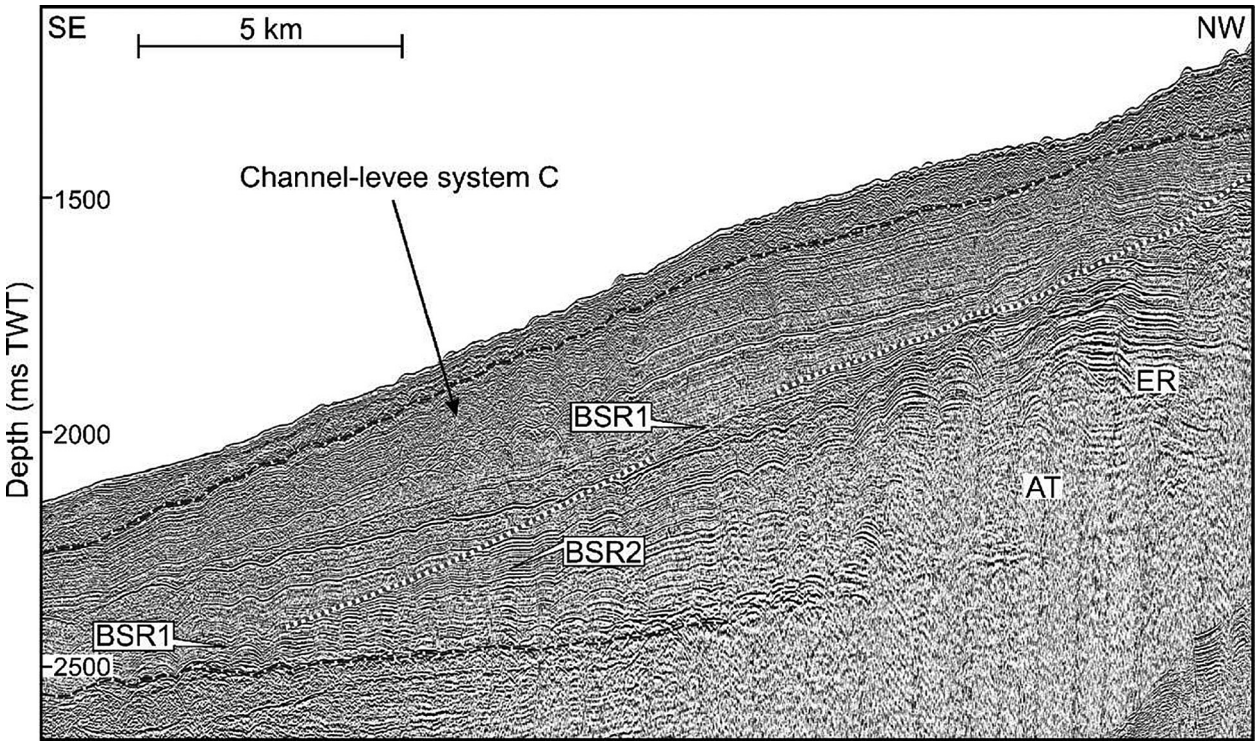

Fig. 40. Double BSR along zone C: part of the seismic reflection profile b007-miniGI, location in Fig. 1. Seismic facies are indicated as in Fig. 37.

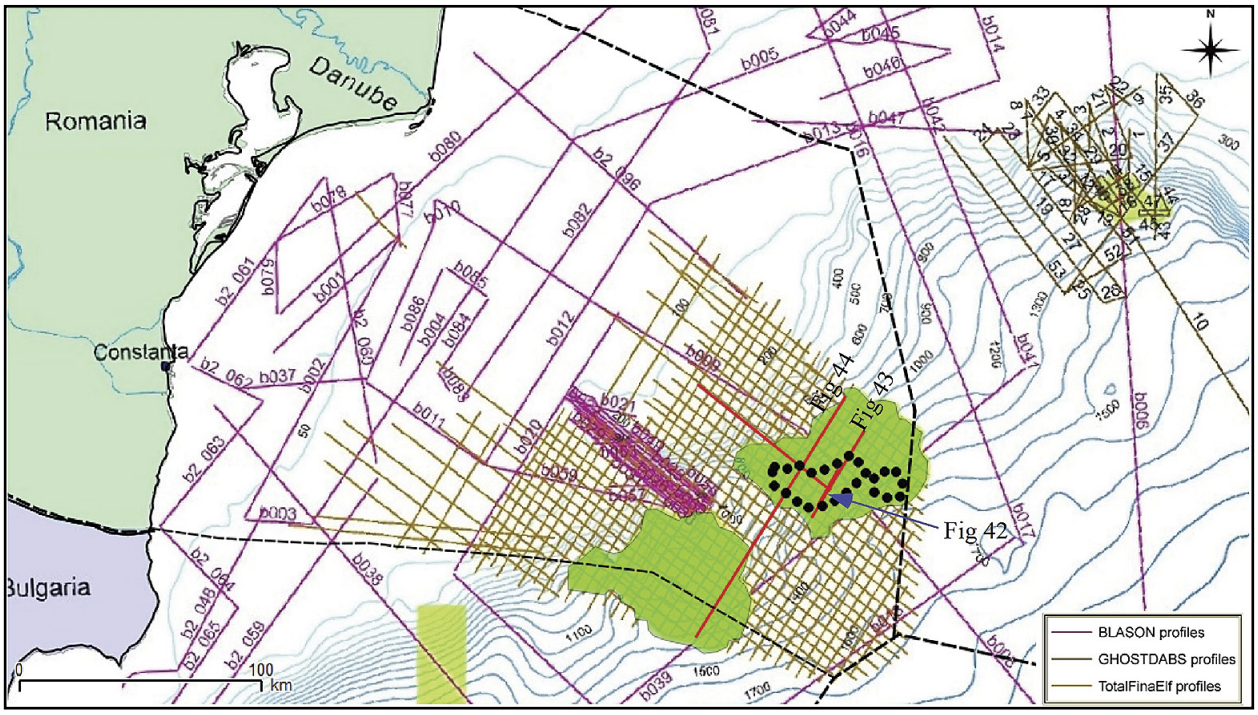

Fig. 41. Location of seismic profiles across the western Black Sea: **red** – high-resolution BlaSON profiles, **black** – profiles from GHOSTDABS, **brown** – profiles from industry. (Lüdmann *et al.*, 2007).

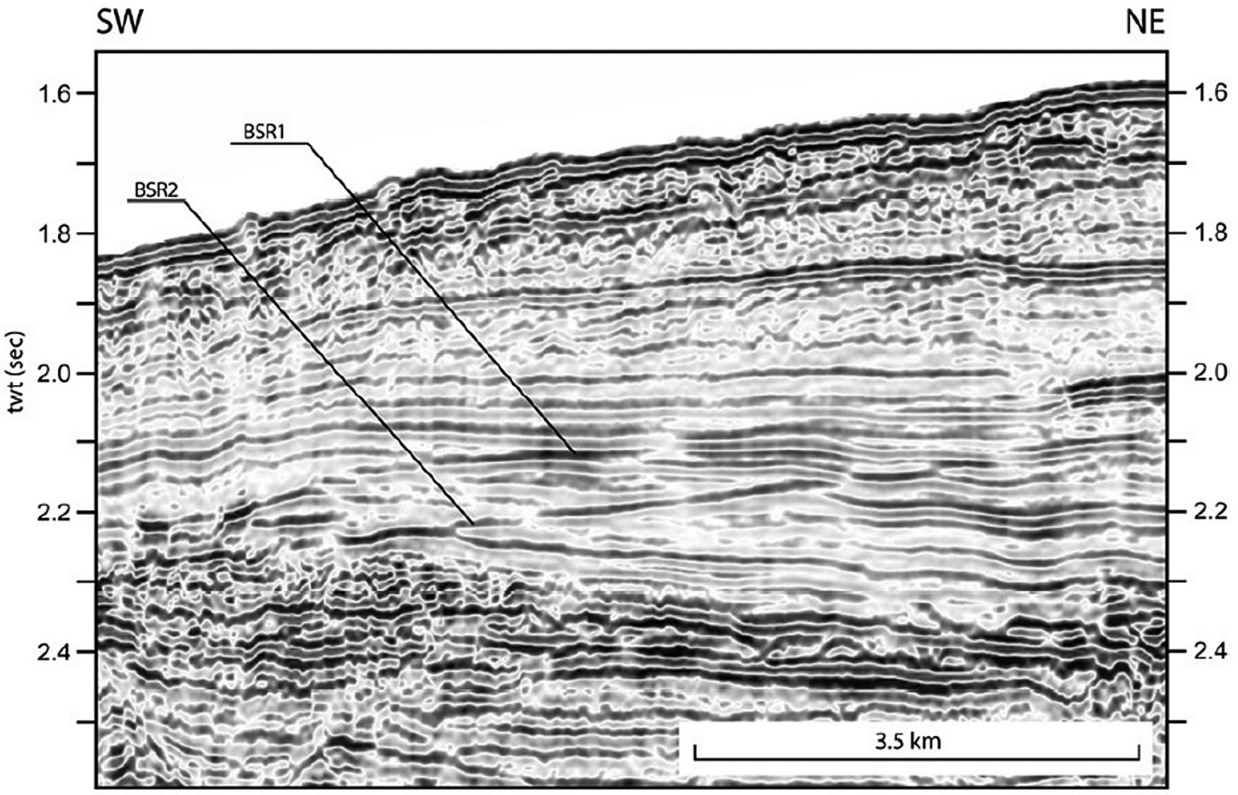

Fig. 42. Part of seismic line 17 showing BSR1 that marks the base of the methane hydrate stability zone and BSR2, the stability zone of a mixture of methane and higher homologues.

fans of the northern hemisphere, the right-hand (western) levees are more pronounced than the left-hand (eastern) levees because of the Coriolis force (Popescu *et al.*, 2001). Several older channels can be identified from the bathymetry such as a channel westwards of the Danube channel named SUGAR channel in this study (Fig. 47).

The upper limit of the gas hydrate stability zone (GHSZ), calculated for the observed bottom water temperature of 9 °C and a limnic pore water salinity of 3‰, is located in a water depth of 665 m. This is supported by the observation of numerous gas flares in water depths shallower than 665 m and much fewer gas flares at greater water depth in parts of the Danube fan (Zander *et al.*, 2017), and other areas of the Black Sea such as the Dnieper fan (Naudts *et al.*, 2006) or the Don-Kuban fan (Römer *et al.*, 2012). The expelled gas is primarily composed of methane of biogenic origin with concentrations of 99.1 – 99.9 % (Poort *et al.*, 2005; Römer *et al.*, 2012).

The shallowest BSR occurs in depths of about 320-380 m below the seafloor and generally runs parallel to the seafloor. It can be identified in large patches throughout the Danube deep-sea fan, as already observed in previous studies (Popescu *et al.*, 2006; Bialas, 2014).

The reflection amplitudes are generally low in an almost transparent seismic facies above the BSR, while they are high and of reversed polarity below the BSR (Fig. 48 C, D). The appearance of the BSR is continuous and sharp where it crosscuts strata (Fig. 48 B). Where it is parallel to the strata, the BSR is characterized by an abrupt amplitude increase with depth. The strongest amplitudes below the BSR are observed underneath the eastern levee, where several high-amplitude reflections pass from below the BSR into the transparent zone while undergoing a phase reversal at the BSR (Fig. 48D). The observed increased amplitudes below the BSR are often limited to individual reflectors that underlie a reflector of weaker amplitude (Fig. 48D).

Three additional BSRs are observed in the MCS data, named BSR 2-4 from top to bottom, underlying the shallowest BSR described above (Fig. 48 B, E). These BSRs are generally weaker in amplitude compared to the shallowest BSR, but they also represent a sharp and continuous boundary towards increased amplitudes below.

The stack of BSRs 2-4 is only observed in the well-stratified levee deposits of a buried channel levee system (BCL) identified in the subsurface (Fig. 49). The BSRs are generally limited to the western levee of the BCL, but on few RMCS profiles we also observed the BSR stack in the eastern levee (Fig. 48 B) where the overburden is thicker compared to the western levee (Fig. 49). The multiple BSRs are not observed in or underneath the channel axis, and the reflections of all BSRs fade out where they intersect with the base of the BCL (Fig. 49A).

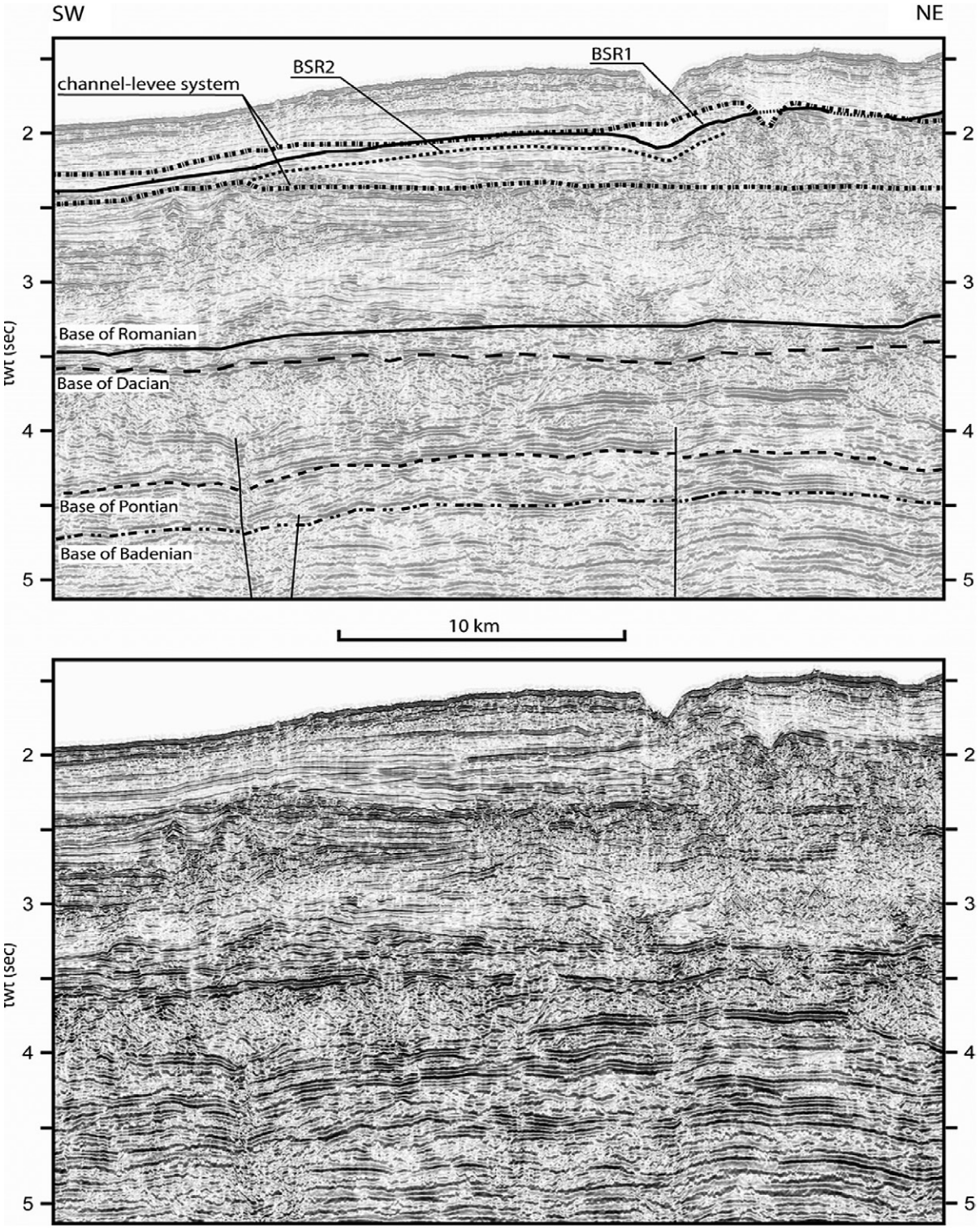

Fig. 43. Part of profile 17 showing that the BSR is confined to the channel-levee and overbank deposits. Note the diffuse reflection pattern throughout the sedimentary column which is interpreted to be a result of gas accumulations.

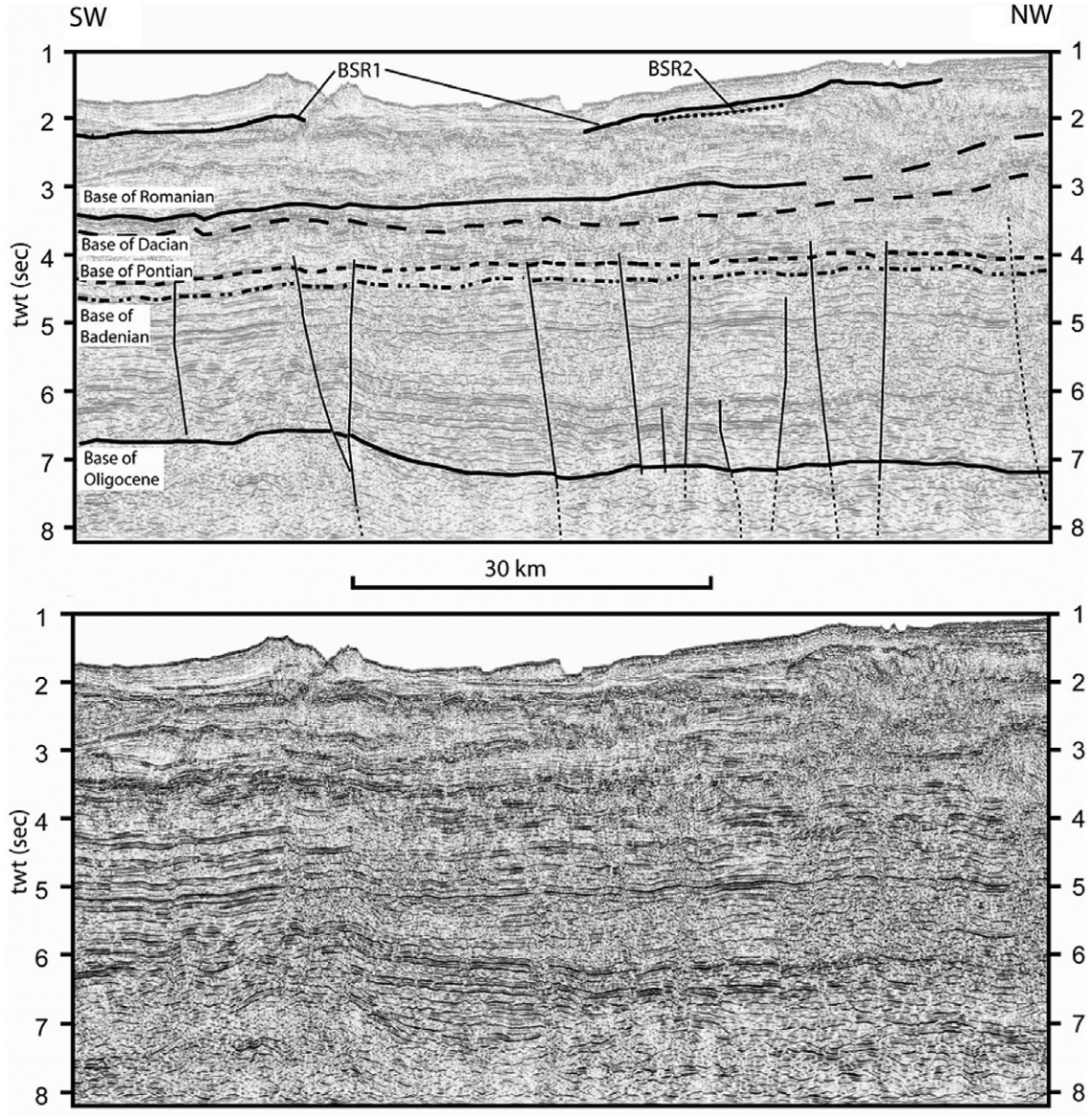

Fig. 44. Part of profile 20 which crosses the 2 BSR areas. Deep-seated faults which penetrate the base of the Pontian are also shown. Note the diffuse reflection pattern throughout the sedimentary column which is interpreted to be a result of gas accumulations.

The BCL is overlain by the outer levee deposits of the Danube channel (Fig. 49A). A sediment unit (layer A) exists between the BSL and the Danube levee and is characterized by an average thickness of about 80 m. The structure of layer A is homogeneous and layered sub-horizontally. Earlier studies by Winguth *et al.* (2000) indicate the depositional ages of the main depositional units in this area. The Danube levee was deposited over the past 75 ka during the last major glacial cycle, and the BCL was deposited during the period of 500 – 320 ka BP. Layer A consequently was deposited during the period of 320 – 75 ka BP.

The existence of previously identified multiple BSRs of the Danube deep-sea fan has been confirmed by new 2D multichannel seismic data. A stack of four BSRs was observed in the levee deposits of a buried channel-levee system. The multiple BSRs do not represent gas composition changes or over-pressured compartments, but reflect past pressure and temperature conditions. Our modelling results suggest that temperature effects of rapid sediment deposition rather than bottom-water temperature change or sea level variations dominate the pressure and temperature conditions leading to the multiple BSRs.

The analysis of new high-resolution 2D seismic data reveals that the distribution of anomalous multiple BSRs is limited to the levees of a buried channel-levee system of the Danube deep-sea fan. Up to four BSRs overlying each other are observed. The shallowest BSR thereby mimics the theoretical base of the GHSZ calculated from regional geothermal gradients and salinity data.

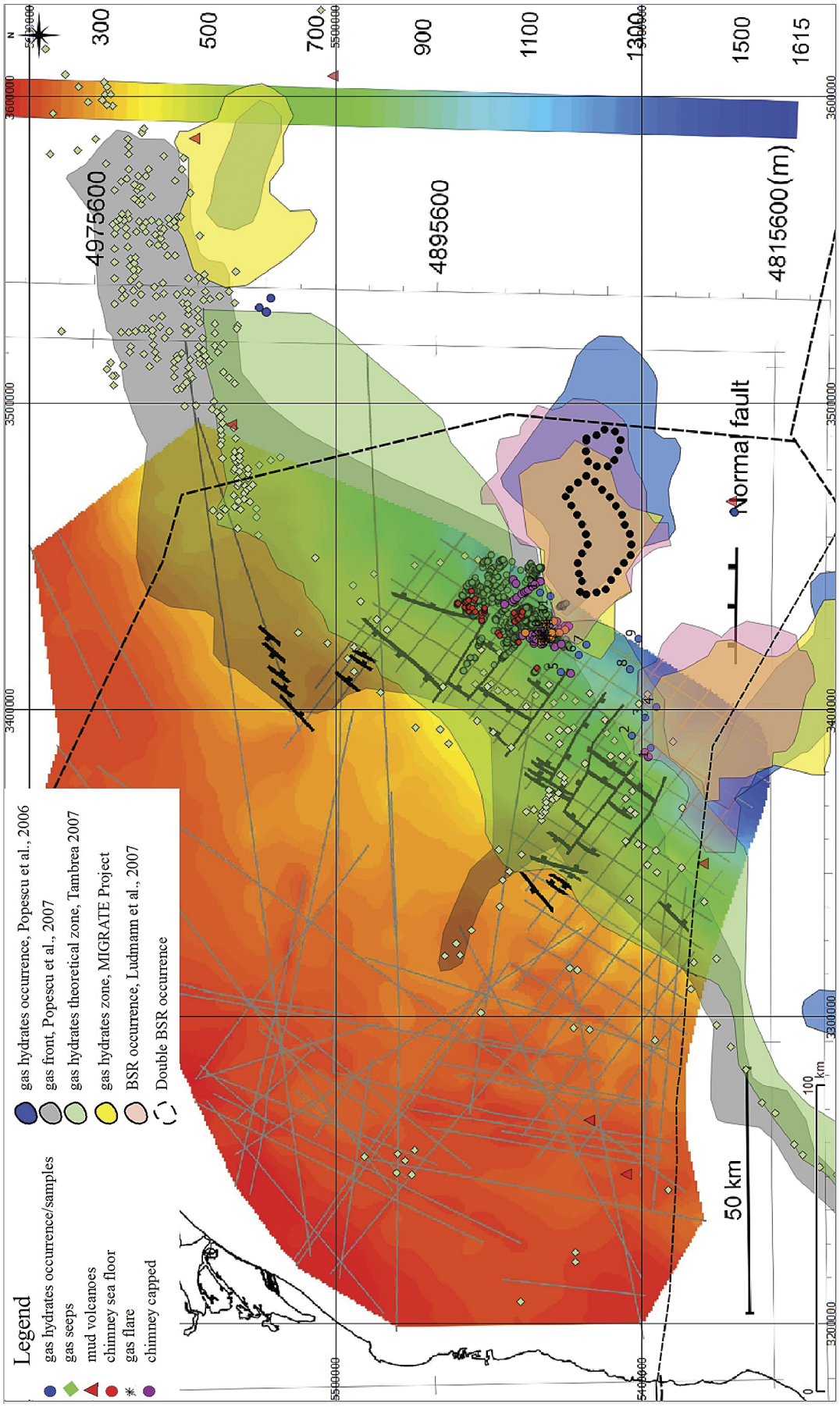

Fig. 45. Base Romanian-Quaternary sequence depth map (MBSL), illustrating the fault pattern (after Konerding *et al.*, 2010), on which we have superposed the gas hydrates, gas flares and seeps, gas chimneys, BSR occurrences areas (after Lüdmann *et al.*, 2007, Popescu *et al.*, 2006, 2007, Tambrea, 2007, Egorov *et al.*, 2011).

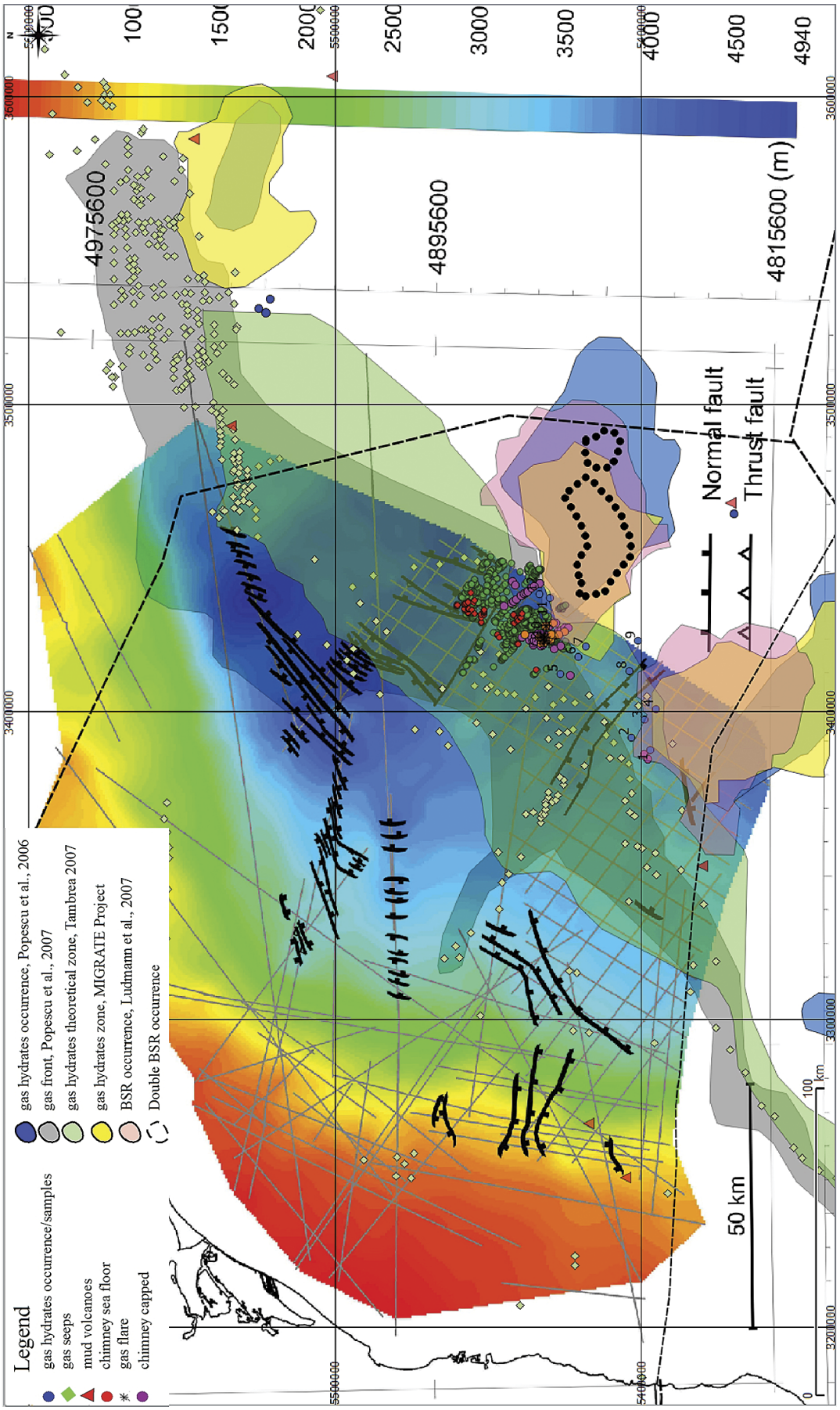

Fig. 46. Base Pontian depth map (MBSL), illustrating the fault pattern, after Konerding *et al.*, 2010; on which we have superposed the gas hydrates, gas flares and seeps, gas chimneys, BSR occurrences areas (after Lüdmann *et al.*, 2007, Popescu *et al.*, 2006, 2007, Tambrea, 2007, Egorov *et al.*, 2011).

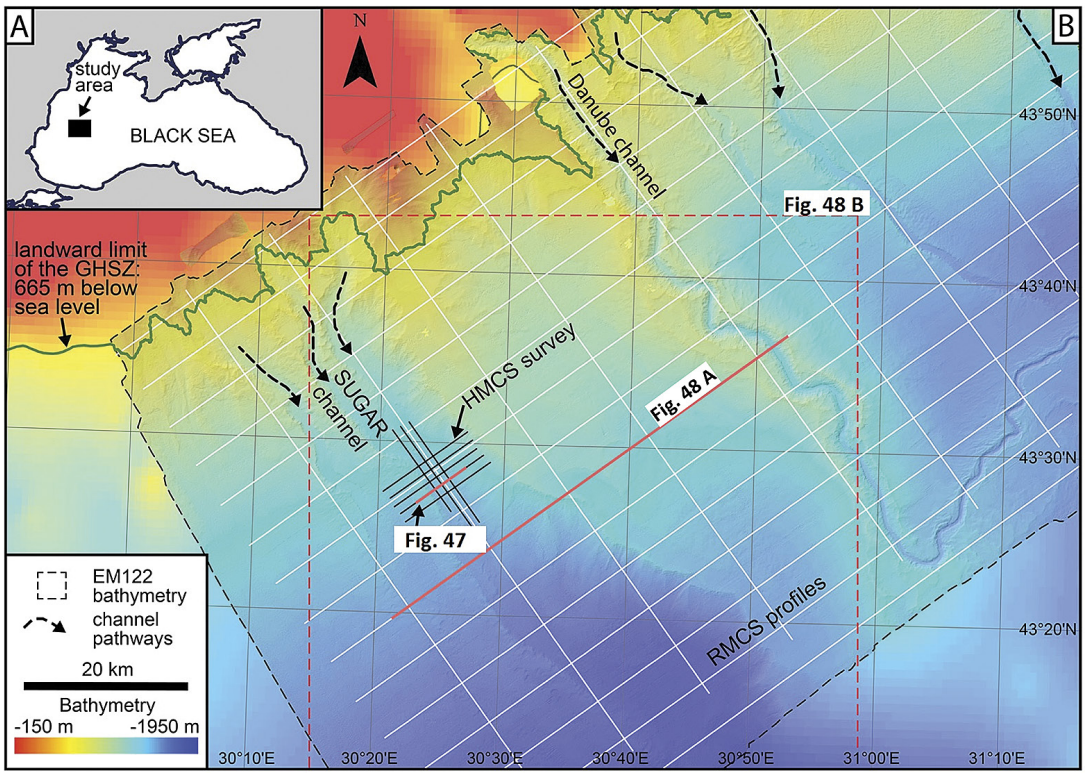

Fig. 47. Location of the study area in the northwestern Black Sea. (**b**) Overview map of the study area in the Danube deep-sea fan. **GHSZ** – gas hydrate stability zone, **HMCS** – 2D high-resolution multichannel seismic survey, **RMCS** – 2D regional multichannel seismic survey. Bathymetry and seismic data were acquired during R/V Maria S. Merian cruise MSM34 in 2013-2014 (Zander *et al.*, 2017).

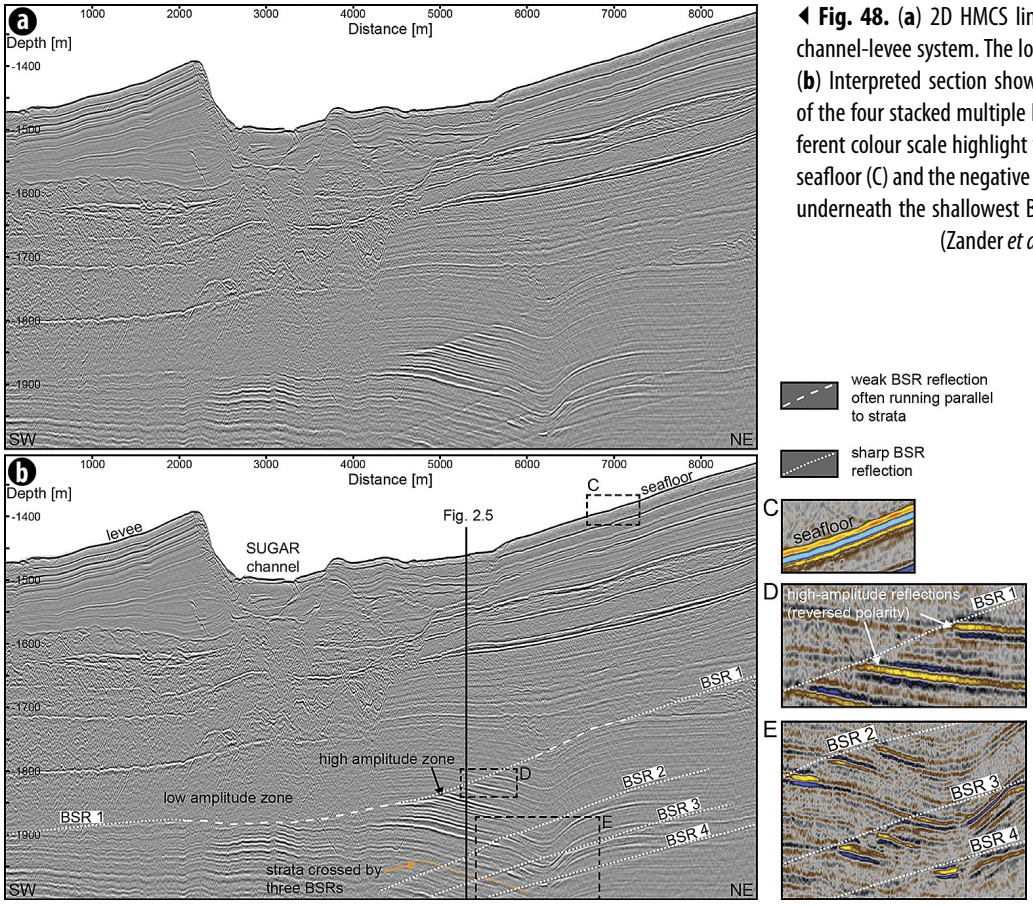

◂ **Fig. 48.** (**a**) 2D HMCS line 1107 across the SUGAR channel-levee system. The location is shown in Fig. 2.1. (**b**) Interpreted section showing the general character of the four stacked multiple BSRs. (**c-e**) Insets with different colour scale highlight the positive polarity of the seafloor (C) and the negative polarities of the reflections underneath the shallowest BSR 1 (D) and BSRs 2-4 (E) (Zander *et al.*, 2017).

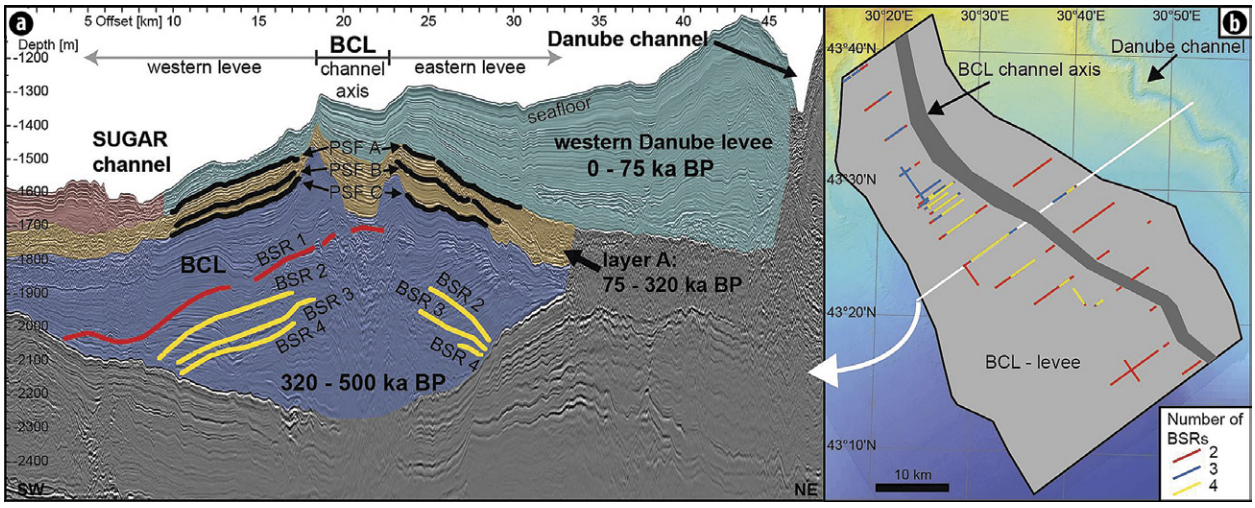

Fig. 49. (**a**) 2D RMCS line 09 across the SUGAR channel (red unit) and the western Danube channel levee (green unit) in the northeast. A buried channel-levee system (BCL) is identified in the subsurface (blue unit), underneath layer A (brown unit). The multiple BSRs (yellow lines) are solely observed in the levees of the BCL. Time frames for the deposition of the different facies units are adapted from the interpretation of Winguth *et al.* (2000) (Fig. 4 in their study). Three paleo seafloors were defined for the modelling of the BGHSZ under paleo conditions (black lines PSF A-C). (**b**) Extent of the BCL based on seismic data and highlighting the occurrence of more than one BSR. Locations of A and B are shown in Fig. 47 (Zander *et al.*, 2017).

Over-pressured gas compartments can be excluded as the cause for the formation of the deeper BSRs, because the height of the necessary gas column would significantly exceeds the vertical distance between two overlying BSRs. Instead, the results indicate that the deeper BSRs are paleo-BSRs, which could be related to paleo seafloor horizons located between the buried channel-levee system and the levee deposits of the Danube channel, the subsequent changes in paleo sea-floor change also the gas hydrates stability zone as this is affected by temperature and pressure.

The modelling results suggest that temperature effects of rapid sediment deposition rather than bottom-water temperature change or sea level variations dominate the pressure and temperature conditions leading to the multiple BSRs (Zander *et al.*, 2017). These changes are more distinctive in the Black Sea, and especially in the Danube area, because of the isolation of the Black Sea from the Mediterranean during sea level lowstands. The BSRs are therefore interpreted to reflect stages of stable sea level lowstands during glacial times. Their observation in seismic data indicates that small amounts of free gas are still present beneath each of the paleo-BSRs, and that buoyancy-driven upward gas migration is inhibited by the low gas concentrations. In addition, the paleo-BSRs may reflect the real geotherm (around 35 °C km^{-1}). These results suggest that the Danube area is not in a thermally steady state and is therefore still adapting to increasing bottom-water temperatures since the last glacial maximum. The multiple BSRs do not represent gas composition changes or over-pressured compartments, but reflect past pressure and temperature conditions.

Because hydrate dissociation may not occur for several thousands of years, such paleo BSRs remain well defined in seismic data. The authors propose that small amounts of free gas are present beneath each of the paleo BSRs. The gas saturation is high enough to cause an impedance contrast in seismic data, but low enough to inhibit buoyancy-driven upward migration. The paleo BSRs possibly reflect the real geotherm in the order of 35 ± 5° C/km, which is higher than the local geotherm of 24.5 ± 0.5° C/km derived from the shallowest BSR.

Riboulot *et al.*, 2017, analysed the gas hydrates from Romanian Black Sea shelf. The authors consider that this area deserves attention because here is located the Danube deep-sea fan, one of the largest sediment depositional systems in the largest anoxic sea in the world, having also a high energy potential. Due to the high sediment accumulation rate, presence of organic matter and anoxic conditions, the Black sea sediments offshore the Danube delta are rich in gas and thus show Bottom Simulating Reflectors (BSR). The cartography of the BSR over the last 20 years, exhibits its widespread occurrence, indicative of extensive development of hydrate accumulations and a huge gas hydrate potential. By combining old and new datasets acquired in 2015 during the GHASS campaign, Riboulot *et al.* performed a geomorphological analysis of the continental slope north-east of the Danube canyon compared with the spatial distribution of gas seeps in the water column and the predicted extent of the gas hydrate stability zone. This analysis provides new evidence of the role of geomorphological setting and gas hydrate extent in controlling the location of the observed gas expulsions and gas flares in the water column.

In the Romanian sector, BSR observation from conventional High Resolution (HR) seismic profiles, acquired during the BLASON and BLASON2 cruises, provides indirect evidence of GH occurrence (Fig. 50). It represents the base of the GHSZ that appears as strong, negative-polarity, high-impedance seismic reflection caused by free gas at the base of the phase boundary (Holbrook *et al.*, 1996). The BSR in the study area is characterized by a distinct seismic reflection, sub-parallel to the seafloor, showing reversed polarity, semi-continuous, crosscutting the sedimentary stratification and their position can also be inferred on the basis of aligned amplitude terminations as Bangs *et al.* (2005) described offshore Oregon (Fig. 18). The appearance of a strong impedance contrast at the location of the BSR with an enhancement of the seismic reflection amplitude is an indication of the presence of gas beneath GHs (Paull *et al.*, 1995). The absence of gas signature on seismic data over the BSR, presented in Fig. 51, provides useful information about the location of the gas, trapped beneath the BSR. The seal formed by GHs could be impermeable. At the landward termination of the GHSZ, the observed seismic hyperbola and deformation zone in the surficial sedimentary layers suggest gas migration or the presence of GHs close to the seafloor (Fig. 18).

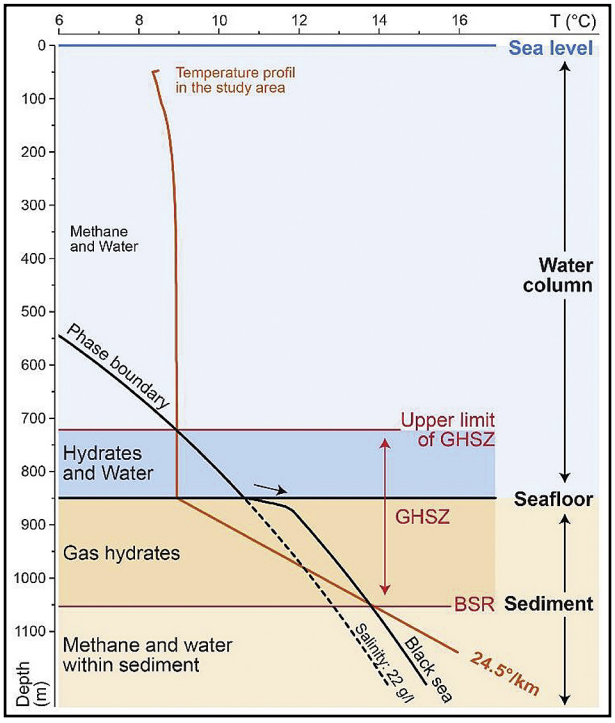

Fig. 50. Gas hydrate stability using pure s-I methane hydrate and the water column (S = 22 psu) and porewater (S=2; in depth higher than 25 mbsf) salinities. For this example used to illustrate the calculation (Seafloor: 850 m water depth), the minimum water depth where GHs are stable is 720 mbsl. The considered bottom water temperature, 8.9°C. For the regional geothermal gradients of 24.5°C/km, the base of GHSZ is 200 mbsf. These results are calculated in 2D and change with depth of the seafloor due to the evolution of the salinity within the sediment (Riboulot *et al.*, 2017).

Once the Riboulot *et al. 2017* established the presence of the gas hydrate in the Romanian Black Sea shelf, they tried to predict gas hydrate stability zone.

Theoretically determined phase equilibrium allow to distinguish natural GHs from water ice, and can therefore be used to calculate the temperature and pressure at which hydrates form from a given gas composition (Sloan and Koh, 2007). The variations of water column temperature, pore pressure and geothermal gradient affect the thickness of the GHSZ.

Seafloor temperature was considered to be 8.9 °C at 850 m water depth, determined by Sippican measurements during GHASS cruise. A hydrostatic pore-pressure gradient of 0.1 bar/m was assumed to calculate the depth scale (Kvenvolden, 1993). The geothermal gradient was measured with 7 temperature sensors welded at regular intervals along a 12 m long core barrel. The geothermal gradient considered in this study is 24.5 °C/km. The composition of the gas enclathrated in hydrate form is a primordial parameter to estimate the boundaries of GHSZ (Sloan, 2003). It is known that the main component of gas from the Black Sea hydrates is CH4 (93.3-99.7%: Vassilev & Dimitrov, 2003). As Poort *et al.*,2005 did, the authors assumed a composition of 100% methane for the composition of the hydrates (Judd *et al.*, 2002), but heavier hydrocarbons could be present and would shift the hydrate stability curve towards higher temperatures (Sloan and Koh, 2007).

The calculation of the GH stability curve was complicated because it is usually performed for a system composed of water with a constant concentration of salt (0 psu to >35 psu). In the study area, Soulet *et al.* (2010) showed a gradual fall in salinity from 21.9 psu at the seafloor level to near 2 psu at around 28 m below the sea floor. In the case presented (Fig. 50), the calculation has been made using a salinity of 22 psu for the water column (850 m), a gradual fall of the salinity for the uppermost 28 m of sediment (the salinity of 22 psu at the seafloor reaching 2 psu in sediment at 28 mbsf) and a constant salinity of 2 psu for the rest of sedimentary column. The intersection of the GH stability curves with the water column temperature curve denotes the minimum water depth at which GHs are stable for a given water depth (Fig. 50), while the intersection with the geothermal gradient reveals the predicted base of the GHSZ (Kvenvolden, 1993).

The calculation to obtain a predicted GHSZ was made at different water depths. An example of the calculation for a water column of 850 m is shown in Fig. 50. For this example, the intersection of the GH stability curves with the water column temperature curve at around 730 m indicates the water depth at which GHs are stable in this location of the Black Sea. The thickness of the GHSZ is 200 m. The predicted base of GHSZ is in agreement with the depth of the BSR observed in the study area (215 mbsf at 850 m water depth: Fig. 50). The minimum water depth where GHs begin to be stable is 660 m at around 20 mbsf and the thickness of the GHSZ would

be 20 m. Riboulot *et al.*2017, theoretically find stable GHs at the seafloor starting from 720 m water depth towards deeper waters.

8. DISCUSSION

Impact of geomorphology and neo-tectonics in free gas expulsion, the distribution of gas flares observed in the water column of the Romanian shelf are in agreement with the free gas areas defined in Popescu *et al.* (2007) or gas hydrates zone of Tambrea (2007). However, in some cases, several gas flares are detected downward the areas defined in the literature: many gas flares are inside the BSR zone defined in (Popescu *et al.*, 2006) close to the landward termination of the BSR (Fig. 51). The causes of this mismatch could be attributed to an evolution of the degassing zone in the water column over the last 10 years and/or to the variety of the data analysis. The free gas area described by Popescu *et al.* (2006) was derived from seismic data interpretation while the gas flare areas defined by Ribollout *et al.* (2017) comes from analysis of acoustic data, a methodology used recently for the identification of seepage activity at continental margins. Another explanation for this mismatch might be due to the paleo-BSR recorded in the seismic data, which locally if two or three of them appears, hence a separation between current and paleo BSR can be made (Lüdmann *et al.*, 2007).

The seepage activity is a relatively widespread phenomenon that has recently, during the last decades, enter into attention of researchers and oil industry companies with the development of water column mapping and technology (Popescu *et al.*, 2007).

The distribution of the gas seeps in the Romanian sector of the Black Sea coincides in most cases with the presence at the seafloor of sediment deformation features. Most of the gas flares are located above canyons (Fig. 51), landslides, pockmarks and fault/ crest line (Figs. 44, 45 and 51).

The spatial distribution of pockmarks suggests that all the discontinuities within the sedimentary column represent potential drains for fluid flow, and that simple diffusion through the sediments cannot explain the observed pattern of fluid expulsion. The spatial distribution of a large proportion of the gas flares in the Romanian Black Sea shelf seems to be associated with gas contained in underlying sediment using discontinuities formed by landsliding. The discontinuities resulted from mass wasting processes inside and outside the canyons are probably responsible for the gas seepages, by providing preferential migration pathways to gas as Riboulot *et al.* (2013) demonstrated in the Niger delta where a buried landslide controls the distribution of the seafloor pockmarks.

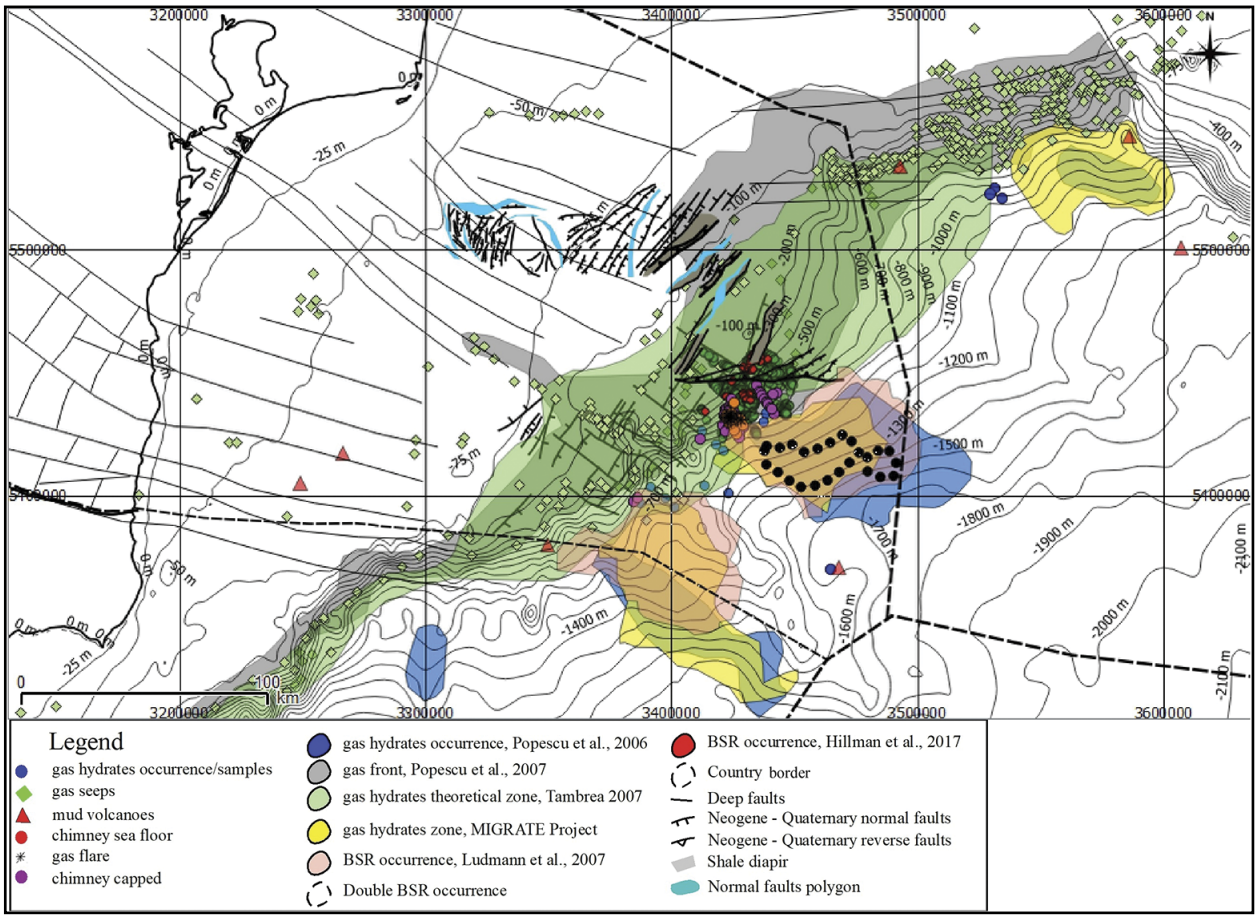

Fig. 51. Map with the location of gas related structures, integrating all the study's results.

Ribolot *et al.*, (2017) inferred that numerous gas seeps have been described above a crest line that represents 2% of the whole gas seeps detected in area. They interpret that the crest line as the seafloor evidence of the presence of a fault affecting the underlying sedimentary sediments (Fig. 44, Popescu *et al.*, 2004). If this is the case, it is supposed that the fluids accumulate under the base of the hydrate stability zone form a layer of free gas and the generation of excess pore fluid pressure in the free gas accumulation leads to the release of fluids along faults of the highly faulted interval responsible of the presence of free gas at the seafloor and in the water column.

Due to the concentration of gas seepages outside and at the landward termination of the GHSZ (98% of the whole degassing site) and the seismic anomalies observed under the BSR, they suggest that the presence of gas hydrates at the base of GHSZ constitutes an impermeable caprock over an accumulation of free gas. Indeed, gas hydrates may fill pore spaces and reduce sediment permeability, so that in some cases hydrate-bearing sediment may act as seal and result in gas traps. This interpretation is in agreement with the observations of Naudts *et al.* (2006) in the Dnieper paleo-delta area where the depth limit for the majority of the detected seeps coincides with the phase boundary of pure methane hydrate at 725 m water depth. They suggest gas hydrates play the role of seal for the upward migration of methane gas and thus prevent seepage of methane bubbles into the water column as it was proposed by Popescu *et al.* (2007) in the Danube Deep-Sea fan.

Indeed, the analysis of the seafloor morphology inside the GHSZ combined with the seismic stratigraphy provides useful information on the impact of gas hydrates on sedimentary deformation. The seafloor deformation, characteristics of the features named "gas-hydrate pockmarks" and described around the world are not observed in the study area. Gas hydrates pockmarks characterize seafloors where gas hydrates are present in the shallow sedimentary layers. Sediment deformation at the landward termination of the BSR may be induced by gas hydrates dynamics (Ribulot *et al.*, 2017). The presence of gas hydrates close to the seafloor generates a disturbance of the sedimentary deposits and the loss of their original sedimentary structures. It may be noted that several headwall scarps are observed at around 650 m water depth. The landward termination of the GHSZ coincides with these escarpments. One third of the gas seeps observed in the water column are localized right above scarps at the boundary with the GHSZ. It suggests gas hydrates dynamics may have an implication in sediment failure as it was interpreted by Westbrook *et al.* (2009). Further investigation will be needed to confirm this hypothesis.

9. CONCLUSIONS

Significant amount of data and new insights have been brought during the past decade for the understanding of gas expulsion and gas hydrates localization offshore Romania. An important advance which comes with the recent data is in the description of continental slope morphology of the Romanian sector of the Black Sea. The Black Sea shelf is affected by several landslides inside and outside canyons. It is a complex geological area where sedimentary processes such as: seafloor erosion and instability, mass wasting, formation of GHs, fluid migration, gas escape, have been identified by numerous studies and the geomorphology seems to dictate the location where gas seep occurs (Fig. 51). Most gas seeps tend to follow a pattern, they occur along canyon flanks, scarps, crest lines, faults and in association with pockmarks and mounts.

The depth limit of the gas seeps coincides with the predicted landward termination of GHSZ. This suggests that gas hydrates formed at the base of the GHSZ act as an effective seal preventing gas to reach the seafloor and the water column. The extent and the dynamics of gas hydrates have a probable impact on the sedimentary destabilization observed at the seafloor and the stability of the gas hydrates is dependent on the salinity gradient through the sedimentary column and thus on the Black Sea recent geological history.

One future area of research should focus on deciphering of connection between deep seated faults and gas hydrates formation and gas expulsion zones, which are still poorly understood. One reason for this is the technical gap between the shallow penetration of academic seismic lines and the lack of resolution of industry focused seismic lines. The cover of this gap might bring significant clues over the gas origin and accumulation pathways.

ACKNOWLEDGEMENTS

Mihaela Muresan is gratefully acknowledged for her constructive comments and suggestions.

REFERENCES

Afanasenkov, A.P., Nikishin, A.M., Obukhov, A.N., 2007. Geology of the Eastern Black Sea, Scientific World, Moscow, 198 p. (in Russian).

Andreassen, K., Mienert, J., Bryn, P., Singh, S.C., 2000. A double gas-hydrate related bottom-simulating reflector at the Norwegian continental margin. *Ann. N.Y. Acad. Sci*., **912**, 126–135.

Bega, Z., Ionescu, G., 2009. Neogene structural styles of the NW Black Sea region, offshore Romania. The Leading Edge, **28**, 1082-1089.

Baba, K., Yamada, Y., 2004. BSRs and associated reflections as an indicator of gas hydrate and free gas accumulation: an example of accretionary prism and forearc basin system along the Nankai Trough, off central Japan. *Resour. Geol*., **54**, 11–24.

Bialas, J. (Ed.), 2014. FS Maria S. Merian Fahrtbericht/Cruise Report MSM-34/1 & 2 SUGAR Site. Berichte aus dem GEOMAR Helmholtz-Zentrum für Ozeanforschung Kiel, **15**.

Clennell, M.B., Hovland, M., Booth, J.S., Henry, P., Winters, W.J., 1999. Formation of natural gas hydrates in marine sediments: 1. Conceptual model of gas hydrate growth conditioned by host sediment properties. *J. Geophys. Res.*, **104**, 22985-23003.

Cloetingh, S., Spadini, G., Van Wees, J.D., Beekman, F., 2003. Thermo-mechanical modelling of Black Sea Basin (de)formation. *Sedimentary Geology*, **156**, 169-184.

Constantinescu, A.M., Toucanne, S., Dennielou, B., Jorry, S.J., Mulder, T., Lericolais, G., 2015. Evolution of the Danube Deep-Sea Fan since the Last Glacial Maximum: new insights into Black Sea water-level fluctuations. *Marine Geology*, **367**, 50-68.

Dickens G.R, Quinby-Hunt MS, 1994. Methane hydrate stability in sea water. *Geophys Res Lett*., **21**(*19*), 2115–2118.

Dimitrov, L.I., 2002. Mud volcanoes – the most important pathway for degassing deeply buried sediments. *Earth-Science Reviews*, **59**, 49-76.

Dinu, C., Wong, H.K., Tambrea, D., Matenco, L., 2005. Stratigraphic and structural characteristics of the Romanian Black Sea shelf. *Tectonophysics*, **410**, 417-435.

Doglioni, C., Busatta, C., Bolis, G., Marianini, L., Zanella, M., 1996. Structural evolution of the eastern Balkans (Bulgaria). *Marine and Petroleum Geology*, **13**, 225-251.

du Fornel, 1999. Architecture du cône profond du Danube en sismique réflexion 2D. MSc Thesis, Université de Montpellier II, France.

Duley, P., Fogg, A., 2009. Old dogs and new tricks; unlocking the hydrocarbon potential of the Romanian Black Sea: Ana and Doina gas fields and the role of inversion in derisking. *The Leading Edge*, **28**, 1090-1096.

Egorov, V., Nasu, C., Gulin, S.B., Artemov, Y., Stokozov, N., Kostova, S., 2003. Modern concepts of the Medium-efficiency and environmental role of earth methane gas deposits from the Black Sea bottom. *Marine Environmental Journal*, **3**, 5-26.

Egorov, V., Artemov, Y., Gulin, S., Polikarpov, G., 2011. Methane seeps in the Black Sea: discovery, quantification and environmental assessment. *Black Sea/Mediterranean Enviroment Journal*, **17**, 171-185.

Erickson A.J., Von Herzen R. P., 1978. Downhole temperature measurements and heat flow data in the Black Sea – DSPD Leg 42B, in Ross DA, Neprochnov YP and the Scientific Party of DSDP Leg 42B - Initial reports of the Deep Sea Drilling Project Leg 42B. Washington, DC, 1085-1101.

Finetti, I., Bricchi, G., Del Ben, A., Pipan, M., Xuan, Z., 1988. Geophysical study of the Black Sea. Bollettino di Geofisica Teorica ed Applicata XXX, 197-324.

Garcia-Gil, S., Vilas, F., Garcia-Garcia, A., 2002. Shallow gas features in incised-valley fills (Ría de Vigo, NW Spain): a case study. *Cont Shelf Res*., **22**, 2303-2315

Gillet, H., Lericolais, G., Rehault, J.-P., Dinu, C., 2003. La stratigraphie oligo-miocene et la surface d'érosion messinienne en mer Noire, stratigraphie sismique haute résolution. C. R. *Geoscience*, **335**, 907-916.

Gillet, H., 2004. La stratigraphie tertiaire et la surface d'errosion messinienne sur les marges occidentales de la Mer Noire: stratigraphie seismique haute resoulution, L'universite de Bretagne Occidentale, Brest, 260 p.

Gillet, H., Lericolais, G., Réhault, J.-P., 2007. Messinian event in the black sea: Evidence of a Messinian erosional surface. *Marine Geology*, **244**, 142-165.

Ginsburg, G.D., Soloviev, V.A., 1998. Submarine Gas Hydrates, St. Petersburg, Russia.

Görür, N., 1988. Timing of opening of the Black Sea basin. *Tectonophysics*, **147**, 247-262.

Golmshtok, A.Y., Zonenshain, L.P., Terekhov, A.A., Shainurov, R.V., 1992. Age, thermal evolution and history of the Black Sea Basin based on heat flow and multichannel reflection data. *Tectonophysics*, **210**, 273-293.

Graham, R., Kaymakci, N., Horn, B., 2013. The Black Sea: Something Different? Geo Expro, 60-63.

Greinert, J., Artemov, Y., Egorov, V., De Batist, M., McGinnis, D., 2006. 1300-m-high rising bubbles from mud volcanoes at 2080m in the Black Sea: Hydroacoustic characteristics and temporal variability. *Earth and Planetary Science Letters*, **244**, 1-15.

Hillman, J. I. T., Klaucke, I., Bialas, J., Feldman, H., Drexler, T., Awwiller, D., Atgin, O., Çifçi, G., Badhani, S., 2018. Gas migration pathways and slope failures in the Danube Fan, Black Sea. *Marine and Petroleum Geology*, **92**, 1069-1084.

Holbrook, W. S., Hoskins, H., Wood, W. T., Stephen, R. A., Lizarralde, D., 1996. Methane Hydrate and Free Gas on the Blake Ridge from Vertical Seismic Profiling. *Science*, **273**, *5283*, 1840 p.

Hsü, K.J., Giovanoli, F., 1979. Messinian event in the black sea. *Palaeogeography, Palaeoclimatology, Palaeoecology,* **29**, 75-93.

Hunt, J.M., 1974. Hydrocarbon geochemistry of the Black Sea. In: Degens ET, Ross DA (eds) The Black Sea-geology, chemistry and biology. AAPG Memoir 20. Tulsa, Oklahoma, 499-504.

Hyndman, R.D., Spence, G.D., 1992. A seismic study of methane hydrate marine bottom simulating reflectors. *J. Geophys. Res*., **97**(*5*), 6683-6698.

Ion, G., Lericolais, G., Nouze, H., Panin, N., Ion, E., 2002. Seismo-acoustic evidence of gases in sedimentary edifices of the paleo-Danube realm. CIESM Workshop, **17**, 91-95.

Ivanov, M.V, Vainstein, M.B, Galchenko, V.F, Gorlator, S.N, Lein, A.Y., 1983. Distribution and geochemical activity of bacteria in sediments of the western part of the Black Sea. In: Geochemical processes in the western part of the Black Sea. Bulgarian Academy of Science, Sofia, 150-181.

Ivanov, M.K, Limonov, A.F, van Weering, TjCE, 1996. Comparative characteristics of the Black Sea and Mediterranean Ridge mud volcanoes. *Mar Geol*., **132**, 253-271.

Ivanov, M.K., Limonov, A.F., Woodside, J.M., 1998. Extensive deep fluid flux through the sea floor on the Crimean continental margin (Black Sea). Geological Society, London, Special Publications, **137**, 195.

Ivanov, M.V, Pimenov, N.V, Rusanov, II, Lein, AYu., 2002. Microbial processes of the methane cycle at the north-western shelf of the Black Sea. *Estuarine, coastal and shelf science*, **54**, 589-599.

Ivanov, Z., 1988. General Framework of the Rhodope Massif Geological and Structural Development, in the Balkanides Setting. *Bulletin De La Societe Geologique De France*, **4**, 227-240.

Jipa, D.C., Olariu, C., 2009. Dacian basin: depositional architecture and sedimentary history of a Paratethys sea. National Institute of Marine Geology and Geo-ecology, Bucharest.

Judd, A., Hovland, M., 2007. Seabed Fluid Flow: the Impact on Geology, Biology and the Marine Environment. Cambridge University Press, Cambridge, UK.

Karstens, J., and Berndt, C., 2015, Seismic chimneys in the Southern Viking Graben – Implications for palaeo fluid migration and overpressure evolution. *Earth and Planetary Science Letters*, **412**, p. 88-100.

Kazmin, V.G., Shreider, A.A., Shreider, A.A., 2007. Age of the Western Black Sea Basin according to an analysis of the anomalous magnetic field and geological data. *Oceanology*, **47**, 571-578.

Kvenvolden, K.A., 1998. A primer on the geological occurrence of gas hydrate. Geological Society Special Publication, 9-30.

Kvenvolden, K.A., 1993. Gas hydrates-geological perspective and global change. *Reviews of Geophysics*, **388**/*31*, 173-173.

Khriachtchevskaia, O., Stovba, S., Popadyuk, I., 2009. Hydrocarbon prospects in the Western Black Sea of Ukraine. *The Leading Edge*, **28**, 1024-1029.

Khriachtchevskaia, O., Stovba, S., Stephenson, R., 2010. Cretaceous-Neogene tectonic evolution of the northern margin of the Black Sea from seismic reflection data and tectonic subsidence analysis. Geological Society, London, Special Publications, **340**, 137-157.

Konerding, C., 2005. Mio-Pliocene sedimentation and structure of the Romanian shelf, northwestern Black Sea, Geowissenschaften. Hamburg University, Hamburg, 140 p.

Konerding, C., Dinu, C., Wong, H.K., 2010. Seismic sequence stratigraphy, structure and subsidence history of the Romanian Black Sea shelf. Geological Society, London, Special Publications, **340**, 159-180.

Kruglyakova, R.P., Byakov, Y.A., Kruglyakova, M.V., Chalenko, L.A., Shevtsova, N.T., 2004. Natural oil and gas seeps on the Black Sea floor. *Geo-Marine Letters*, **24**, 150-162.

Kutas, R.I., Kobolev, V.P., Tsvyashchenko, V.A., 1998. Heat flow and geothermal model of the Black Sea depression. *Tectonophysics*, **291**, 91-100.

Kutas, R.I., Paliy, S.I., Rusakov, O.M., 2004. Deep faults, heat flow and gas leakage in the northern Black Sea. *Geo-Marine Letters*, **24**, 163-168.

Kutas, R., Poort, J., 2008. Regional and local geothermal conditions in the northern Black Sea. *International Journal of Earth Sciences*, **97**, *2*, 353-363.

Kvenvolden, K.A., 1998. A primer on the geological occurrence of gas hydrate. Geological Society Special Publication, 9-30.

Lericolais, G., Guichard, F., Morigi, C., Minereau, A., Popescu, I., Radan, S., 2010. A post Younger Dryas Black Sea regression identified from sequence stratigraphy correlated to core analysis and dating. *Quaternary International*, **225**, 199-209.

Lericolais, G., Bourget, J., Popescu, I., Jermannaud, P., Mulder, T., Jorry, S., Panin, N., 2013. Late Quaternary deep-sea sedimentation in the western Black Sea: New insights from recent coring and seismic data in the deep basin. *Global and Planetary Change*, **103**, 232-247.

Letouzey, J., Biju-Duval, B., Dorkel, A., Gonnard, R., Krischev, K., Montadert, L., Sungurlu, O., 1977. The Black Sea: a marginal basin: geophysical and geological data, in: Biju-Duval, B., Montadert, L. (Eds.), Structural History of the Mediterranean Basins. Editions Technip, Paris, 363-376.

Limonov, A.F, van Weering, TjCE, Kenyon, N.H, Ivanov, M.K, Meisner, L.B, 1997. Seabed morphology and gas venting in the Black Sea mud volcano area: Observations with the MAK-1 deep-tow sidescan sonar and bottom profiler. *Mar Geol*., **137**, 121-136.

Lüdmann, T., Wong, H.K., Konerding, P., Zillmer, M., Petersen, J., Flüh, E., 2004. Heat flow and quantity of methane deduced from a gas hydrate field in the vicinity of the Dnieper Canyon, northwestern Black Sea. *Geo-Marine Letters*, **24**, 182-193.

Lüdmann, T., Wong, H.K., Baristeas, N., 2007. Characterization of gas hydrates and free gas occurrences in the northwestern Black Sea, unpublished work.

Matenco, L., Bertotti, G., Leever, K., Cloetingh, S., Schmid, S., Tărăpoancă, M., Dinu, C., 2007. Large-scale deformation in a locked collisional boundary: Interplay between subsidence and uplift, intraplate stress, and inherited lithospheric structure in the late stage of the SE Carpathians evolution. *Tectonics*, **26**, TC4011.

Matenco, L., Krézsek, C., Merten, S., Schmid, S., Cloetingh, S., Andriessen, P., 2010. Characteristics of collisional orogens with low topographic build-up: an example from the Carpathians. *Terra Nova*, **22**, 155-165.

Matoshko, A., Gozhik, P., Semenenko, V., 2009. Late Cenozoic fluvial development within the Sea of Azov and Black Sea coastal plains. *Global and Planetary Change*, **68**, *4*, 270-287.

Merey, S., Sinayuc, C., 2016. Analysis of the Black Sea sediments by evaluating DSDP Leg 42B drilling data for gas hydrate potential. *Marine and Petroleum Geology*, **78**, 151-167.

Merten, S., Matenco, L., Foeken, J.P.T., Stuart, F.M., Andriessen, P.A.M., 2010. From nappe-stacking to out-of-sequence post-collisional deformations: Cretaceous to Quaternary exhumation history of the SE Carpathians assessed by low-temperature thermochronology. *Tectonics*, **29**, 1-28.

Michaelis W, Seifert R, Nauhaus K, Treude T, Thiel V, Blumenberg M, Knittel K, Gieseke A, Peterknecht K, Pape T, Boetius A, Amann R, Jørgensen BB, Widdel F, Peckmann J, Pimenov N, Gulin MB, 2002. Microbial reefs in the Black Sea fueled by anaerobic oxidation of methane. *Science*, **297**, 1013-101.

Munteanu, I., Matenco, L., Dinu, C., Cloetingh, S., 2011. Kinematics of back-arc inversion of the Western Black Sea Basin.*Tectonics*, **30**, *5*, 21.

Munteanu, I., 2012. Evolution of the western Black Sea: Kinematic and sedimentological inferences from geological observations and analogue modelling, Amsterdam, Ipskamp Drunkkers B.V., Utrecht Studies in Earth Sciences.

Munteanu, I., Matenco, L., Dinu, C., Cloetingh, S., 2012. Effects of large sea-level variations in connected basins: the Dacian-Black Sea system of the Eastern Paratethys. *Basin Research*, **24**, 583-597.

Munteanu, I., Willingshofer, E., Sokoutis, D., Matenco, L., Dinu, C., Cloetingh, C., 2013. Transfer of deformation in back-arc basins with a laterally variable rheology: constraints from analogue modelling of the Balkanides - Western Black Sea inversion. Tectonophyiscs.

Munteanu, I., Willingshofer, E., Matenco, L., Sokoutis, D., Cloetingh, S., 2014. Far-field contractional polarity changes in models and nature. *Earth and Planetary Science Letters*, **395**, *0*, 101-115.

Naudts, L., Greinert, J., Artemov, Y., Staelens, P., Poort, J., Van Rensbergen, P., De Batist, M., 2006. Geological and morphological setting of 2778 methane seeps in the Dnepr paleo-delta, northwestern Black Sea. *Marine Geology*, **227**, 177-199.

Neprochnov, Y.P., Kosminskaya, I.P., Malovitsky, Y.P., 1970. Structure of the crust and upper mantle of the Black and Caspian Seas. *Tectonophysics*, **10**, 517-525, 531-538.

Neretin, L.N, Böttcher, M.E, Jørgensen, B.B, Volkov, II,, Lüschen, H., Hilgenfeldt, K., 2004. Pyritization processes and greigite formation in the advancing sulfidization front in the Upper Pleistocene sediments of the Black sea. *Geochim Cosmochim Acta*, **68**/*9*, 2081-2093.

Nikishin, A. M., Korotaev, M. V., Ershov, A. V., Brunet, M.-F., 2003. The Black Sea basin: tectonic history and Neogene-Quaternary rapid subsidence modelling. *Sedimentary Geology*, **156**, 1-4, 149-168.

Nikishin, A.M., Ershov, A.V., Nikishin, V.A., 2010. Geological History of Western Caucasus and Adjacent Foredeeps Based on Analysis of the Regional Balanced Section. *Doklady Earth Sciences*, **430**, 155-157.

Nikishin, A.M., Okay, A.I., Tüysüz, O., Demirer, A., Amelin, N., Petrov, E., 2015a. The Black Sea basins structure and history: New model based on new deep penetration regional seismic data. Part 1: Basins structure and fill. Marine and Petroleum Geology, **59**, 638-655.

Nikishin, A.M., Okay, A., Tüysüz, O., Demirer, A., Wannier, M., Amelin, N., Petrov, E., 2015b. The Black Sea basins structure and history: New model based on new deep penetration regional seismic data. Part 2: Tectonic history and paleogeography. *Marine and Petroleum Geology*, **59**, 656-670.

Okay, A.I., Sahinturk, O., 1997. Geology of the Eastern Pontides, in: Robinson, A.G. (Ed.), Tectonic-Sedimentary Evolution of the North-Tethyan Margin in the Central Pontides of Northern Turkey, 291-312.

Paull, C.K., Ussler, W., Borowski, W.S., Spiess, F.N., 1995. Methane-rich plumes on the Carolina 424 continental rise: associations with gas hydrates. *Geology*, **23**, 89-92.

Panin, N., Jipa, D., 2002. Danube River Sediment Input and its Interaction with the North-western Black Sea. *Estuarine, Coastal and Shelf Science*, **54**, 551-562.

Panin, N., 2003. The Danube Delta. Geomorphology and Holocene Evolution: a Synthesis / Le delta du Danube. Géomorphologie et évolution holocène : une synthèse. Géomorphologie : relief, processus, environnement, 247-262.

Peckmann, J., Reimer, A., Luth, U., Luth, C., Hansen, B.T, Heinicke, C., Hoefs, J., Reitner, J., 2001. Methane-derived carbonates and authigenic pyrite from the northwestern Black Sea. *Mar. Geol.*, **177**, 129-150.

Popescu, I., Lericolais, G., Panin, N., Wong, H. K., Droz, L., 2001. Late Quaternary channel avulsions on the Danube deep-sea fan, Black Sea. *Marine Geology*, **179**, *1-2*, 25-37.

Popescu, I., Lericolais, G., Panin, N., Normand, A., Dinu, C., Le Drezen, E., 2004. The Danube submarine canyon (Black Sea): morphology and sedimentary processes. *Marine Geology*, **206**, *1-4*, 249-265.

Popescu, I., De Batist, M., Lericolais, G., Nouzé, H., Poort, J., Panin, N., Versteeg, W., Gillet, H., 2006. Multiple bottom-simulating reflections in the Black Sea: Potential proxies of past climate conditions. *Marine Geology*, **227**, 163-176.

Popescu, I., Lericolais, G., Panin, N., Batist, M., Gillet, H., 2007. Seismic expression of gas and gas hydrates across the western Black Sea. *Geo-Marine Letters*, **27**, 173-183.

Poort, J., Vassilev, A., Dimitrov, L., 2005. Did postglacial catastrophic flooding trigger massive changes in the Black Sea gas hydrate reservoir?: *Terra Nova*, **17**, *2*, 135-140.

Popov, S.V., Shcherba, I.G., Ilyina, L.B., Nevesskaya, L.A., Paramonova, N.P., Khondkarian, S.O., Magyar, I., 2006. Late Miocene to Pliocene palaeogeography of the Paratethys and its relation to the Mediterranean. *Palaeogeography, Palaeoclimatology, Palaeoecology*, **238**, 91-106.

Riboulot, V., Cattaneo, A., Sultan, N., Garziglia, S., Ker, S., Imbert, P., Voisset, M., 2013. Sea-level change and free gas occurrence influencing a submarine landslide and pockmark formation and distribution in deepwater Nigeria. *Earth and Planetary Science Letters*, **375**, 78-91.

Riboulot, V., Cattaneo, A., Scalabrin, C., Gaillot, A., Jouet, G., Ballas, G., Marsset, T., Garziglia, S., Ker, S., 2017. Control of the geomorphology and gas hydrate extent on widespread gas emissions offshore Romania. *Bull. Soc. géol. Fr.*, **188**, 26.

Ricou, L.E., Burg, J.P., Godfriaux, I., Ivanov, Z., 1998. Rhodope and vardar: the metamorphic and the olistostromic paired belts related to the Cretaceous subduction under Europe. *Geodinamica Acta*, **11**, 285-309.

Robinson, A., Spadini, G., Cloetingh, S., Rudat, J., 1995. Stratigraphic evolution of the Black Sea: inferences from basin modelling. *Marine and Petroleum Geology*, **12**, 821-835.

Rögl, F., 1999. Mediteranean and Paratethys. Facts and hypotheses of an Oligocene to Miocene paleogeography. *Geologica Carpathica*, **50**, 339-349.

Römer, M., Sahling, H., Pape, T., Bahr, A., Feseker, T., Wintersteller, P., Bohrmann, G., 2012. Geological control and magnitude of methane ebullition from a high-flux seep area in the Black Sea – the Kerch seep area. *Marine Geology*, **319-322**, 57-74.

Ross, A.D., Stoffers, P., Trimonis, E.S., 1978. Black Sea sedimentary framework, in: Institution, W.H.O. (Ed.), DSDP Leg. 42 B. Woods Hole Oceanographic Institution, Washington, D.C., 359-372.

Saulea, E., Popescu, I., Sandulescu, J., 1969. Lithofacias map atlas, 1:200000 (in Romanian and French), IGR (Ed.). IGR, Bucharest.

Senes, J., 1973. Correlation hypotheses of the Neogene Tethys and Paratethys. *Giorn. Geol*., **39**, 271-286.

Shillington, D.J., White, N., Minshull, T.A., Edwards, G.R.H., Jones, S.M., Edwards, R.A., Scott, C.L., 2008. Cenozoic evolution of the eastern Black Sea: A test of depth-dependent stretching models. *Earth and Planetary Science Letters*, **265**, 360-378.

Sloan, E.D., 2003. Fundamental principles and applications of natural gas hydrates. *Nature*, **426**, 353-363.

Sloan, E.D., Koh, C., 2007. Clathrate hydrates of natural gases. CRC press.

Shnyukov, E., F., 1999. Mud Volcanoes in Black Sea. *Petroleum Geology*, **34**, 323-328.

Soulet, G., Delaygue, G., Vallet-Coulomb, C., Böttcher, M.E., Sonzogni, C., Lericolais, G., Bard, E., 2010. 459 Glacial hydrologic conditions in the Black Sea reconstructed using geochemical pore water profiles. *Earth 460 and Planetary Science Letters*, **296**, 57-66.

Spadini, G., Robinson, A.G., Cloetingh, S.A.P.L., 1997. Thermomechanical Modelling of Black Sea Basin Formation, Subsidence, and Sedimentation, in: Robinson, A.G. (Ed.), Regional and Petroleum Geology of the Black Sea and Surrounding Region, 19-38.

Starostenko, V., Buryanov, V., Makarenko, I., Rusakov, O., Stephenson, R., Nikishin, A., Georgiev, G., Gerasimov, M., Dimitriu, R., Legostaeva, O., Pchelarov, V., Sava, C., 2004. Topography of the crust–mantle boundary beneath the Black Sea Basin. *Tectonophysics*, **381**, 211-233.

Steininger, F.F., Muller, C., Rögl, F., 1988. Correlation of Central Paratethys, Eastern Paratethys, and Mediterranean Neogene Stages, in: Royden, L.H., Horvath, F. (Eds.), The Pannonian Basin, A Study in Basin Evolution. AAPG Memoir, 79-87.

Tambrea, D., Sindilar, V., Olaru, R., 2000. Pontian from Romanian continental plato of Black Sea (in romanian). *Romanian oil journal*, **7**, 9-21.

Tambrea, D., 2007. Subsidence analysis and thermo-tectonic evolution of Histria Depresion (Black Sea). Implications in hydrocarbon generation, Faculty of Geology and Geophysics. University of Bucharest, Bucharest, 165 p.

Tarapoanca, M., 2004. Architecture, 3D geometry and tectonic evolution of the Carpathians foreland basin, Faculty of Earth and Life Sciences. VU University Amsterdam, Amsterdam, 120 p.

Vasiliev, I., Krijgsman, W., Stoica, M., Langereis, C.G., 2005. Mio-Pliocene magnetostratigraphy in the southern Carpathian foredeep and Mediterranean–Paratethys correlations. *Terra Nova*, **17**, 376-384.

Vasiliev, I., Iosifidi, A.G., Khramov, A.N., Krijgsman, W., Kuiper, K., Langereis, C.G., Popov, V.V., Stoica, M., Tomsha, V.A., Yudin, S.V., 2011. Magnetostratigraphy and radio-isotope dating of upper Miocene–lower Pliocene sedimentary successions of the Black Sea Basin (Taman Peninsula, Russia). *Palaeogeography, Palaeoclimatology, Palaeoecology*, **310**, 163-175.

Vassilev, A., Dimitrov, L., 2003. Model evaluation of the Black Sea gas hydrates. *Comptes Rendus de l'Academie bulgare des Sciences*, **56**, 3-15.

Veliciu, S., 2002. Heat flow of the North-Western Black Sea region, in: Dinu, C., Mocanu, V. (Eds.), Geology and Tectonics of the Romanian Black Sea shelf and its Hydrocarbon Potential. *BGF Special Volume*, **2**, 53-58.

Westbrook, G.K., Thatcher, K.E., Rohling, E.J., Piotrowski, A.M., Pälike, H., Osborne, A.H., Nisbet, E.G., Minshull, T.A., Lanoiselle, M., James, R.H., 2009. Escape of methane gas from the seabed along the West Spitsbergen continental margin. *Geophysical Research Letters*, **36**.

Winguth, C., Wong, H.K., Panin, N., Dinu, C., Georgescu, P., Ungureanu, G., Krugliakov, V.V., Podshuveit, V., 2000. Upper Quaternary water level history and sedimentation in the northwestern Black Sea. *Marine Geology*, **167**, 127-146.

Wong, H. K., Panin, N., Dinu, C., Georgescu, P., Rahn, C., 1994. Morphology and post-Chaudian (Late Pleistocene) evolution of the submarine Danube fan complex. *Terra Nova*, **6**, *5*, 502-511.

Wong, H.K., Winguth, C., Panin, N., Dinu, C., Wollschlager, M., Georgescu, P., Ungureanu, G., Krugliakov, V.V., Podshuveit, V., 1997. The Danube and Dniper Fans: Morphostructure and Evolution. *Geoecomarina,* **2**, 77-101.

Yefremova, A. G., Zhizhchenko, B. P., 1974. Occurrence of crystal hydrates of gas in sediments of modern marine basins. *Doklady Akademii Nauk SSSR*, **214**, 1179-1181.

Zander, T., 2017. Methane hydrates in Black Sea deep-sea fans: Characteristics, implications, and related geohazards. Phd Thesis, Kiel, der Mathematisch-Naturwissenschaftlichen Fakultät der Christian-Albrechts-Universität zu Kiel: 160 p.

Zander, T., Haeckel, M., Berndt, C., Chi, W.-C., Klaucke, I., Bialas, J., Klaeschen, D., Koch, S., Atgin, O., 2017. On the origin of multiple BSRs in the Danube deep-sea fan, Black Sea. *Earth and Planetary Science Letters,* **462**, 15-25.

Zillmer, M., Flueh, E.R., Petersen, J., 2005. Seismic investigation of a bottom simulating reflector and quantification of gas hydrate in the Black Sea. *Geophysical Journal International,* **161**, 662-678.

Zonenshain, L.P., Le Pichon, X., 1986. Deep basins of the Black Sea and Caspian Sea as remnants of Mesozoic back-arc basins. *Tectonophysics,* **123**, 181-211.